Anonymous Referee #1
General comments:

In their paper “Single particle characterization using the soot particle aerosol mass spectrometer (SP-AMS)”, Lee et al. describe the first deployment of a soot particle aerosol mass spectrometer coupled with a light scattering probe, enabling single particle and ensemble analysis of both refractory black carbon and non-refractory species. They apply k-means clustering to the single particle mass spectra, and compare to the results of positive matrix factorization analysis of the ensemble data. The paper is well and clearly written and provides relevant information on the methods of single particle and ensemble analysis with the SP-AMS, as well as some interesting insights into particle mixing state. However, since the main focus of the paper is rather on a technical (method) development, it could be argued that this paper would be more suitable for AMT than for ACP. I therefore recommend publication either in AMT or as a “Technical Note” in ACP, subject to the following comments.

Response:
Thanks for the reviewer's encouraging comments.

The focus of our paper is on the investigation of carbonaceous particle mixing states in an urban environment. While our single particle measurements do represent the first application of the combined light scattering module with the soot particle aerosol mass spectrometer (LS-SP-AMS), the combined light scattering – aerosol mass spectrometer (LS-AMS) technique has been developed elsewhere (Cross et al. 2009, Freutel et al. 2013, Liu et al. 2013). Here we are applying the technique with a new focus on refractory black carbon (rBC)-containing particles enabled by the laser vaporizer in the SP-AMS. Since this is the first time that a light scattering module was deployed with the SP-AMS to measure ambient particles, some technical details have to be included in our manuscript. However, we do not believe that this paper should be limited to a technical note, as we are applying a recently developed technique to a new problem, not developing a brand new technique.

To make our focus clear, the title of the paper has been modified to "Mixing state of carbonaceous aerosol in an urban environment: Single particle characterization using the soot particle aerosol mass spectrometer (SP-AMS)". We have also modified three key sentences, one in the abstract, one in the introduction, and one in the conclusions to help ensure clarity on the science focus. Finally, in responding to the helpful and constructive comments from the reviewers (here and below), we have further enhanced the scientific content of the paper by adding two new sections (Section 3.6 and 3.7) and a several new figures (Figure 9, 10, S15, S16 and S17) to the revised version. With this additional information, the mixing state of rBC and other NR-PM components measured in an urban environment is better described in the paper. We feel that the insights into the mixing states of rBC-containing particles obtained as part of this work are important and are of interest in the aerosol community served by ACP.

References:

Cross, E. S., Onasch, T. B., Canagaratna, M., Jayne, J. T., Kimmel, J., Yu, X. -., Alexander, M. L., Worsnop, D. R. and Davidovits, P.: Single particle characterization using a light scattering module coupled to a time-of-flight aerosol mass spectrometer, Atmos. Chem. Phys., 9, 7769-7793, 2009.

Freutel, F., Drewnick, F., Schneider, J., Klimach, T. and Borrmann, S.: Quantitative single-particle analysis with the Aerodyne aerosol mass spectrometer: development of a new classification algorithm and its application to field data, Atmos. Meas. Tech., 6, 3131-3145, 2013.

Liu, S., Russell, L. M., Sueper, D. T. and Onasch, T. B.: Organic particle types by single-particle measurements using a time-of-flight aerosol mass spectrometer coupled with a light scattering module, Atmos. Meas. Tech., 6, 187-197, 2013.

Specific comments:

1. It is not made clear from the experimental section what data is acquired in LSSP mode and how this data is processed. Specifically, the statement on p. 15329, lines 24-25, is not correct: the computer is not triggered to save “the corresponding mass spectrum from the single particle”, it saves the whole PToF trace, from which afterwards the single particle mass spectrum is obtained. This is especially important as both PToF traces and integrated mass spectra are used later on (in Figs. 5 and 7, I think; this should be stated more clearly). Is the dva from LS or MS signal used in Fig. 7?

   Response:
   The reviewer is correct; the whole PTOF trace is saved for each light scattering event and the single particle mass spectrum is obtained from the saved PTOF trace. The sentence under question has been corrected in Section 2.5 as the reviewer suggested. It now reads:

   "Once a light scattering signal is detected, the computer is triggered to save the whole PToF trace, from which the single particle mass spectrum is subsequently obtained."

   Figure 7 shows the integrated single particle PTOF ion signals for different chemical species for the IR laser off (a) and on (b) conditions. The D_{va} used in Figure 7 is from the PTOF ion signals, and not from the LS light scattering signal.

2. The categorization of single particle mass spectra. First of all, “rotten” sounds rather colloquial to me to describe a category of mass spectra. The single particle data the authors describe rather seem to be “low in LS signal” or something similar. By looking at Fig. S1, it seems that the threshold during the data acquisition was set rather low, i.e. many saves were triggered by noise in the LS signal. So, instead of

using rather arbitrary values ("signal < 0.2"), why not simply calculate a new threshold from the data in Fig. S1 using some kind of "baseline" region (e.g., dva < 40nm)? A similar approach could be used to determine a threshold for "null" mass spectra.

Response:
The term "rotten" has be replaced by "noise" to describe the light scattering threshold crossing events that were likely caused by noise, rather than real particles. We used "rotten" in the original version because it is a default terminology used in the software package - Sparrow.

The reviewer points out an important issue that we actually set the threshold very close to the limit of our light scattering module during data acquisition. The primary reason is that we wished to maximize our particle counts from LS, especially for nearly pure BC particles that may have a weaker LS signal. The major drawback is that we detected significant numbers of LS noise events (i.e., false positive particle signals). As we have two direct measurements per single particle event, light scattering and mass spectrum, we use two different thresholding criteria, one based on light scattering signal and one based on ion signals. The mass spectrum ion threshold criteria is actually the more stringent threshold. The threshold of > 6 ions was established, in part, using the "effective noise level" shown in the new Figure S3e and f, following the concept described by the reviewer. The > 6 ions threshold was also chosen, in part, based on having sufficient ion signal per mass spectrum to enable useful chemical detection from the mass spectrum. With the chemical ion signal as the primary (i.e., most effective) threshold, the light scattering threshold (0.2 volts) helps to further refine the discrimination between real particle events and noise.

In relation to this, I am not quite sure about the comparison to the fraction of "null" particles found by Cross et al. and Liu et al. (p. 15336). While most of the reasoning seems valid, I am not sure on which evidence the authors base their assumption they had "a more sensitive light scattering detection system" than Liu et al. (lines 13-14). Furthermore, as said above, the threshold settings for data acquisition may have a large influence here; there may also be influences like different size distributions / chemical composition.

Response:
Liu et al. (2012) reported that their LS laser was not well aligned. However, to avoid any confusion, the related sentence has been removed in the revised version.

3. As written, there seem to be some contradictions regarding the collection efficiencies: on p. 15332, the authors claim CE = 1 for NR-PM after comparison to an SMPS system. They do not base this CE on any theoretical reasoning (average chemical composition to justify this?). Later on (Section 3.3), it is observed that NR-PM components are biased low by 10-20% in laser off compared to laser on mode, which

implies CE >1 for laser on mode. Then in several places (e.g., p. 15337), particle bounce is discussed, implying CE <1. Furthermore, when single particle data are analyzed, it becomes obvious that about half of the particles giving an LS signal do not give significant ion signal, i.e. CE <1. This needs some clarification.

Response:
Thank you for pointing out the confusion concerning the CE issue. It is important that we present a clear discussion of CE. Figure S5 and corresponding calculation details have been added to the supplementary information to discuss the CE correction factors applied for different particle types based on our single particle observations. In brief, we assume inorganic species (internal mixtures of ammonium nitrate and ammonium sulfate) vaporized by the heated tungsten vaporizer have CE equal to 0.5, which is commonly applied for ambient aerosols. On the other hand, oil-like organic droplets (HOA and COA) dominated the total organic aerosol mass, and they are unlikely to have a significant particle bounce on the tungsten vaporizer surface. Therefore, we assume that the CE of the total organic aerosol equal to one and, furthermore, the total organic signal is likely dominated by vaporization from the tungsten vaporizer. However, OOA that is likely internally mixed with inorganics may have CE lower than unity from the heated tungsten vaporizer, and this adds a potential uncertainty. The CE for rBC vaporized by the laser is assumed to be 1, but it is actually highly uncertain as discussed in Willis et al (2014). However, due to the low mass loading of rBC, the calculation is not sensitive to the CE of rBC. The overall correlation between LS-SP-AMS, using the various CE's stated above, and SMPS-derived particle mass, assuming spherical particles, is close to 1, suggesting our assumptions on CE's are reasonable.

Sections 3.1, 3.3 and 3.4 have been modified accordingly to ensure all the discussion related to CE is consistent throughout the manuscript.

Reference: Willis, M. D., Lee, A. K. Y., Onasch, T. B., Fortner, E. C., Williams, L. R., Lambe, A. T., Worsnop, D. R., and Abbatt, J. P. D., Collection efficiency of the soot-particle aerosol mass spectrometer (SP-AMS) for internally mixed particulate black carbon, Atmos. Meas. Tech. Discussion, 7, 5223-5249, 2014.

4. Concerning the statement on p. 15339, lines 22-25 (and related statements elsewhere): "In contrast, the clustering analysis clearly suggests that two major types of particles contributed to the PMF-HOA factor. The different size distributions of the two clusters also indicate two distinct particle types." This claims there are two particle types, wholly unconnected, separated into two clusters. Is it not more likely that there is a gradual degree of mixing between HOA and rBC? This could be easily tested by plotting e.g. HOA vs rBC mass for particles from these two clusters. Moreover, in other places of the manuscript the authors seem to contradict themselves on this topic (e.g., on p. 15341, lines 17 and 21, they suggest that also the "pure" HOA particles contain a small rBC core, which rather seems an indication of gradual degree of mixing). This needs clarification. Furthermore, can the detection limit of

rBC be somehow approximated? It is discussed on p. 15342, line 12, that rBC may be underestimated due to low ion counts. Could this be tested by comparing the average chemical composition derived from ensemble and single particle measurements?

Response:
Thanks for the reviewer's suggestion. We agree that HOA and rBC are likely gradually mixed in ambient aerosol particles. Based on the reviewer’s comments, we have done an extensive re-examination of the single particle data with the specific focus of understanding the potential for gradual mixing between different particle types. Figure 10 and Section 3.7 have been added to the revised manuscript to explicitly show the gradual mixing of HOA and rBC in both HOA-rich and rBC-rich particle classes, as suggested by the reviewer.

Onasch et al. (2012) reported that the 3σ detection limit for rBC mass concentration measurements is 0.03 μgm−3 for 1 min collection. This information has been added to the experimental section (Section 2.3). However, it is not straightforward to compare the average composition derived from ensemble and single particle measurements for rBC-containing particles because the light scattering detection bias to the large particles (e.g. > 200 nm). Most of the rBC particles are smaller than the light scattering cut size (please see Figure 2c and 5).

Reference: Onasch, T. B., Trimborn, A., Fortner, E. C., Jayne, J. T., Kok, G. L., Williams, L. R., Davidovits, P. and Worsnop, D. R.: Soot Particle Aerosol Mass Spectrometer: Development, Validation, and Initial Application, Aerosol Sci. Technol., 46, 804-817, 2012.

5. Similar to the discussion of distinct particle types vs gradual degree of mixing of rBC and HOA, it should be noted that the four particle cluster types of nitrate, sulfate, OOA cluster 1 and 2 likely represent four “extremes” of a large group of particles, all of the same type (internal mixture of sulfate, nitrate, OOA). This again should be easy to see in an according diagram (e.g. ternary plot).

Response:
We agree that all the secondary species (i.e., nitrate, sulfate and OOA1 and OOA2) are gradually mixed to some degree. As described above, we have done an extensive re-examination of the single particle data with the specific focus of understanding the potential for gradual mixing between different particle types. In order to better describe the mixing state of the secondary aerosol species in the accumulation mode (d_{va} peak at ~ 400 nm), ternary diagrams of mass fractions of nitrate, sulfate and total organics are shown in Figure 9 and S15 of the revised version as suggested by the reviewer. A new section (Section 3.6) has been added to the revised manuscript to describe the relative contributions of each secondary species in the particle classes identified by cluster analysis.

6. p. 15327, line 15: Can the measurement location be described a bit more in detail? Is it adjacent to a road, or rather in a backyard? What's the traffic density, inlet height?

   Response:
   A paragraph has been added to Section 2.1 (Sampling location and instruments) to describe the sampling locations. A map has been also added to the supplementary information (Figure S1).

7. p. 15332, line 15: provide model of SMPS instrument. What assumptions were used to infer mass from the SMPS measurements, and how well did it correlate exactly (slope?)

   Response:
   The model of the SMPS instrument has been added to Section 2.1. Please refer to comments 3 above about the assumptions used for SMPS mass calculation.

8. p. 15332, lines 20-24: Which m/z range was investigated in this study? I think the information on fullerenes could be easily improved by a simple back-of-the-envelope calculation: assuming the ratio found by Onasch et al. from the fullerenes to the smaller Cx ions, would a significant signal of fullerenes be expected at the observed signal of lower Cx fragments?

   Response:
   Thanks for the reviewer's suggestion. Based on a previous laboratory study, small Cx fragments only have small contributions (~10%) to the total rBC mass of fullerenes (information from AMS users meeting wiki site - http://cires.colorado.edu/jimenez-group/UsrMtgs/UsersMtg11/SPAMSpresentationOnasch.pdf). Since fullerene is likely a minor contributor to the total rBC mass in ambient rBC-containing particles (Onasch et al., 2012) and there is only limited information available in the literature, we have modified the original sentences as follow instead of doing the estimation.

   "Fullerene type rBC spectral features (i.e., C_x^+ fragments with carbon number > 32) cannot be evaluated because their C_x^+ peaks are out of the m/z range (up to ~300) investigated in this study. Onasch et al. (2012) observed carbon cluster ions up to C_{82}^+ in laboratory generated ethylene flame soot particles and detected C_{32}^+ to C_{70}^+ that accounted for about 4% of the total rBC signals at an urban roadside environment."

9. p. 15335, line 21: KNO3 is not a good example of refractory species, since it is very easily thermally decomposed and detected very well with the AMS. Why should more acidic material be present in internally mixed rBC particles than in others? For very aged material, this does not seem very likely.

   Response:

> To avoid any confusion, the discussion about the KNO3 and acidic particles has been removed from Section 3.3. The revised sentences are shown as below:
>
> "For inorganic species, the enhancement of NH_4^+ mass between the two operational modes is smaller than those observed in the case of NO_3^- and SO_4^{2-} (Figure S10). The reason of this observation is unclear but one of the possibilities is that some refractory nitrate and sulfate (e.g., Na_2SO_4) coexisted with rBC."

Technical corrections:

The authors use the different terms "LS-SP-AMS" and "SP-AMS" sometimes on purpose to distinguish between SP-AMS with and without light scattering module; but sometimes, both terms seem to be used interchangeably (e.g., p. 15342: In line 3, it is "SP-AMS" on purpose, because here we talk about an "usual" SP-AMS. But in line 7, again "SP-AMS" is used, where it is talked about the single particle data from this work. So, it should be more precisely "LS-SP-AMS" here.) More care should be taken in the whole manuscript to use the more appropriate of both terms in each situation.

Response:
Done

Also, it might be confusing to the reader that on the one hand, there is the "LS-SPAMS", on the other hand, there is the "LSSP mode". Maybe it could be shortened to "LS mode" to make the difference more clear? Especially since in one case SP means "soot particle", in the other "single particle".

Response:
Done

p. 15324, line 18; Section 3.6; and p.15344, line 4: "low to mid-range aerodynamic diameter" could mean anything from a few nanometers to several _m. Please specify at least once the size range.

Response:
We define low-to-mid range aerodynamic diameter as ~200-400 nm.

p. 15325, line 13: "quantitative single particle detection": do you really mean that the (optical) detection of the particles should be quantitative (i.e., the number concentration should be correct), or do you mean quantitative chemical composition analysis of the single particles which were detected (i.e., getting quantitative mass per particle information, i.e. do you want to stress the difference between AMS and ATOFMS single particle data)? Maybe reword to make more clear.

Response:

This is a sentence to generally describe the features of ideal techniques for single particle detection. The sentence has been revised to specify the meaning of "quantitative single particle detection" in the introduction.

"Real-time quantitative single particle detection (i.e. number concentrations and chemical composition by mass in a single particles basis) is necessary to determine the mixing state of ambient particles."

p. 15326, line 20: “which is able to quantify and characterize rBC and NR-PM”: sounds strange. How do you “characterize rBC”?

Response:
It has been reported within the AMS community that ambient particles can consist of different types of rBC (e.g. flame soot, fullerene, etc. - http://cires.colorado.edu/jimenez-group/UsrMtgs/UsersMtg11/SPAMSpresentationOnasch.pdf). Furthermore, recent study has reported that soot particles can have different fragmentation patterns and surface properties (functional groups) (Corbin et al. 2014). To make it clear, the related information has been added to the manuscript.

"The utility of the AMS was recently extended by development of the Soot-Particle Aerosol Mass Spectrometer (SP-AMS), which is able to quantify and characterize rBC (i.e. C_x fragmentation pattern and surface functionality) and NR-PM simultaneously (Cross et al. 2010, Onasch et al. 2012, Corbin et al. 2014)."

Reference: "Corbin, J. C., Sierau, B., Gysel, M., Laborde, M., Keller, A., Kim, J., Petzold, A., Onasch, T.B., Lohmann, U. and Mensah, A. A.: Mass spectrometry of refractory black carbon particles from six sources: carbon cluster and oxygenated ions, Atmos. Chem. Phys., 14, 2591-2603, 2014."

p. 15327, line 6: “SP-AMS ensemble measurement data”

Response:
Done

p. 15327, lines 13 and 22: give a reference for “standard HR-ToF-AMS” and “V-mode”.

Response:
A reference has been added.

"DeCarlo, P. F., Kimmel, J. R., Trimborn, A., Northway, M. J., Jayne, J. T., Aiken, A. C., Gonin, M., Fuhrer, K., Horvath, T., Docherty, K. S., Worsnop, D. R., and Jimene, J. L.: Field-deployable, high-resolution, time-of-flight aerosol mass spectrometer, Anal. Chem., 78, 8281–8289, 2006."

p. 15328, line 2: “the NR-PM that is internally mixed with rBC core”: strange wording. Maybe just delete “core”?

Response:
The word "core" has been deleted.

p. 15328, lines 18-19; and p. 15330, line 4: As reference, the URL should be provided where Squirrel / PIKA / Sparrow can be obtained.

Response:
Two URL have been provided in the revised version.

AMS data analysis software (Squirrel, version 1.51H for unit mass resolution (UMR) data and Pika, version 1.10H for high resolution peak fitting) -
http://cires.colorado.edu/jimenez-group/ToFAMSResources/ToFSoftware/index.html

Single particle data processing software, Sparrow (1.04E) -
http://cires.colorado.edu/jimenez-group/ToFAMSResources/ToFSoftware/index.html

p. 15330, line 18: “number of ions is the sum” should read “number of ions was calculated as the sum”

Response:
Done

p. 15331, line 8: this should read “total ion signals in a single particle mass spectrum” more precisely

Response:
Done

p. 15333, line 4: specify “SOA”

Response:
Secondary organic aerosol (SOA) has been changed to oxygenated organic aerosol (OOA) in the revised version as suggested by another reviewer.

p. 15337, line 4: “Chi” should read “S”. Also, the same equation is given before (p. 15328). Maybe break up into a separate line there and simply refer to “Eq. (1)” later.

Response:
The symbol has been changed in the Eq. 1 of the revised manuscript. Also, the latter part of the manuscript refers to Eq. 1 if needed.

p. 15337, line 26-28: It is unclear what this sentence is supposed to say in the present form. If I understand correctly, what is meant is that clusterings of both laser on and laser off datasets were performed, and here only laser on clustering results are shown as an example. This should be made clearer here, especially since the results from both clusterings are compared later on.

Response:
Thanks for the suggestions. Below is the revised sentence in Section 3.5:

"The k-means clustering algorithm was used to separately classify all the prompt particle mass spectra into chemically distinct groups for both laser-on and laser-off datasets. The overall cluster analysis results for NR-PM are similar for both the IR laser-on and off datasets, with the primary exception being an additional particle class, rBC, obtained from the laser-on mode single particle data. The major NR-PM particle classes obtained via independent cluster analysis for both datasets included nitrate, sulfate, HOA, COA, and 2 types of OOA (Figure 8). These particle classes represented similar particle number fractions and time series, and differed only slightly in average mass spectra (not shown)."

To demonstrate the capability of the LS-SP-AMS to investigate the mixing state of ambient aerosol particles, the twelve-cluster solution from the laser-on mode measurements is presented here...."

p. 15338, line 3: should read "reduces" to not mix different tenses within one sentence.

Response:
Done

p. 15338, line 11: "procedure" – do the authors mean "produce"?

Response:
Done

p. 15339, line 9: rather "do not contain any inorganic species"

Response:
Done

p. 15339, line 10: considering the associated uncertainty, "about 6%" seems more appropriate than “6.4%”

Response:
It has been changed to "about 6%".

p. 15343, line 18: comma missing: “other, non-refractory”

Response:
Done

Table 2: define “NA”. What does “measurable m/z 36 signal” mean? Any signal larger than zero? Signal above a certain threshold?

Response:
NA has been defined as "Not applicable" in Table 2. "Measurable m/z 36 signal" means any signal larger than zero and has been defined in Table 2.

Figure 2: define “Org44”; it should be noted that these data are from ensemble measurements.

Response:
The caption of Figure 2 has been revised as below:

"Figure 2: Summary of ensemble measurements (a) Time series (local time) of laser-off (Org, NO_3, SO_4, NH_4) and laser-on (rBC) aerosol compositions. (b) The average mass spectrum of laser-on ambient rBC and Regal Black (insert). (c) Average size distributions of laser-off (Org, NO_3, SO_4, Org44) and laser-on (rBC) aerosol compositions. Org 44 represents organic signal at m/z 44 (e.g., CO_2^+)."

Figures 2 and 4: Is this local time? Please specify.

Response:
They are local time. The information has been added to the captions.

Figures 5, 7 and S9: The purple and grey lines are hard to distinguish.

Response:
The purple lines have been changed to pink lines in Figure 5, 7 and S12 of the revised version.

Figure 6: b) how thin is a “thin” coating? Maybe would be better described as an “internal mixture of rBC and HOA”. c) should be “is classified” instead of “are”.

Response:
The caption of Figure 6 has been modified as follow:

"Figure 6: Examples of single particle mass spectra of rBC-containing particles: (a) Black carbon, (b) black carbon internally mixed with HOA, and (c) black carbon internally mixed with OOA and sulfate. Particles (a) and (b) are sorted into the rBC cluster, and particle (c) is classified into the OOA cluster 2 identified in this study (See Section 3.5)."

Figure 8: For clarity, it could be stated in the figure caption that these are results for the clustering of the "laser on" dataset. Also, what is the inset in panel (d)? Please clarify.

Response:
The caption of Figure 8 has been modified as follow:

"Figure 8: Normalized mass spectra (left column), normalized histograms displaying the relative frequency of each m/z (middle column), and size distributions (right column) of different particle classes identified from k-means clustering of LS-SP-AMS single particle dataset (laser-on): (a, h and p) NO_3 class, (b, i and q) SO_4 class, (c, j and r) HOA class, (d, k and s) rBC class, (e, m and t) COA class, (f, n and u) OOA class 1 – less oxygenated, (g, o and v) OOA class 2 – more oxygenated. The insert in 8d shows the organic mass spectrum associated with the rBC-rich particle class."

Figure S7: in which units are the signal intensities given?

Response:
They are ion signals. The information has been added to the figure caption (Figure S10 in the revised version).

" Figure S10: Comparison between the IR laser on and off measurements (ion signals): (a) NH_4^+ (b) SO_4^{2-} (c) NO_3^- and (d) Organic. Dashed line = 1:1 line, red line = data fitting."

Figure S9b: Label on the right y-axis is unclear. Should this read ": : :ratio or Total: : :"?

Response:
The correction has been made. It should be "ratio or total".

Anonymous Referee #2

Lee et al., describe results obtained with the Aerodyne Soot-Particle Aerosol Mass Spectrometer equipped with a light scattering module to enable single particle characterization of both refractory and non-refractory particle constituents (for particles larger than the optical detection limit of the instrument). The manuscript focuses on four days of continuous sampling in downtown Toronto, from which the authors demonstrate the capability of the LS-SP-AMS through single particle k-means cluster analysis and bulk ensemble positive matrix factorization (PMF) approaches. The work is an important contribution to the field especially in the context of improving our understanding of the mixing state of ambient particulate matter (including combustion-derived rBC) within urban environments. The manuscript is well written and the insights drawn from the work warrant publication in ACP. The following comments should be addressed by the authors prior to final publication.

Thanks for the reviewer's encouraging comments.

General Comments

Grey area terminology:

- Throughout the manuscript the authors refer to 'low to mid-range aerodynamic diameter' this range should be explicitly defined. The first mention of an actual mid-range diameter is not found until P15337 L12.

  Response:
  Thanks for the comments. The low to mid range dva has been defined as particle size ranging from ~200-400 nm.

- 'HOA-rich': how is this classified?

  Response:
  As mentioned in Section 3.5.2 of the revised manuscript, particles with mass spectral fragmentation patterns of hydrocarbons are identified as HOA particles. In the current study, the HOA-rich particles are primarily composed of HOA-like organics (e.g. > 90 wt%).

- 'Nearly external mixing': I believe the authors wish to convey the fact that they measure nearly chemically pure, distinct, particle populations within the ensemble. For example, a chemically pure rBC-only particle type or HOA+rBC particle type or pure HOA particle type. The authors should carefully consider what they mean by 'nearly external mixing' and discuss external and internal mixing from the ensemble and single particle perspectives. Within any given urban environment there will be a gradient of mixing and the exact nature of this gradient is dependent on many factors.

The authors should make a concerted effort to more clearly define what they interpret as externally vs. internally mixed particle populations in the context of the real-world gradients of particle chemistry encountered in an urban environment like downtown Toronto.

Response:
Thanks for the reviewer's suggestion. We agree that HOA and rBC are likely gradually mixed in ambient aerosol particles as suggested by other reviewers. We have done an extensive re-examination of the single particle data with the specific focus of understanding the potential for gradual mixing between different particle types. Figures 10, S16, and S17 and Section 3.7 have been added to the revised manuscript to explicitly show the gradual mixing of HOA and rBC in both HOA-rich and rBC-rich particle classes. Furthermore, the degree of mixing of secondary species including nitrate, sulfate, and OOA in the accumulation mode (d_{va} peak at ~ 400 nm) is discussed in Section 3.6 and Figures 9 and S15 of the revised manuscript.

- In paragraph 2 of P15325 the authors introduce the term refractory BC (rBC) in connection with the SP2-defined measurement technique. Prior to (and following) this the authors use ‘BC’. I think it would be helpful to the general reader to include a sentence describing the difference between rBC and BC. The authors should make a point not to switch back and forth between using these two terms throughout the manuscript, if possible.

  Response:
  Thanks for the comment. rBC has been used more frequently than BC throughout the manuscript unless a more general description of ambient BC issues is needed.

- The authors make an effort to differentiate the SP-AMS from the LS-SP-AMS and this ends up causing more confusion than clarity. I recommend that they use LS-SP-AMS throughout the manuscript and describe the menu-switching modes of operation to differentiate single particle from ensemble modes of operation. The introduction of the LSSP mode (which is not defined, when introduced on P15328, L6) further confuses the acronym-overloaded of the text. Consider removing this, while still clearly defining the single particle mode of operation.

  Response:
  LS-SP-AMS has been used throughout the manuscript unless more general SP-AMS issues are discussed. To avoid confusion, "LSSP mode" has been changed to "LS mode".

- P15331, L23: Authors should specify the # of clusters that can be combined with the CAP program – not just ‘a few’.

Response:
We didn't perform any testing on the maximum number of clusters which can be handled by the CAP program. In the current study, we successfully combined 4 nitrate related clusters to a single nitrate-rich cluster. Therefore, we decided to keep the current sentence in the revised version.

Specific comments:

P15324, L20-21: The general reader may not be familiar with ‘the conventional interpretation’ of PMF results and as such, this language should be avoided or more concretely defined.

Response:
As suggested by the reviewer, "conventional" has been removed from the last sentence of the abstract.

"The similar temporal profiles and mass spectral features of the organic classes identified by cluster analysis and the factors from a positive matrix factorization (PMF) analysis of the ensemble aerosol dataset validate the interpretation of the PMF results."

P15325, L1: Do the authors mean to highlight the varying morphology of the ‘coating’ on the BC or the particle as a whole.

Response:
We would like to highlight the varying morphology and thickness of the coating on the BC. To make it clear, additional description about coating morphology (e.g. partly coated and embedded) has been added to the sentence.

"Coatings on BC aerosol surfaces with varying morphology (e.g. partly coated and embedded) and thickness have been observed using electron microscopy (China et al. 2013, 2014)."

P15326, L18: Should read ‘flash vaporize at 600 C’

Response:
Done

P15327, Section 2: Should include a more comprehensive description of the sampling location and sampling inlet configuration relative to near-by source of pollution. Specifically, proximity to major roadways and COA sources (such as food trucks, carts, etc.) would help place the results in a more relevant context. If possible, inclusion of a map of the area surround the sampling site may be particularly useful for the reader.

This inclusion would also allow the authors to draw finer lines of connectivity between their results and important sources of particulate matter within busy, active, urban environments.

They should also make a point of identify the days of week across which sampling occurred (weekday vs. weekend) – and the difference that makes to likely emission sources in the area.

Response:
Thanks for the reviewer's suggestions. A new paragraph has been added to Section 2.1 (Sampling location and instruments) to describe the sampling location and inlet configuration. A map showing the sampling location and surrounding environment has been added to the supplementary information (Figure S1). The sampling period was from Tuesday evening to Saturday afternoon, which has been added to Section 2.1.

P15327, L22: V-mode should be described. This is a meaningless term to readers not familiar with the AMS. Define mass resolving power for your instrument, during this campaign.

Response:
The sentence has been modified.

"The ions are then detected by a high-resolution time-of-flight mass spectrometer operated in V-mode, which provides a lower mass resolving power (~2000) but a higher sensitivity compared to W-mode (mass resolving power ~ 4000) (DeCarlo et al. 2006)."

P15327, L23: It would be helpful to add a sentence describing the motivation behind running the instrument in laser-on vs. laser-off mode throughout your sampling campaign. To the unfamiliar reader, this just looks like you are cutting your duty cycle on sampling rBC down by 50%.

Response:
Thanks for the suggestion. A sentence has been added to Section 2.2 of the revised manuscript.

"The SP-AMS was operated with two vaporizer configurations during sampling, laser-on and laser-off, to maximize the information obtained and to enable comparisons and correlations between the two different vaporizers.. In particular, previous work has shown vaporizer-dependent differences in collection efficiencies and fragmentation patterns (Onasch et al. 2012; Willis et al., 2014)."

P15328, L10: Consider adding a header here: Calibration

Response:
A new heading "Calibration and ensemble data analysis" has been added to Section 2.3.

P15328, L22-28: I would strongly recommend removing the equation for effective density from within the text and writing the formula out with label: Eqn. 1. In fact the authors should define effective density in this section. Once organized as Eqn 1, the authors can more easily refer back to this equation later in the manuscript (P15337 L4-5).
- In connection with the discussion of effective density – as the authors point out – highly non-spherical particles (i.e. soot agglomerates, dominated by rBC) will appear at lower dva values than typical accumulation mode particles. Given the importance of this type of particle to results discussed in this manuscript, the authors should briefly discuss the influence that highly non-spherical shape has on the particle beam width as it transits the time-of-flight chamber of the LS-SP-AMS / intersecting different regions (intensities) of the 405 nm scattering laser and 1064 SP laser.

Response:
Thanks for the suggestion. The equation has been defined as Eq. 1 in the revised version. The highly non-spherical particles result in a wider particle beam than the spherical particles. The SP laser (1064 nm) and particle beam overlapping remains uncertain and has to be further investigated by SP-AMS community. Our group recently studied the particle-beam width of ambient BC particles in urban environments and laboratory-generated BC standard (i.e. Regal Black). We observed that the particle beam width of BC particles decreases with coating thickness. In particular, the collection efficiency of bare Regal Black particle is ~0.6 due to incomplete overlap between SP laser and particle beam (Willis et al. 2014). Such information has been provided in Section 2.3 and 3.1.

The overlapping of LS laser (405 nm) and particle beam is unlikely an issue because the LS laser beam is not focused and diverges in order to ensure a complete overlapping. This information is provided in the original manuscript.

Reference: Willis, M. D., Lee, A. K. Y., Onasch, T. B., Fortner, E. C., Williams, L. R., Lambe, A. T., Worsnop, D. R., and Abbatt, J. P. D., Collection efficiency of the soot-particle aerosol mass spectrometer (SP-AMS) for internally mixed particulate black carbon, Atmos. Meas. Tech. Discussion, 7, 5223-5249, 2014.

P15329, L10: Consider revising sentence: ‘overlaps perpendicularly with the particle beam _ 0.265 m downstream of the chopper and _ 0.130 m upstream of the tungsten vaporizer as shown in Fig. 1.

Response:
Done

P15329, L15: The authors should define what they mean by 50% cut-off diameter.

Response:
The 50% cut-off mobility diameter has been defined.

"The 50% cut-off mobility diameter (d_m) (i.e., a diameter that represents 50% counting efficiency of particle number when compared to a CPC) of our light scattering module determined using dry NH_4NO_3 particles is ~250 nm,..."

P15329, L19: should read: ‘may have a lower cut-off dva than: : :.’

Response:
Done

P15330, L2: Consider adding a sentence describing the width of the chopper slit used in the LS-SP-AMS (0.5, 1, 2%) and how this width would impact the ability to accurately size (LS_dva) and predict arrival times at the vaporizer.

Response:
Thanks for the suggestion. A sentence has been added to describe the chopper slit throughput in Section 2.2.

"A single slit chopper with ~2% throughput was used in our LS-SP-AMS."

Furthermore, two major uncertainties for particle sizing measurement have been added to Section 2.5 of the revised version:

"There are two major timing uncertainties for particle sizing measurement: 1) the initial time of the chopper cycle due to the slit width of the spinning chopper (~2%), and 2) the extra time required for vaporization, ionization and detection."

P15330, L7: Avoid use of term ‘rotten’

Response:
The term "rotten" has been changed to "noise" throughout the revised manuscript as suggested by another reviewer.

P15330, L9: Is it possible to relate the >/= 6 ions/spectra threshold to an estimate of mass-based (fg/particle) detection limit?

Response:
It is not straightforward to provide an estimate of mass-based detection limit based on the ion-based threshold as all chemical species (nitrate, sulfate, ammonium, organics, black

carbon) have different relative ionization efficiency (RIE) in AMS. That is why we use ion-based mass spectra in our manuscript most of the time. However, using 6 ions and mass-based ionization efficiency of rBC determined in the current study, it can be estimated that the detection limit of a pure rBC single particle is 25 fg of rBC per particle. This information has been added to the last paragraph of Section 3.8.

"Using 6 ions as a detection limit of a single particle (i.e. a criteria for “prompt” particle type) and a mass-based ionization efficiency of Regal Black determined by calibration, it can be estimated that the detection limit of a pure rBC single particle is ~25 fg of rBC per particle."

P15330, L13: It would be informative to include the Gaussian distribution figure in the supplemental. Why did the authors choose the 3 sigma boundary as their classification of prompt vaporization-ionization? What is the physical explanation for an ‘early’ ion pulse arrival time?

Response:
A distribution figure has been added to the supplementary information (Figure S2). We choose the 3 sigma boundary because we would like to include most of the particles within the Gaussian boundary. The physical meaning of "early" particle type is not clear. However, they contribute less than 0.2% of particle LS trigger events (Table 1). The information has been added to the second paragraph of Section 2.5.

"The delayed particle type can be due to the phenomenon of particle bounce upon impact with the thermal vaporizer surface (Cross et al. 2009) but the physical meaning of early particle type remains unclear."

P15330, L25-27: The authors reference Fig S1 as evidence of clear separation of the prompt single particles from all other particle types. Although it is clear that their 3 sigma classification for prompt particles has identified the vast majority of real- LS events from noise events – it is not clear that from the graph that early or delayed particle vaporization types are effectively identified. Rather than plotting the MS ion scatter plot vs. LS_dva – the authors could consider plotting and differentiating the early, prompt, and delayed particle types vs MS_dva, whilst leaving out the 25% of LS events that were noise. This, combined with the Gaussian distribution of arrival times may provide a more comprehensive separation of the prompt-vaporization particle types from all other non-noise particle events.

Response:
Thanks for the reviewer's suggestions. Two new plots have been added to Figure S3e and S3f in the supplementary information. These scatter plots (i.e. MS total ion counts vs. MS d_{va}) show how prompt, early and delayed particle types are separated by our particle type classification procedure. It can be found that early and delayed particle types are concentrated at smaller and larger particle size respectively, which is quite reasonable.

- It is very interesting to see the prominence of single particle events that appear in S1b that result from having the SP laser ON – particles comprised of rBC, rBC+HOA. This begins to show the potential for determining a size and chemistry-dependent collection efficiency for the LS-SP-AMS sampling across a matrix of particle types encountered in an urban environment. Did the authors complete any size-dependent CE assessments (whether from the perspective of non-spherical rBC-dominant particle types or larger, accumulation mode particles with higher SO4 content)?

Response:
It would be useful to study a size and chemistry-dependent collection efficiency of SP-AMS with light scattering module. However, the focus of this paper is to investigate the mixing state of carbonaceous aerosols in an urban environment using LS-SP-AMS. Our group has published a paper in Atmospheric Measurement Techniques Discussion that investigated the collection efficiency of rBC-containing particles using the beam width probe approach (Willis et al. 2014). This is an important issue to be future investigation.

Reference: Willis, M. D., Lee, A. K. Y., Onasch, T. B., Fortner, E. C., Williams, L. R., Lambe, A. T., Worsnop, D. R., and Abbatt, J. P. D., Collection efficiency of the soot-particle aerosol mass spectrometer (SP-AMS) for internally mixed particulate black carbon, Atmos. Meas. Tech. Discussion, 7, 5223-5249, 2014.

P15331, L1: The authors should explain their justification for using only the prompt particles in their cluster analysis. Did the early and delayed particle types show consistently lower total ion counts for the same LS_dva when compared to prompt?

Response:
According to our single particle classification approach, early and delayed particle types should have ion counts ≥ 6 ions. Otherwise, they should be classified as "Null" particle type. We haven't tried to include these two particle types in our cluster analysis. The major reason is that we would like to have a more meaningful particle size information. Also, as shown in Table 1, the two particle types only contribute ~1% of the particle LS trigger events. Therefore, we believe the final results and conclusions would not be affected. This information has been added to revised version.

"Including other particle types with a lower confidence on their PToF d_{va} (i.e. early and delayed) to the cluster analysis would not affect the major observations, as they contributed only ~1% of the particle LS trigger events (Table 1)."

P15332, L12-16: Graph or correlation coefficient should explicitly stated comparing LSSP-AMS mass vs SMPS. SMPS assumptions about particle shape and density should be given.

Response:
Figure S5 and some calculation details have been added to the supplementary information to discuss the CE correction for different particle types based on single particle observation. All the calculations and comparisons between LS-SP-AMS and SMPS particle mass are shown there. A sentence has been added to the manuscript as shown below:

"The total particle mass loading measured by the LS-SP-AMS is similar to that inferred from a simultaneous measurement using a Scanning Mobility Particle Sizer (SMPS, TSI Inc.,) (slope ~ 1.02, $R^2 = 0.76$), suggesting that the estimated CEs for NR-PM, vaporized from the heated tungsten vaporizer, and rBC, vaporized from the laser vaporizer, are within reasonable ranges (see Figure S5 in supplementary information)"

P15332, L25: Should read 'average ensemble size distributions..'

Response:
Done

Section 3.1: Opportunities to link the observations of particle chemistry back to details about the sampling site and potential sources – this would follow from a more thorough description of the sampling site back in section 2.1.

Response:
Thanks for the suggestions. Two sentences in Section 3.1 have been modified to link the observations to the sampling site characteristics described in Section 2.1.

"Since ambient rBC is only emitted from primary sources, this suggests that a significant portion of sampled rBC was freshly emitted or only slightly aged particles. This is consistent with the fact that vehicle emission are a major local source of rBC in the downtown area of Toronto."

"The relatively low fraction of oxygenated organic aerosol indicates that the sampling site was strongly influenced by local anthropogenic sources, such as vehicle and cooking related emissions, matching well with the site characteristics (see Section 2.1)."

P15334: The authors introduce Figure 4 at this point in the paper, but only describe the PMF portions of the analysis. The next mention of Figure 4 comes in the very last section of the paper (3.7) – connecting the cluster analysis results (also displayed in Figure 4). Splitting the descriptions of Figure 4's overlapping content is confusing and the authors should re-consider reorganizing this content so that the resultant figure is more coherent with the text or vice versa. One thing that draws the reader's eye is the presence of the three red rectangles in the figure – which are highlighting areas of agreement and disagreement within the data. These are not mentioned until P15342, L23.

Response:
Thanks for the reviewer's comment. This manuscript involves many observations obtained from different data analysis. After considering many factors, we would like to keep the current paper structure. To improve the connections between Figure 4 and discussions, the Figure 4 captions has been modified and an additional sentence has been added to the end of Section 3.2.

Section 3.2: "The comparison between PMF and single particle cluster analysis (Figure 4, line vs. filled area) will be discussed in Section 3.9."

Figure 4 Caption: "Time series (local time) profiles of rBC, PMF factors of organic components (from laser off mode MS measurements) and different organic clusters (from laser on mode LS measurements). The red rectangles indicate three major rBC and HOA peaks throughout the sampling period."

P15339, L16: How does the rBC-rich cluster's C1/C3 ratio of 0.53 impact the quantification of total BC mass concentration, given that the frag table assumes a C1/C3 ratio of 0.61? Related to this, it is not clear why the authors choose to use the C1/C3 ratio obtained from regal black instead of that acquired from the HR analysis of the ambient rBC (which is used in the case of the C4/C3 and C5/C3 ions as described in Table S2).

Response:
This is a very good question. A significant signal of C1 fragment can be contributed by organic aerosol based on the laser off measurements (or standard AMS measurement). The AMS community is still trying to improve the estimation of the C1 signal from rBC using the C1/C3 ratio. Therefore, we decide to use C1/C3 ratio of 0.61 obtained from Regal Black in the current study, which is also a common practice within the community at this stage, and provide the single particle C1/C3 ratio as a reference for future development.

P15341, L14: The authors should take care in explicitly stating that the rBC-rich particles they measure have a 'thin HOA coating'. As the radiative impacts of this particle type vary dramatically based on the nature of the associated HOA on the surface of the BC, it may not be appropriate to classify this as a thinly HOA-coated rBC particle–based on the LS-SP-AMS measurements alone. It is certainly clear that the authors have a particle population that is comprised of rBC+HOA components, but how they are distributed within the particle itself, remains ambiguous with the current instrumentation. Similarly, classifying HOA coatings as 'thick' may also be inappropriate.

Response:
The authors agree that it may be inappropriate to describe internally mixed rBC and HOA that observed by LS-SP-AMS as a thinly or thickly coated particles as we don't have direct evidence of particle morphology. To avoid misunderstanding, the descriptions of

"thin" and "thick" coatings have been minimized unless we have clearly stated the assumption. In particular, the sentences in Section 3.8 have been changed in the revised reversion.

"Quantitatively, the single particle data analysis demonstrates that: (1) a significant portion of HOA- and COA-rich particles (> 90%) with particle d_{va} larger than ~200 nm did not contain a detectable amount of rBC, e.g., organic-rich particles containing a small rBC core or no rBC (with a mass contribution of rBC to the HOA- and COA-rich classes about 3% on average), and (2) the rBC-rich particles were mixed with ~28 wt% HOA-like material on average, e.g., a thinly HOA coated rBC particle, assuming uniform coating thickness. For example, applying a simple core-shell spherical structure (i.e. rBC core plus uniform HOA coating), a 200 nm d_{va} rBC-rich particle has a coating thickness of ~10 nm with HOA and rBC densities equal to 0.9 and 0.8 g/cm^3, respectively."

Comments on Figures

Obviously, the authors put a tremendous amount of effort into this analysis and as a result of the complexity of the dataset and diversity of analysis approaches applied, have generated many figures. I worry that the sheer number of figures obscure the main take home points of the manuscript. Of the 8 figures within the manuscript body itself, Figures 7 and 8 stand out as important demonstration of the power of the technique for single particle characterization. Given the information in Figure 7, Figure 5 becomes somewhat redundant and the color scheme used in Figure 5 leads to some confusion (red, blue, green – signifying metrics that are not sulfate, nitrate, organic). The same comments applies to the colors used in Figure S9. The data displayed in Figures 2a and 4 could also be re-combined into a single figure, along with appropriate reorganization of text within the manuscript itself. Figures S2 and S10 seem unnecessary. Their content could be effectively conveyed with text alone.

If Figure 5 is kept in the manuscript, the authors should plot their empirical data that comprises the NH4NO3 d50 line. Likewise, this data could be included in Figure S9, if it remains in the final manuscript.

Response:

Thanks for the reviewer's suggestions on our figures. The empirical data that comprise the NH_4NO_3 d_{50} line have been added to Figure 5 and S12. The color scheme used in Figure 5 and S12 has been changed. We decide to not combine Figures 2a and 4 as it would it more difficult to follow the discussions. Figure S4 and S13 are not removed because they give the reader a general idea how we interpret the single particle cluster analysis results.

Anonymous Referee #3

The manuscript "Single particle characterization using the soot particle aerosol mass spectrometer (SP-AMS)" by Lee and coworkers reports the first deployment of an Aerodyne aerosol mass spectrometer equipped with both an infrared intracavity laser for black carbon measurement and a single particle light-scattering probe. This combination was used during a four days period in downtown Toronto. The collected data was then analyzed using standard AMS methods, positive matrix factorization as well as cluster analysis using the k-means algorithm.

General comments:

The manuscript is well structured and written, although in a few places the language could use a revision regarding sentence structure, grammar (tenses) and punctuation.

In some parts the use of abbreviations and "AMS" specific terms could be reduced to improve readability for readers less familiar with the Aerodyne AMS. The manuscript has some major shortcomings that should be addressed prior to publication.

Thanks for the reviewer's encouraging comments.

- In large parts it deals with the techniques and methods applied to obtain and analyze the data. The results of the mathematical methods are compared regarding the methods used; the atmospheric relevant results and their implications, however, are only shortly mentioned and not really discussed.

  Response:
  In order to improve the quality of this paper in terms of science and atmospheric relevance, two new sections (Section 3.6 and 3.7) and a few figures (Figure 9, 10, S15, S16 and S17) have been added to the revised version to discuss the degree of mixing state of secondary species in the accumulation mode particles, and HOA and rBC in the two vehicle related particle types (i.e. HOA- and rBC rich particle classes).

- It is not comprehensible nor explained, why the authors use the k-means algorithm instead of its successor. K-means cluster analysis has some major shortcomings that have been addressed long ago by the c-means (Fuzzy) algorithm. K-means requires each data point to belong to one (and only one) cluster, a condition which is difficult to justify for atmospheric aerosols with a history of constant mixing and exchange.

- In general both algorithms (k-means as well as c-means) do require equal distribution of data points into all clusters and thus are prone to oversee small clusters. This issue could be addressed by in addition using a different cluster method for comparison, for example hierarchical clustering or a neuronal network like ART-2A.

  Response:

Cluster analysis of single particle data from Aerodyne LS-ToF-AMS is rather limited in the literature. Liu et al. (2013) first applied k-means clustering to analysis LS-ToF-AMS single particle data. On the other hand, a few previous studies have shown that k-means clustering can classify ambient particle types measured by ATOFMS in good agreement with other cluster analysis techniques such as ART-2a and hierarchical clustering. This information has been added to the introduction and Section 2.6 so that the reader can better understand the potential differences between those cluster analysis techniques.

Introduction: “Previous studies have shown that k-means clustering can classify ambient particle types measured by ATOFMS in good agreement with other clustering algorithms such as ART-2a and hierarchical clustering (Rebotier and Prather, 2007, Giorio et al. 2012).”

Section 2.6: "It is worth noting that k-means clustering can classify ambient particles measured by ATOFMS into particle types that are highly consistent with other clustering algorithms such as ART-2a and hierarchical clustering (Rebotier and Prather, 2007, Giorio et al. 2012)."

- I recommend that the authors reconsider the main focus of the manuscript. If they want to keep the current focus, the methodical part should be enhanced, and the manuscript should be moved to AMT. To merit publication in ACP, the authors have to shift the focus towards a more scientific (non-methodical) discussion and atmospheric relevance.

Response:
Thanks for the reviewer's comments. As described above (in comment 1 to reviewer 1), the focus of our paper is on the investigation of carbonaceous particle mixing states in an urban environment. While our single particle measurements do represent the first application of the combined light scattering module with the soot particle aerosol mass spectrometer (LS-SP-AMS), the combined light scattering – aerosol mass spectrometer (LS-AMS) technique has been developed elsewhere (Cross et al. 2009, Freutel et al. 2013, Liu et al. 2013). Here we are applying the technique with a new focus on refractory black carbon (rBC)-containing particles enabled by the laser vaporizer in the SP-AMS. Two new sections have been added to the revised version to have a more comprehensive discussion about the mixing state of secondary aerosol species (Section 3.6), and HOA and BC (Section 3.7). This modification improves the paper quality in terms of science and atmospheric relevance and makes it more suitable to be published in ACP. Given that light scattering AMS and the SP-AMS have been previously described, we do not consider this paper appropriate for AMT.

References

Cross, E. S., Onasch, T. B., Canagaratna, M., Jayne, J. T., Kimmel, J., Yu, X. -., Alexander, M. L., Worsnop, D. R. and Davidovits, P.: Single particle characterization using a light scattering module coupled to a time-of-flight aerosol mass spectrometer,

Atmos. Chem. Phys., 9, 7769-7793, 2009.

Freutel, F., Drewnick, F., Schneider, J., Klimach, T. and Borrmann, S.: Quantitative single-particle analysis with the Aerodyne aerosol mass spectrometer: development of a new classification algorithm and its application to field data, Atmos. Meas. Tech., 6, 3131-3145, 2013.

Liu, S., Russell, L. M., Sueper, D. T. and Onasch, T. B.: Organic particle types by single-particle measurements using a time-of-flight aerosol mass spectrometer coupled with a light scattering module, Atmos. Meas. Tech., 6, 187-197, 2013.

Specific comments:

P15324, L21: What is "the conventional interpretation of the PMF results"?

Response:
As suggested by the reviewer, "conventional" has been removed from the sentence.

"The similar temporal profiles and mass spectral features of the organic classes identified by cluster analysis and the factors from a positive matrix factorization (PMF) analysis of the ensemble aerosol dataset validate the interpretation of the PMF results."

P15324, L25-26: "Processes such as : : : are the primary sources of ambient BC." This suggests that there are other sources for atmospheric black carbon particles. Which sources would that be?

Response:
Thanks for the comments. The sentence has been changed as below:

"Fossil fuel combustion and biomass burning are the primary sources of ambient BC."

P15325, L13: "Real-time, quantitative single particle: : : ": the comma is unnecessary.

Response:
Done

P15326, L1: "In contrast, the Aerodyne : : : separates the particle vaporization and ionization steps : : :": "In contrast" should be removed because in this context it is wrong. For example, the SPLAT II (Zelenyuk et al., 2009) also uses a two-step vaporization and ionization process.

Response:

Done

P15326, L3-5: (Jayne et al., 2003) should be cited as a reference for the Q-AMS (when mentioning different versions of the AMS).

Response:
A reference for the Q-AMS has been added to the revised manuscript.

"Jayne, J.T., Leard, D.C., Zhang, X., Davidovits, P., Smith, K.A., Kolb, C.E. and Worsnop, D.R.: Development of an Aerosol Mass Spectrometer for Size and Composition. Analysis of Submicron Particles, Aerosol Science and Technology, 33, 49-70, 2000."

P15327, L1: "Clustering analysis" should be changed to "Cluster analysis" or simply "Clustering".

Response:
Corrections have been made throughout the manuscript.

P15327, L9ff: More details on the measurement location would be favorable, e.g., was it close to a major street, restaurants, etc.

Response:
A paragraph has been added to Section 2.1 (Sampling location and instruments) to describe the sampling locations.

P15327, L23: "The IR laser was switched on and off during data acquisition." This sentence sounds very trivial.

Response:
It is an important description about the LS-SP-AMS operation. To make it clear, the sentence has been modified as below:

"The SP-AMS was operated with two vaporizer configurations during sampling, laser-on and laser-off, to maximize the information obtained and to enable comparisons and correlations between the two different vaporizers.. In particular, previous work has shown vaporizer-dependent differences in collection efficiencies and fragmentation patterns (Onasch et al. 2012; Willis et al., 2014)."

P15327, L23-26: Please correct the grammar: ": : : the SP-AMS was operated : : :., whereas the instrument : : : detects both : : :"

Response:
Done

P15328, L14: “Regal 400R Pigment” should be “Regal 400R Pigment black”.

Response:
Done

P15329, L10: “: : : of a particle sizing chamber : : :” should be “: : : of the particle sizing chamber : : :”.

Response:
As suggested by another reviewer, this sentence has been revised to better describe the instrument.

"Briefly, the light scattering module consists of a 50 mW diode pumped 405 nm continuous wave laser (CrystaLaser, LC BCL-050-405) that overlaps perpendicularly with the particle beam ~0.265 m downstream of the chopper and ~0.130 m upstream of the tungsten vaporizer as shown in Figure 1."

P15329, L15: What was the lower cut-off diameter for the “Regal black” particles?

Response:
We did not determine the lower cut-off diameter of light scattering laser for the Regal black particles during the field study. Unfortunately, our instrument is in a new configuration and the data acquisition algorithm does not allow us to perform such testing.

P15330, L5-6: “The weak scattering trigger events (i.e., : : :).” Where do these values come from? What is the unit of the scattering signal?

Response:
The unit of light scattering signal is volts. A total scattering signal of 0.2 volts is roughly the average value of the noise signal as shown in Figure S3. However, it should be noted that a signal-to-noise ratio plays a more critical role in screening out the useless data.

P15330, L7: Please replace “rotten” with another expression, for example “useless”. Or just paraphrase it.

Response:

The term "rotten" has been changed to "noise" throughout the revised manuscript as suggested by another reviewer.

P15330, L8-9: How is a “strong” scattering signal defined? Why six ions? And how are the ions calculated? By integrating over the mass spectrum divided by the (measured) single ion?

Response:
Based on Figure S3, 6 ions is a reasonable cut-off to remove the MS signals close to the noise level. As mentioned by the reviewer, the total ions calculated by integrating over the mass spectrum divided by the measured single ion during the calibration. To avoid confusion, the sentence has been modified as below:

"For particles that gave a sufficiently strong LS trigger event (i.e. those are not classified to as “noise”) and a total number of ions ≥ 6 in their mass spectra (calculated by integrating the ion signals in the single particle mass spectrum), they were either categorized as “prompt”, “early” or “delayed” particle types based on their PToF information (see supplementary information for information on setting the LS signal and total number of ions thresholds)."

P15330 L10-12: “: : : could accurately predict : : : the particle is categorized : : :” Correct the grammar. Why “Specifically: : :”?

Response:
"Specifically" has been deleted in the revised version.

P15330, L19: Was there a reason for removing potassium? If so, where did the high background come from? For sure, it did not come from the gas phase. Did you use the high resolution data do check if m/z 39 really was potassium, and not for example C3H3+?

Response:
Surface ionization on the heated tungsten vaporizer can be a significant source of potassium. The sentence has been modified as below:

"... the total number of ions was calculated as the sum of all ion signals except m/z 14 (N^+), 15 (NH^+), 16 (NH_2^+), 17 (NH_3^+), 18 (H_2O^+), 28 (N_2^+), 32 (O_2^+) and 39 (K^+) either due to the strong interferences from air and instrument background (i.e. surface ionization on the tungsten vaporizer for K^+) or the noisy baseline of ammonium fragment ions."

P15331, L1-8: Again, c-means should be favored over k-means, especially for an atmospheric data where a distinct separation of different populations is very unlikely.

Response:
Please refer to the previous response.

P15331, L17: “A Clustering Analysis Panel was developed : : :”: This is “IGOR slang”. A reader not familiar with Wavemetrics IGOR Pro will not understand, what a panel is (in this context), or why it is worth mentioning. Please rephrase.

Response:
We agree with the reviewer that IGOR Pro has a built in k-means cluster analysis function. However, it is not designed for ambient single particle mass spectra so that the direct output cannot fit the specific needs of our application. The Cluster analysis panel used in our study is a template that can be used to analyze output from Sparrow and provide some output (for example, size distribution, time series, etc.) for presentation. Also, we wrote a function that can used to combine a few clusters to a single class. We understand the concern from the reviewer. We rephrased the sentence in Section 2.6 as following.

"A Cluster Analysis Panel (CAP) recently developed by our group was used to perform the built-in k-means clustering algorithm in IGOR Pro. The following information for each cluster can be directly generated by CAP:..."

P15332, L7-8: Why is the “collection efficiency” for uncoated Regal Black particles lower than for coated? Besides, I find the term “collection efficiency” not really suitable when used with the intracavity laser vaporizer. Wouldn’t “incandescence efficiency” be a better term?

Response:
Our group recently published a paper in Atmospheric Measurement Technique Discussions regarding the collection efficiency (CE) of ambient black carbon and laboratory generated Regal Black in SP-AMS (Willis et al. 2014). The heavily coated Regal Black has a more spherical particle morphology than bare Regal black. As a result, the coated Regal Black beam width is narrower than the bare one, resulting in larger overlap of the particle and laser beams. Since it has been discussed in our previous publication and is not the focus of this paper, we decide to refer the details to our previous publication. Also, the CE has been widely used in the AMS community and therefore we would like to keep this term in our paper.

Reference: Willis, M. D., Lee, A. K. Y., Onasch, T. B., Fortner, E. C., Williams, L. R., Lambe, A. T., Worsnop, D. R., and Abbatt, J. P. D., Collection efficiency of the soot-particle aerosol mass spectrometer (SP-AMS) for internally mixed particulate black carbon, Atmos. Meas. Tech. Discussion, 7, 5223-5249, 2014.

P15332, L21-24: Why are these observations by Onasch et al. mentioned, if the authors did not see anything alike (as mentioned before)?

Response:
The sentence has been changed as below. We did not have the similar observation but it is worth noting some recent literature highly relevant to this work.

"Fullerene type rBC spectral features (i.e., C_x^+ fragments with carbon number > 32) cannot be evaluated because their C_x^+ peaks are out of the m/z range (up to ~300) investigated in this study. Onasch et al. (2012) observed carbon cluster ions up to C_{82}^+ in laboratory generated ethylene flame soot particles and detected C_{32}^+ to C_{70}^+ that accounted for about 4% of the total rBC signals at an urban roadside environment."

P 15333, L1: Why is that? Are there only local sources for rBC, or are there any sinks? If so, what could these local sources be? Could it be that particles containing aged rBC are simply not vaporized by the laser (e.g., low black carbon content, high organic and inorganic content, low absorption at 1064 nm)?

Response:
Thanks for the comments. The sentence has been modified in the last paragraph of Section 3.1 to describe the possible local sources of rBC in our sampling location. Furthermore, our group recently reported that particles with 5 wt% of rBC can be vaporized and detected accurately by SP-AMS (Willis et al. 2014), supporting our argument regarding local sources as major contributors to the observed rBC.

"Since ambient rBC is only emitted from primary sources, this suggests that a significant portion of sampled rBC was freshly emitted or only slightly aged particles. This is consistent with the fact that vehicle emission are a major local source of rBC in the downtown area of Toronto."

P15334, L6, and Figure S4: The residual (of the PMF analysis) is quite high, especially in the first two days and at the end (10% and higher). Any explanation?

Response:
This is mainly because the aerosol loading is quite low during the first two days of our sampling period. This information has been added to the caption of Figure S7.

"Figure S7: Mass fraction contributions of each PMF factor (Blue: HOA, Red: COA, Orange: OOA, Grey: Residual) to the total organics from IR laser-off measurement. The relatively high residual for the first two days of our sampling period is mainly due to a low loading of organic aerosol."

P15334, L28: If there was significant particle bounce, why did the authors assume a

CE=1 for the tungsten vaporizer?

Response:

Thank you for pointing out the confusion concerning the CE issue. It is important that we present a clear discussion of CE. Figure S5 and corresponding calculation details have been added to the supplementary information to discuss the CE correction factors applied for different particle types based on our single particle observations. In brief, we assume inorganic species (internal mixtures of ammonium nitrate and ammonium sulfate) vaporized by the heated tungsten vaporizer have CE equal to 0.5, which is commonly applied for ambient aerosols. On the other hand, oil-like organic droplets (HOA and COA) dominated the total organic aerosol mass, and they are unlikely to have a significant particle bounce on the tungsten vaporizer surface. Therefore, we assume that the CE of the total organic aerosol equal to one and, furthermore, the total organic signal is likely dominated by vaporization from the tungsten vaporizer. However, OOA that is likely internally mixed with inorganics may have CE lower than unity from the heated tungsten vaporizer, and this adds a potential uncertainty. The CE for rBC vaporized by the laser is assumed to be 1, but it is actually highly uncertain as discussed in Willis et al (2014). However, due to the low mass loading of rBC, the calculation is not sensitive to the CE of rBC. The overall correlation between LS-SP-AMS, using the various CE's stated above, and SMPS-derived particle mass, assuming spherical particles, is close to 1, suggesting our assumptions on CE's are reasonable.

Sections 3.1, 3.3 and 3.4 have been modified accordingly to ensure all the discussion related to CE is consistent throughout the manuscript.

Reference: Willis, M. D., Lee, A. K. Y., Onasch, T. B., Fortner, E. C., Williams, L. R., Lambe, A. T., Worsnop, D. R., and Abbatt, J. P. D., Collection efficiency of the soot-particle aerosol mass spectrometer (SP-AMS) for internally mixed particulate black carbon, Atmos. Meas. Tech. Discussion, 7, 5223-5249, 2014.

P15335, L28: 75% in "laser on" mode, in "laser off" mode, or total?

Response:

To avoid confusion, the sentence has been revised as below:

"75% of them in both laser-on and laser-off mode were recognized as particle LS trigger events."

P15336, L13-15: How do the authors know that their light scattering system was more sensitive than the one used by Liu et al. (2012)?

Response:

Liu et al. (2012) reported that their LS laser was not well aligned. However, to avoid any confusion, the related sentence has been removed in the revised version.

P15336, L22-24: “: : : the single particle size distributions measured : : : are generally consistent with the ensemble PToF data (Fig. 2c).” This cannot be seen in this Figure.

Response:
Thanks for the comments. The sentence has been removed in the revised version.

P15337, L20-21: How should the laser vaporizer have bounce effects?

Response:
This sentence has been rewritten as below:

"The former is suggestive of potential bounce effects on the tungsten vaporizer and/or better ion transmission efficiency in the laser-on mode as discussed in Section 3.3; the latter, for particles smaller than 200 nm, is likely due to rBC particles dominating the ion signals (Figure S12b)."

P15337, L26ff: It would be helpful to mention why the twelve-cluster solution was selected.

Response:
More information has been provided in Section 3.5. Also, a few sentences were used to briefly describe the selection criteria (see Section 2.6 in the revised version).

"Increasing the number of clusters from 12 to 25 only gradually reduces the total Euclidian distance between the cluster centers and each single particle mass spectrum (Figure S4), and does not generate any new particles classes with significant physical meaning (i.e. determined by clusters re-combination as discussed in the next paragraph). Note that an rBC-rich particle class (see Section 3.5.2) can be clearly identified starting from the nine-cluster solution (up to twenty five-cluster solution). However, for the eleven-cluster solution, the rBC-rich particle class cannot be separated from OOA in the accumulation mode (i.e. dva peak at ~ 400 nm). Therefore, the twelve-cluster solution is considered as the optimal clustering solution."

Section 2.6: "All single particle mass spectra were normalized by their total ion signal, and solutions with up to 25 clusters were tested. Euclidian distance (the square root of the sum of the squares of the differences between corresponding values) was used to evaluate the total distance between the cluster centers and each single particle. In general, increasing the number of clusters can better represent the dataset mathematically (i.e., reduce the total distance) as shown in Figure S4. However, a very large number of clusters compromises the physical meaning of each cluster."

P15340, L17: What does low-range Dva, what mid-range Dva stand for?

Response:
As commented by other reviewers, we defined low-to-mid range aerodynamic diameter ranging from ~200-400 nm.

P15344, L8-9: As stated by the authors before, it could well be that they were not able to detect rBC in larger particles. Thus this statement should be modified.

Response:
Thanks for the reviewer's comment. The sentence has been revised in the last paragraph of Section 4.

"During our study, most of the rBC was likely freshly emitted from nearby vehicle exhaust and therefore we did not observe significant mixing, even though missing ion signals from small rBC cores in the aged particle types is also possible"

As suggested by another reviewer, we estimated the detection limit of a pure rBC single particle using 6 ions as a criterion and the mass-based ionization efficiency of Regal Black. The information has been added to last paragraph of Section 3.8.

"Using 6 ions as a detection limit of a single particle (i.e. a criteria for "prompt" particle type) and a mass-based ionization efficiency of Regal Black determined by calibration, it can be estimated that the detection limit of a pure rBC single particle is ~25 fg of rBC per particle."

Table 2: What are the uncertainties and errors of these values? Is a difference of 6.4% between "laser on" and "laser off" HOA significant at all?

Response:
We don't have a good estimation of uncertainties and errors of single particle counting. Even though the percentage difference is only a few percent for HOA type particles, the absolute number of HOA type particles in laser-on mode is 5 times higher than that in laser-off mode. Therefore, the difference between the two modes is significant.

Figure 2: Please hyphenate "laser on" and "laser off", or use it with quotes (throughout the manuscript).

Response:
Both terms have been hyphenated throughout the manuscript.

Figure S1: The sharp cut-off for "laser on" prompt particles should be explained either in the diagram or in the caption.

Response:
The shape cut-off for laser-on prompt particles in Figure S1b is due to the fact that we set the absolute total ion threshold at 6 ions. The similar cut-off is also observed for the case of laser-off mode as shown in Figure S1d.

Figure S2: Why did the authors select 12 clusters for their analysis? Is there a relation with the cluster distance? What is the purpose of this plot?

Response:
Similar to the above response, a few sentences have been modified or added in the main text (Section 3.5 and 2.6) to briefly explain the selection of 12 clusters in our analysis.

Anonymous Referee #4

Lee et al. describe a unique set of ambient particle measurements obtained with a soot particle aerosol mass spectrometer (SP-AMS) that was combined with a light scattering module to obtain the first light scattering single-particle (LSSP) SP-AMS measurements of the size and chemical composition of black carbon and non-black carbon containing particles. A few days of measurements of ambient aerosol in downtown Toronto are analyzed. These exemplary results and the associated data analysis method used provide a good illustration of this instrumental method's ability to assess the mixing state of black carbon containing particles, and also reveals some of the method's limitations. The single-particle data analysis is inherently complex, and the manuscript would benefit from some major revisions to clarify certain key aspects of the data analysis and interpretation of the results. Issues related to particle sizes measured were particularly unclear to me, as were changes in the ionization/collection efficiencies in the different analysis modes. This manuscript should be suitable for publication in ACP after the issues below are addressed. I am ambivalent as to whether this manuscript is more suitable for AMT or ACP; depending on the revisions it could be suitable for either journal.

Response:
Thanks for the overall comments on our manuscript. We have made major changes in the revised manuscript to make it more suitable for ACP. To improve the quality of this paper in terms of science and atmospheric relevance, two new sections (Section 3.6 and 3.7) and a few figures (Figure 9, 10, S15, S16 and S17) have been added to the revised version to have a more comprehensive discussion about the degree of mixing state of secondary species in the accumulation mode particles, and HOA and rBC in the two vehicle related particle types (i.e. HOA- and rBC rich particle classes). Given that the light scattering AMS and the SP-AMS have already been described in previous publications, this paper does not seem appropriate for AMT, with the focus more on the new science from the new measurements.

The measurable particle size ranges should be stated and discussed more upfront, and even mentioned in the abstract. The LS-AMS can typically only measure individual particles > _200-250 nm (Dva). Due to the fractal nature of soot and effective density effects, smaller vacuum aerodynamic diameter black carbon particles were measured here with the LS-SP-AMS. Can you impose any constraints on what the physical or other equivalent diameter of these BC particles detected may have been, perhaps by comparison to the SMPS data? It is important to clarify these particle size issues as fresh combustion-derived BC-containing particles are initially emitted at sizes well below 100 nm, especially for gasoline vehicles. If the LS-SP-AMS can only measure significantly larger BC particle sizes, it will have an inherent bias towards the more aged/coated BC particles, and against the fresh less coated BC. I realize this issue is difficult to constrain due to the complexities of particle effective density on the measure Dva, but some additional and earlier discussion of this important issue is warranted. The first paragraph on Page 15326 where the different types of AMS instruments are discussed would be a good place to bring in the particle size limitations. The AMS also typically measures only a few ions in single-particle mode, which also hampers the analysis.

Response:
The cut-size limitation of light scattering has been mentioned in the introduction.

"LS-ToF-AMS typically measure individual particles in ambient air with vacuum aerodynamic diameters (d_{va}) > 350 nm due to the lower sizing limit of the light scattering module (Cross et al. 2009, Freutel et al. 2013, Liu et al. 2013). It is crucial to investigate whether the LS-SP-AMS can detect fresh, less-coated rBC-containing particles derived from vehicle combustion, which are generally emitted at d_{va} well below the typical light scattering cut-off diameter (Massoli et al. 2012)."

Ellis et al. (2013) recently reported the unique application of the LS-AMS to study mixing of organic aerosol populations in a smog chamber. As this is one of the few other papers to use the LSSP mode of the AMS the authors should consult this paper and include any relevant discussion that relates to their analysis here.

Response:
The information about the single particle study by Ellis et al (2013) has been added to the introduction.

“Ellis et al. (2013) recently deployed LS-ToF-AMS to determine the mixing state of laboratory-generated organic aerosol in a smog chamber.”

The references to other single-particle mass spectrometry based paper come largely from one group (Greg Evans) at U. Toronto associated with these authors. A more complete discussion and references to other related SP-MS measurements should be provided. For example, there is a series of ATOFMS papers from Kim Prather’s group focused on vehicular and carbonaceous particle measurements (Cahill et al., 2012; Moffet and Prather, 2009; Shields et al., 2007, 2008; Sodeman et al., 2005; Toner et al., 2006, 2008).

Response:
Thanks for the important suggestion. The suggested references have been added to the introduction of revised version.

I do not agree with this statement: “Specifically, the application of positive matrix factorization (PMF) analysis to AMS measurements is well developed for source apportionment of organic aerosol and evaluation of aerosol aging.” (Page. 15326) The AMS induces extensive fragmentation precluding the true identification of the aerosol sources. This combined with the fact that the AMS only measures the non-refractory aerosol (except when the soot particle mode is used, of course) such that it cannot measure the primary particles makes it quite unable to truly do source apportionment on the complete aerosol. Also the PMF factorization typically only segregates the organic aerosol mass fraction, ignoring the inorganic components. Thus the PMF factors have more to do with the average chemical composition of different slices of the organic aerosol segregated based on their ion fragments. The factors obtained are typically associated with hydrocarbon-like (HOA) or oxygenated (OOA) organic aerosol, and thus do provide insight into “aerosol aging” as stated. While factors these have some connection to “sources” they are not really aerosol source profiles in the typical sense. COA, BBOA, and a marine OA factor, which are more closely related to the actual aerosol source, have also been retrieved in some cases. Considering these issues it is not accurate to say that PMF applied to AMS data can produce source apportionment. It is really a statistical analysis of the OA’s chemical composition, which /may/ indicate something about its sources.

Response:
Thanks for the reviewer's comments. The sentence has been changed as follow:

"Specifically, the application of positive matrix factorization (PMF) analysis to AMS measurements has been developed to provide information on possible sources of organic aerosol and the extent of aerosol aging"

Some discussion and justification of why k-means was used as the clustering algorithm is warranted. One issue with k-means is that the number of clusters must be prescribed. And it tends to more evenly distribute members throughout the clusters, and can thus miss small numbers of unique particle types. Reviewer #3 brought up c-means (fuzzy or non-exclusive clustering). While this can better reflect the mixed/evolving nature of atmospheric aerosol mixing state, a non-exclusive clustering can also complicate the analysis. How do you decide which particle belong to which clusters/classes, or do you never assign the particles to one class? An advantage of ART-2a is it finds the number of clusters required to sort the dataset at the prescribed vigilance factor, and thus provides a quantitative measure of the heterogeneity of the aerosol population. Rebotier and Prather (2007) have I believe the most extensive discussion and comparison of clustering methods for SP-MS data – please consult and cite this paper. While using k-means is fine, the authors should better justify their choice of 12 clusters to solve their dataset. Something was said about gaining little additional separation with higher cluster number, but what was lost when fewer than 12 clusters were used?

Similarly, in Sect. 3.5: While the use of more than 12 clusters is explained, why fewer than 12 clusters was not used to “solve” this dataset is not explained. Since the 12 cluster solution produces several quite similar clusters than are they manually regrouped, the authors should explain what happens when fewer than 12 clusters are used. Why is the 12 cluster solution considered optimal?

Response:
A sentence with the support of references (Rebotier and Prather, 2007, Giorio et al. 2012) has been added to the introduction and Section 2.8 to highlight the comparison between

k-means and other clustering algorithm from previous studies.

Introduction: “Previous studies have shown that k-means clustering can classify ambient particle types measured by ATOFMS in good agreement with other clustering algorithms such as ART-2a and hierarchical clustering (Rebotier and Prather, 2007, Giorio et al. 2012).”

Section 2.6: "It is worth noting that k-means clustering can classify ambient particles measured by ATOFMS into particle types that are highly consistent with other clustering algorithms such as ART-2a and hierarchical clustering (Rebotier and Prather, 2007, Giorio et al. 2012)."

More information has been provided in Section 3.5 to better explain the use of 12 clusters results. Also, a few sentences were used to briefly describe the selection criteria (see Section 2.6 in the revised version).

Section 3.5: "To demonstrate the capability of the LS-SP-AMS to investigate the mixing state of ambient aerosol particles, the twelve-cluster solution from the laser-on mode measurements is presented here. The number of particles and the ion fractions of nitrate, sulfate, organics and rBC in each cluster are shown in Figure S13. Increasing the number of clusters from 12 to 25 only gradually reduces the total Euclidian distance between the cluster centers and each single particle mass spectrum (Figure S4), and does not generate any new particles classes with significant physical meaning (i.e. determined by clusters re-combination as discussed in the next paragraph). Note that an rBC-rich particle class (see Section 3.5.2) can be clearly identified starting from the nine-cluster solution (up to twenty five-cluster solution). However, for the eleven-cluster solution, the rBC-rich particle class cannot be separated from OOA in the accumulation mode (i.e. dva peak at ~ 400 nm). Therefore, the twelve-cluster solution is considered as the optimal clustering solution."

Section 2.6: "All single particle mass spectra were normalized by their total ion signal, and solutions with up to 25 clusters were tested. Euclidian distance (the square root of the sum of the squares of the differences between corresponding values) was used to evaluate the total distance between the cluster centers and each single particle. In general, increasing the number of clusters can better represent the dataset mathematically (i.e., reduce the total distance) as shown in Figure S4. However, a very large number of clusters compromises the physical meaning of each cluster."

A note on terminology. For SP-MS data, when similar clusters are manually combined or “regrouped” into one group this is often referred to as a particle “class”. For this dataset there would be a nitrate class, rBC class, etc. The authors might adopt this terminology for consistency, and to distinguish between classes and clusters.

Response:

Thanks for the reviewer's comment. The terminology has been changed to describe the clustering results after combining clusters.

Appropriate black carbon calibrant standards remain an issue, for both the SP-AMS and SP2. More justification to support the use of Regal Black to calibrate the SPAMS's response to ambient combustion-derived particles should be provided. While the spectra do appear similar, it is a bit hard to believe that printer toner ink really simulates combustion soot.

Response:
We agree with the reviewer that calibration standards of BC can be an issue and it should be further investigated in the future. Regal Black is a recommended rBC standard based on a study of SP-AMS development (Onasch et al. 2012) and has been widely used within the SP-AMS community. Since the focus of this paper is not to describe the details of the SP-AMS development, we decide to modify a related sentence as below:

"Similarly, a water suspension of Regal Black (Regal 400R Pigment Black, Cabot Corp., a calibration standard recommended by Onasch et al. 2012) was atomized to generate standard BC particles."

Reference: Onasch, T. B., Trimborn, A., Fortner, E. C., Jayne, J. T., Kok, G. L., Williams, L. R., Davidovits, P. and Worsnop, D. R.: Soot Particle Aerosol Mass Spectrometer: Development, Validation, and Initial Application, Aerosol Sci. Technol., 46, 804-817, 2012.

This sentence is a real mouthful (page 15328): "The product of density and shape factor, derived from the ratio of the vacuum aerodynamic diameter (dva) measured by the PToF mode of the SP-AMS to the mobility diameter (dm) determined by the DMA (DeCarlo et al., 2004): : :". Can you reword so the meaning is clearer?

Response:
The sentence has been revised as follow:

"The product of density and shape factor of the dried 300 nm Regal Black particles is ~0.8 g/cm^3, which is derived from the ratio of the vacuum aerodynamic diameter (d_{va}) measured by the PToF mode of the LS-SP-AMS to the mobility diameter (d_m) determined by the DMA (DeCarlo et al. 2004) as follows:"

Do the RIEs of the various components measured not change with the IR laser is used? Was this tested?

Response:
This is a good question. The RIEs of NR-PM do change if they are evaporated from the

rBC surface. We mention a few possibilities in Section 3.3 and it is an issue that should be investigated in the future. To make this message clear, a sentence in Section 3.3 has been modified.

"(2) Particle vaporization by the IR laser and the tungsten vaporizer do not occur at exactly the same location inside the ion chamber, possibly resulting in different ionization rates and ion transmission efficiencies (i.e., from the ion chamber to the ion focusing optics) between the two operational modes. This difference may also be a reason for the observed enhancements in the RIE of NR-PM evaporated from rBC particles."

Section. 2.2. The light scattering module's cut-off size should really be characterized with particles more appropriate to these ambient BC measurements than ammonium nitrate aerosol. Some speculation about the cut off size for hydrocarbon oil droplets is given but these were not actually measured. Why not? Some attempt to also determine the cut-off LS detection size for size-selected black carbon particles should have also been made, though I realize the fractal particle shape would complicate this.

Response:
We agree with the reviewer that it would be ideal to have other particle types for determining the LS cut-off diameter of our instrument. Unfortunately, our instrument is in a new configuration and the data acquisition algorithm does not allow us to perform such testing. Nevertheless, it is worth noting that our estimation of cut-off size for oil-like particles (i.e. HOA and COA) matches well with the shape of ambient single particle size distribution.

Why was the K+ signal at m/z 39 excluded from the clustering analysis? This is a useful marker for biomass-combustion derived particles. While it seems likely that most of the combustion particles detected here were vehicular, it can be quite useful to include markers such as K+ in the analysis.

Response:
Surface ionization of heated thermal vaporizer can be a significant source of potassium in AMS. Therefore, K^+ is removed in our analysis in this study. However, we agree with the reviewer that K^+ is an important tracer for biomass burning. In another urban study, we observed a much higher K^+ signal during biomass burning influence period compared to the instrumental background. This will be discussed in our future publication. To provide this information, a sentence has been modified in the revised manuscript.

"... the total number of ions was calculated as the sum of all ion signals except m/z 14 (N^+), 15 (NH^+), 16 (NH_2^+), 17 (NH_3^+), 18 (H_2O^+), 28 (N_2^+), 32 (O_2^+) and 39 (K^+) either due to the strong interferences from air and instrument background (i.e. surface ionization on the tungsten vaporizer for K^+) or the noisy baseline of ammonium fragment ions."

Similarly, no mention of metals detected from the laser on mode of the SP-AMS analysis is given. Metals may be present in traffic-dominated aerosol from brake dust, or calcium from lubricating oil, for example. There has been some discussion of the SPAMS being able to detect metals that the normal mode of the AMS would not detect as they do not evaporate at 600 C. Were metals detected in these measurements? It seems like metals were not detected looking at the spectra. Any discussion the authors can add to the paper about what they have determined for the SP-AMS's ability to measure metals in PM would be valuable. Dallmann et al. (2014) recently reported SP-AMS measurements of vehicular combustion aerosol, and did detect trace metals such as zinc and phosphorous.

Response:
We agree that the SP-AMS has great potential to detect trace metals in the particle phase and we believe that this is an important area to explore in the future. To highlight this information, the following sentences have been added to Section 3.1.

"Furthermore, Dallmann et al. (2014) have demonstrated the capability of the SP-AMS to detect trace metals such as zinc in on-road gasoline and diesel vehicles emissions. However, no trace metals were clearly observed in this study."

Section 3.1. The authors should make it clear that this and the following sections discuss results only from the ensemble (not single-particle mode) measurements. While the section title does say "ensemble measurements", it took me awhile to realize that this was not discussing single-particle data, since the rest of the paper had thus far focused on single-particle measurements. A disclaimer at the beginning of the section's text would help clarify this.

Response:
Thanks for the suggestion. A short paragraph has been added at the beginning of Section 3.

"The results and discussion section is divided into two main parts. The first part (Section 3.1-3.3) presents the observations from SP-AMS ensemble aerosol mesurements and PMF analysis of the organic components. The second part (Section 3.4-3.9) focuses on identification of particle types and characterizing the mixing state of carbonaceous aerosols based on cluster analysis of LS-SP-AMS single particle measurements."

Much of the discussion of the results would be greatly improved if the size range of the reported measurements was stated. For example, "In general, organics dominated the particulate mass, whereas rBC contributed 5–8 % of the average particle mass: : :" (page 15332, line 5). For what size range do these mass measurements refer to? Starting on line 25 some discussion of the sizes measured for NR-PM and rBC is given. It would be very useful if the typical measurable size ranges for these two aerosol types was provided in a clear summary statement early in the results. Also make it clear if the measurable size range from LSSP mode differs from the ensemble measurements. The authors need to make the instrument's measurement capabilities much more clear. What was it capable of measuring reliably, and what did it likely not measure?

Response:

The measurable size range of single particle data has been discussed in Section 3.4. In particular, a few particle types which show different light scattering cut-off diameters have been discussed in the original manuscript. To make it clear, a sentence has been added at the beginning of results and discussion section.

"Note that the ensemble measurements detect particles with d_{va} starting from ~50 nm and up to ~1 µm, whereas the single particle measurements only detect particles greater than 200 nm d_{va} (the LS cut-off diameter for different particle types will the discussed in Section 3.4)."

How is assuming that the collection efficiency for all NR-PM evaporated from the tungsten vaporizer is equal to 1 justified? (Page 15332, line 9) CE is typically _0.5 for ambient aerosol, but can experience significant variations with changing PM composition. This statement really confuses me.

Response:

Thank you for pointing out the confusion concerning the CE issue. It is important that we present a clear discussion of CE. Figure S5 and corresponding calculation details have been added to the supplementary information to discuss the CE correction factors applied for different particle types based on our single particle observations. In brief, we assume inorganic species (internal mixtures of ammonium nitrate and ammonium sulfate) vaporized by the heated tungsten vaporizer have CE equal to 0.5, which is commonly applied for ambient aerosols. On the other hand, oil-like organic droplets (HOA and COA) dominated the total organic aerosol mass, and they are unlikely to have a significant particle bounce on the tungsten vaporizer surface. Therefore, we assume that the CE of the total organic aerosol equal to one and, furthermore, the total organic signal is likely dominated by vaporization from the tungsten vaporizer. However, OOA that is likely internally mixed with inorganics may have CE lower than unity from the heated tungsten vaporizer, and this adds a potential uncertainty. The CE for rBC vaporized by the laser is assumed to be 1, but it is actually highly uncertain as discussed in Willis et al (2014). However, due to the low mass loading of rBC, the calculation is not sensitive to the CE of rBC. The overall correlation between LS-SP-AMS, using the various CE's stated above, and SMPS-derived particle mass, assuming spherical particles, is close to 1, suggesting our assumptions on CE's are reasonable.

Sections 3.1, 3.3 and 3.4 have been modified accordingly to ensure all the discussion related to CE is consistent throughout the manuscript.

Reference: Willis, M. D., Lee, A. K. Y., Onasch, T. B., Fortner, E. C., Williams, L. R., Lambe, A. T., Worsnop, D. R., and Abbatt, J. P. D., Collection efficiency of the soot-particle aerosol mass spectrometer (SP-AMS) for internally mixed particulate black carbon, Atmos. Meas. Tech. Discussion, 7, 5223-5249, 2014.

Page 15333, line 4: To be accurate and consistent, better to say that m/z 44 is a tracer for oxidized OA (OOA), rather than of SOA.

Response:
The suggested change has been made.

Page 15334, line 19: “Based on the PMF analysis, the rBC associated with HOA, COA and OOA accounted for: : :”. What does “associated” mean here? Correlated with, or the mass of rBC in each of those PMF factors?

Response:
The sentence has been changed.

"Based on the PMF analysis, the rBC mass in HOA, COA and OOA factors accounted for about 51% (±20%), 9% (±11%) and 40% (±18%), respectively, of the total rBC mass loading on average (± standard deviation)."

Sect. 3.3. “The IR laser on mode exhibited a higher sensitivity to all NR-PM components than 25 the IR laser off mode by _ 10–20 %”. This goes back to my earlier question regarding how the IE changes with the laser on versus off. It seems that this “higher sensitivity” might be explained by changes in IE in addition to changes in CE, but this is difficult to tease out from the text here as the term ionization efficiency is not actually stated. Please clarify this section. Page 15336, line 8: “a higher mass spectral sensitivity in the laser on mode as described in Sect. 3.3.”. As discussed above, this important effect was not actually described very well in Sect. 3.3.

Response:
Similar to our previous response. We think that the RIE of NR-PM would be enhanced if it is evaporated from rBC surface. We mention this possibility in Section 3.3 and this is something to be investigated in the future. To make this message clear, a sentence in Section 3.3 has been modified.

"(2) Particle vaporization by the IR laser and the tungsten vaporizer do not occur at exactly the same location inside the ion chamber, possibly resulting in different ionization rates and ion transmission efficiencies (i.e., from the ion chamber to the ion focusing optics) between the two operational modes. This difference may also be a reason for the observed enhancements in the RIE of NR-PM evaporated from rBC particles."

Page 15334, line 30: “particle bounce issues for tungsten vaporizers” is mentioned, which goes back to my earlier question about the CE for NR-PM being assumed to be 1, when it is known that the CE is variable and less than 1 for ambient PM. Please explain the earlier assumption of CE = 1.

Response:
Please refer to the above response regarding CE issue. Sections 3.1, 3.3 and 3.4 have been modified accordingly to ensure all the discussion related to CE is consistent throughout the manuscript.

Page 15335, line 18: “This is indirect evidence that a larger fraction of HOA material was internally mixed with rBC compared to the COA and OOA components.” This sentence was part of my original confusion in reading this section, as it wasn’t immediately clear that the ensemble measurements were being discussed. The authors might add a sentence here stating that the direct measurements of mixing state from the single particle data will be discussed in the following section, so the connection is clear.

Response:
Thanks for the comments. A sentence has been added to the end of Section 3.3.

"The direct measurements of mixing state from the single particle data will be discussed in the following sections."

Page 15338, line 17: “Note that the overall clustering analysis results for NR-PM are quite similar for both the IR laser on and off data sets.” Could the authors add some brief discussion of the implications of this finding? As this is a very new type of analysis I don’t think it will be clear to most readers. It could also suggest that little additional data is collected using the SP laser, but I do not think that is true. Would be good to clarify what additional data the IR laser on mode provides even if the clusters are similar.

Response:
Thanks for the suggestions. The sentence has been extended and moved to the beginning of this section to better highlight the difference between laser on and laser off mode clustering results.

"The overall cluster analysis results for NR-PM are similar for both the IR laser-on and off datasets, with the primary exception being an additional particle class, rBC, obtained from the laser-on mode single particle data. The major NR-PM particle classes obtained via independent cluster analysis for both datasets included nitrate, sulfate, HOA, COA, and 2 types of OOA (Figure 8). These particle classes represented similar particle number fractions and time series, and differed only slightly in average mass spectra (not shown)."

Page 15339, line 9: Should be “HOA-rich particles are largely externally mixed /from/ inorganic species: : :”

Response:
Based on the suggestion by another reviewer, the sentence has been revised as below.

"Most of the HOA-rich particles do not contain any inorganic species (Figure 8c and 8j)."

Sect. 3.6. I find the term “low to mid-range dva particles” really confusing and meaningless. Can you please just state the actual size range being discussed?

Response:
As commented by other reviewers, we define low-to-mid range aerodynamic diameter ranging from ~200-400 nm.

Sect. 3.6: Nothing is said here about what the LS-SP-AMS actually determined regarding the mixing state of rBC with HOA and other components, which I thought was a major point of this paper. Please summarize these findings here.

Response:
We agree with the reviewers that we need to extend the discussion about the mixing state of rBC and HOA in more detail. Section 3.7 and Figures 10, S16 and S17 have been added to the revised version. Furthermore, as suggested by reviewer 1, Section 3.6 and Figure 9 and S15 have been added to discuss the mixing state of secondary aerosol species in accumulation mode particles.

“This suggests that the HOA-rich particles were likely associated with small rBC cores.” This seems like an important, though not concrete finding that warrants more than one sentence of discussion.

Response:
Similar to the above response, Section 3.7 and a few figures have been added to the revised version to discuss the mixing state of rBC and HOA. Moreover, a simple core-shell structure model has been applied to estimate organic coating thickness on rBC particles in Section 3.8 (see details in later response)

“a significant portion of HOA- and COA-rich particles (> 90 %) with particle dva larger than _ 200 nm did not contain a detectable amount of rBC, i.e., the particles can be thought of containing a small rBC core with a thick HOA coating: : :” Couldn’t these particles also just have had no rBC?

Response:
The sentence has been modified in Section 3.8.

"(1) a significant portion of HOA- and COA-rich particles (> 90%) with particle d_{va} larger than ~200 nm did not contain a detectable amount of rBC, e.g., organic-rich particles containing a small rBC core or no rBC (with a mass contribution of rBC to the HOA- and COA-rich classes about 3% on average),..."

A lot of discussion of thinly coated rBC particles is given here in Sect. 3.6. Can you put any constrains on just how thin these coatings were that would explain your results for the average _28 wt% of HOA on the typical range of rBc core sizes?

Response:
Thanks for the comments. The estimation of coating thickness based on a simple core-shell spherical structure and uniform coating thickness has been done in Section 3.8.

"(2) the rBC-rich particles were mixed with ~28 wt% HOA-like material on average, e.g., a thinly HOA coated rBC particle, assuming uniform coating thickness. For example, applying a simple core-shell spherical structure (i.e. rBC core plus uniform HOA coating), a 200 nm d_{va} rBC-rich particle has a coating thickness of ~10 nm with HOA and rBC densities equal to 0.9 and 0.8 g/cm^3, respectively."

“We cannot rule out that the SP-AMS is missing ion signals from small rBC cores”. Any constraints on how small an rBc core has to be to go undetected?

Response:
The single particle detection limit of a pure rBC particle is estimated and the information has been added in the last paragraph of Section 3.8.

"Using 6 ions as a detection limit of a single particle (i.e. a criteria for “prompt” particle type) and a mass-based ionization efficiency of Regal Black determined by calibration, it can be estimated that the detection limit of a pure rBC single particle is ~25 fg of rBC per particle."

Sect. 3.7. It is important to make it clear that the LS-SP-AMS provides a rather selective lens for determining aerosol mixing state. As it cannot detect many potentially important primary aerosol components, the mixing state measurements obtained are rather skewed from the real total mixing state. This is not to say that the LS-SP-AMS measurements are not valuable, but the limitations should be made clear, especially to a non-expert reader.

Response:
Thanks for the comments. A sentence has been added to the first paragraph of Section 4 to highlight the limitation of single particle measurements by LS-SP-AMS.

"That being said, it is important to note that because the LS-SP-AMS may not be able to detect certain primary aerosol components, such as mineral dust, and non-IR absorbing refractory PM, and therefore the mixing state measurements obtained may not reflect the mixing state of the entire aerosol population."

Sect. 4. The summary has a lot of valuable and interesting discussion. While it is a summary, it would benefit from some expansion. For example, this deserves elaboration, as I don't think it was clearly explained earlier in the paper: "While it is recognized that HOA factors, identified by PMF analysis of standard HR-ToF-AMS data, and rBC originate from combustion sources, the mixing states of these primary aerosol species cannot be easily characterized in this manner." And again, a more quantitative measure than "thinly" and "thickly" coated particles would really increase the scientific value of these results.

Response:
The following information has been added to further elaborate that PMF analysis of ensemble measurements can only provide information to evaluate the potential sources and aging of organic aerosol but not mixing state without the support of measurements in single particle basis.

"PMF analysis of ensemble measurements can provide information to evaluate the potential sources and aging of organic aerosol. While it is recognized that HOA factors, identified by PMF analysis of standard HR-ToF-AMS data, and rBC originate from combustion sources, the mixing states of these primary aerosol species cannot be easily characterized in this manner without the support of single particle measurement."

We agree that a more quantitative measure of coating thickness would be valuable. Please refer to the previous response to the comments about the estimation of organic coating thickness. The information has been added to Section 3.8.

"The single particle data also provide insight to the sources of low to mid-range dva organics in a typical urban environment. According to our clustering analysis, those organics are mainly composed of HOA- and COA-rich particles emitted from primary sources such as vehicle exhaust and kitchen emissions instead of processed particles associated with condensed secondary materials." Please clarify if these "low-to-mid range dva organics" (and use a more specific description of their size) were or were not mixed with rBC, or if you could not reliably determine this.

Response:
The additional information has been added to the revised sentence.

"The single particle data also provide insight to the sources of low to mid-range d_{va} organics (~200-400 nm) in a typical urban environment. According to our cluster analysis, those organics are mainly composed of HOA- and COA-rich particles (with rBC content about 3% on average) emitted from primary sources such as vehicle exhaust and kitchen emissions instead of processed particles associated with condensed secondary materials."

Table 2 is a nice way to present this data.

Response:
Thanks for the reviewer's encouraging comments.

Fig. 2: The figure legend could be clarified. I believe the data from the laser on and off modes is combined here, but this is not clearly stated.

Response:
This information has been clearly stated in the caption of Figure 2.

"Figure 2: Summary of ensemble measurements (a) Time series (local time) of laser-off (Org, NO_3, SO_4, NH_4) and laser-on (rBC) aerosol compositions. (b) The average mass spectrum of laser-on ambient rBC and Regal Black (insert). (c) Average size distributions of laser-off (Org, NO_3, SO_4, Org44) and laser-on (rBC) aerosol compositions. Org 44 represents organic signal at m/z 44 (e.g., CO_2^+).

Fig. 3: I think this figure would be easier to interpret if C from OA was in green while C from rBC was in black. That will make the difference from laser on vs off more obvious.

Response:
Thanks for the suggestions. We prefer to keep the original color scheme because it is not straightforward to differentiate whether the C atom from OA or rBC for the laser on data set.

Fig. 5: Again, the LS cut-off detection size should really be measured using aerosol more appropriate to the combustion and OA focus of these measurements.

Response:
We agree with the reviewer that it would be ideal to have other particle types for determining the LS cut-off diameter of our instrument. Unfortunately, our instrument is in a new configuration and the data acquisition algorithm does not allow us to perform such testing. Nevertheless, it is worth noting that our estimation of cut-off size for oil-like particles (i.e. HOA and COA) matches well with the shape of ambient single particle size distribution.

Fig. 6: Are all these spectra from ambient data? The caption does not specify. Is a presumably "fresh" BC particle with almost no coating and dva = 549 nm realistic for ambient combustion aerosol? That seems huge for fresh vehicular soot, unless the effective density can explain such a large dva for a fresh combustion particle.

Response:
The three examples are ambient data. The caption of Figure 6 has been changed as below. The black carbon with almost no coating (in panel a) is only an example of this particle types. In Figure 8, it can be found that most of the particles classified to the rBC classes have a relatively small dva (peak at ~200 nm).

"Figure 6: Examples of single particle mass spectra of rBC-containing particles in ambient air:..."

Fig. 8: As suggested earlier, I would call these "classes" rather than "clusters", since they are produced by manually regrouping some k-means clusters into particle type classes.

The figure caption should specify that these classes come from k-means clustering applied to LS-SP-AMS single-particle data. A better way to display the richness of single-particle mass spectra is using a "digital color stack". This is basically a combination of the spectra in the left and middle panels, where the height of the bar represents the fraction of particles in that cluster/class that had that ion, while the color stack at each m/z displays the ion peak area measured for that fraction of particles. For example, see Figure 1 in Sullivan et al. (2007).

Response:
The "clusters" have been changed to "classes" in Figure 8. The caption of Figure 8 has been revised as below:

"Figure 8: Normalized mass spectra (left column), normalized histograms displaying the relative frequency of each m/z (middle column), and size distributions (right column) of different particle classes identified from k-means clustering of LS-SP-AMS single particle dataset (laser on)..."

Thanks for the suggestions about modifying Figure 8. However, we decide to keep the current format as the color scheme (blue: nitrate, red: sulfate, green: organics and black: rBC) used in the right column helps the reader to identify the aerosol chemical composition in each particle classes.

Cited References

Cahill, J. F., Suski, K., Seinfeld, J. H., Zaveri, R. a. and Prather, K. a.: The mixing state of carbonaceous aerosol particles in northern and southern California measured during CARES and CalNex 2010, Atmos. Chem. Phys., 12(22), 10989–11002, doi:10.5194/acp-12-10989-2012, 2012.

Dallmann, T. R., Onasch, T. B., Kirchstetter, T. W., Worton, D. R., Fortner, E. C., Herndon, S. C., Wood, E. C., Franklin, J. P., Worsnop, D. R., Goldstein, A. H. and

Harley, R. A.: Characterization of particulate matter emissions from on-road gasoline and diesel vehicles using a soot particle aerosol mass spectrometer, Atmos. Chem. Phys., 14(14), 7585–7599, doi:10.5194/acp-14-7585-2014, 2014.

Moffet, R. C. and Prather, K. A.: In-situ measurements of the mixing state and optical properties of soot with implications for radiative forcing estimates, Proc. Natl. Acad. Sci., 106(29), 11872–11877, 2009.

Rebotier, T. P. and Prather, K. A.: Aerosol time-of-flight mass spectrometry data analysis: a benchmark of clustering algorithms., Anal. Chim. Acta, 585(1), 38–54, doi:10.1016/j.aca.2006.12.009, 2007.

Robinson, E. S., Saleh, R. and Donahue, N. M.: Organic aerosol mixing observed by single-particle mass spectrometry., J. Phys. Chem. A, 117(51), 13935–45, doi:10.1021/jp405789t, 2013.

Shields, L. G., Qin, X. Y., Toner, S. M. and Prather, K. A.: Detection of ambient ultrafine aerosols by single particle techniques during the SOAR 2005 campaign, Aerosol Sci. Technol., 42(8), 674–684, doi:10.1080/02786820802227378, 2008.

Shields, L. G., Suess, D. T. and Prather, K. A.: Determination of single particle mass spectral signatures from heavy-duty diesel vehicle emissions for PM2.5 source apportionment, Atmos. Environ., 41(18), 3841–3852, 2007.

Sodeman, D. A., Toner, S. M. and Prather, K. A.: Determination of single particle mass spectral signatures from light-duty vehicle emissions, Environ. Sci. Technol., 39(12), 4569–4580, 2005.

Sullivan, R. C., Guazzotti, S. A., Sodeman, D. A. and Prather, K. A.: Direct observations of the atmospheric processing of Asian mineral dust, Atmos. Chem. Phys., 7, 1213–1226, 2007.

Toner, S. M., Shields, L. G., Sodeman, D. A. and Prather, K. A.: Using mass spectral source signatures to apportion exhaust particles from gasoline and diesel powered vehicles in a freeway study using UF-ATOFMS, Atmos. Environ., 42(3), 568–581, 2008.

Toner, S. M., Sodeman, D. A. and Prather, K. A.: Single particle characterization of ultrafine and accumulation mode particles from heavy duty diesel vehicles using aerosol time-of-flight mass spectrometry, Environ. Sci. Technol., 40(12), 3912–3921, 2006.

Mixing state of carbonaceous aerosol in an urban environment: single particle characterization using the soot particle aerosol mass spectrometer (SP-AMS)

A. K. Y. Lee[1], M. D. Willis[1], R. M. Healy[2,3], T.B. Onasch[4], J. P. D. Abbatt[1]

[1] {Department of Chemistry, University of Toronto, Toronto, Canada}

[2] {Department of Chemistry and Environmental Research Institute, University College Cork, Ireland}

[3] {Southern Ontario Centre for Atmospheric Aerosol Research, University of Toronto, Toronto, Canada}

[4] {Aerodyne Research, Inc., Billerica, Massachusetts, USA}

Correspondence to: A.K.Y. Lee (klee@chem.utoronto.ca)

Abstract

Understanding the impact of atmospheric black carbon (BC) containing particles on human health and radiative forcing requires knowledge of the mixing state of BC, including the characteristics of the materials with which it is internally mixed. In this study, we examine the mixing state of refractory BC (rBC) and other aerosol components in an urban environment (downtown Toronto) utilizing the Aerodyne Soot-Particle Aerosol Mass Spectrometer equipped with a light scattering module (LS-SP-AMS).. K-means cluster analysis was used to classify single particle mass spectra into chemically distinct groups. One resultant particle class is dominated by rBC mass spectral signals (C_1^+ to C_5^+) while the organic signals fall into a few major particle classes, identified as hydrocarbon-like organic aerosol (HOA), oxygenated organic aerosol (OOA), and cooking emission organic aerosol (COA). A gradual mixing is observed with small rBC particles only thinly coated by HOA (~28% by mass on average), while over 90% of the HOA-rich particles did not contain detectable amounts of rBC. Most of the particles classified into other inorganic and organic particle classes were not significantly associated with rBC. The single particle results also suggest that HOA and COA emitted from anthropogenic sources were likely major contributors to organic-rich particles with vacuum aerodynamic

diameter (d_{va},) ranging from ~200-400 nm. The similar temporal profiles and mass spectral features of the organic classes identified by cluster analysis and the factors from a positive matrix factorization (PMF) analysis of the ensemble aerosol dataset validate the interpretation of the PMF results.

1 Introduction

Atmospheric black carbon (BC) particles play an important role in regional air quality and introduce large uncertainties into radiative forcing estimates of the Earth's atmosphere (Bond et al. 2013). Fossil fuel combustion and biomass burning are the primary sources of ambient BC. Coatings on BC aerosol surfaces with varying morphology (e.g. partly coated and embedded) and thickness have been observed using electron microscopy (China et al. 2013, 2014). These coatings can be formed through condensation and coagulation of low-volatility materials co-emitted from combustion sources (e.g., unburned organics) and produced via photochemical processing during transport. Current research is evaluating whether particle coatings can significantly enhance the light absorption efficiency of ambient BC (Cappa et al. 2012, Jacobson 2001, Lack et al. 2012, Metcalf et al. 2013). Also, coating materials can modify the hygroscopicity and/or the cloud activation of BC particles, thus affecting their atmospheric lifetime (McMeeking et al. 2011, Tritscher et al. 2011, Wang et al. 2010, Zhang et al. 2008). Improving our understanding of the mixing state of BC and the characteristics of its associated coatings is crucial to evaluate the fate and environmental impacts of ambient BC.

Real-time quantitative single particle detection (i.e. number concentrations, size distributions and chemical composition by mass in a single particle basis) is necessary to determine the mixing state of ambient particles. In particular, the single particle soot photometer (SP2, DMT, Inc.) has been developed to quantify refractory BC (rBC) using single particle incandescence signals (Baumgardner et al. 2004, Stephens et al. 2003). Combining both optical scattering and incandescence signals, the SP2 has been used to evaluate the degree of mixing (internal vs. external) and estimate the coating thickness of BC particles in both field and laboratory studies (e.g., Metcalf et al. 2013, Moteki and Kondo 2007, Schwarz et al. 2006, Shiraiwa et al. 2007, 2010). However, this instrument cannot characterize the chemical composition of the coating materials. Single particle mass spectrometry utilizing laser desorption/ionization methods such as the aerosol time-of-flight mass spectrometer (ATOFMS, TSI, Inc.) or particle analysis by laser mass spectrometry (PALMS) are powerful techniques, which provide rich size-resolved chemical information to examine the mixing state of both refractory (e.g., dust and BC) and non-refractory components in ambient particles (Pratt and Prather 2012 and references therein). In particular, Prather and co-workers have undertaken a series of ATOFMS studies focused on vehicular and carbonaceous particle measurements (Cahill et al., 2012; Moffet and Prather, 2009; Shields et al., 2007, 2008; Sodeman et al., 2005; Toner et al., 2006, 2008). However, these single particle mass spectrometry techniques are number concentration-based methods and the associated pulsed laser desorption and ionization process makes particle mass quantification challenging (Pratt and Prather 2012).

The Aerodyne Aerosol Mass Spectrometer (AMS, Aerodyne Research Inc.) separates the particle vaporization and ionization steps to make quantification of particulate mass possible, with different versions of the AMS deployed to measure mass concentrations and mass-size distributions of non-refractory particulate matter (NR-PM) (e.g., Canagaratna et al. 2007, Drewnick et al. 2005, Jayne et al. 2000, Jimenez et al. 2009, Ng et al. 2010, Zhang et al. 2007). Specifically, the application of positive matrix factorization (PMF) analysis to AMS measurements has been developed to provide information on possible sources of organic aerosol and the extent of aerosol aging (Lanz et al. 2007, Ng et al. 2010, Ulbrich et al. 2009, Zhang et al. 2011). A few previous studies have demonstrated that a time-of-flight AMS in conjunction with a light scattering module (LS-ToF-AMS) can be used to characterize ambient particles on a single particle basis, which allows investigation of the mixing state of NR-PM in ambient (Cross et al. 2009, Freutel et al. 2013, Liu et al. 2013). Different particle categorization approaches have been developed to analyze single particle datasets from the LS-ToF-AMS, including principle component analysis (Cross et al. 2009), k-means cluster analysis (Liu et al. 2013) and a classification algorithm based on comparison with reference mass spectra (Freutel et al. 2013). Ellis et al. (2013) recently deployed the LS-ToF-AMS to determine the mixing state of laboratory-generated organic aerosol in a smog chamber. However, the LS-ToF-AMS is only able to detect non-refractory aerosol species that flash vaporize at ~600°C.

The utility of the AMS was recently extended by development of the Soot-Particle Aerosol Mass Spectrometer (SP-AMS), which is able to quantify and characterize rBC (i.e. C_x fragmentation pattern and surface functionality) and NR-PM simultaneously (Cross et al. 2010, Onasch et al. 2012, Corbin et al. 2014). An infrared (IR) laser vaporizer has been incorporated into the standard high resolution time-of-flight AMS (HR-ToF-AMS) to facilitate the detection of rBC components and associated coating materials. Incorporation of the light scattering module into the SP-AMS (LS-SP-AMS) allows the instrument to detect both rBC and NR-PM on a single particle basis. Thus, this technique enables the characterization of the mixing state of ambient carbonaceous particles, including rBC-containing, while simultaneously measuring the average size-resolved chemical compositions and mass loadings of the ensemble aerosol. However, LS-ToF-AMS typically measure individual particles in ambient air with vacuum aerodynamic diameters (d_{va}) > 350 nm due to the lower sizing limit of the light scattering module (Cross et al. 2009, Freutel et al. 2013, Liu et al. 2013). It is crucial to investigate whether the LS-SP-AMS can detect fresh, less-coated rBC-containing particles derived from vehicle combustion, which are generally emitted at d_{va} well below the typical light scattering cut-off diameter (Massoli et al. 2012).

The primary objective of this study is to investigate the mixing state of ambient rBC-containing particles in an urban environment utilizing the single particle capabilities of the LS-SP-AMS. Cluster analysis using the k-means algorithm, which has been widely applied to analyze ATOFMS data, is performed to classify mass spectra from ambient single particles. Previous studies have shown that k-means clustering can classify ambient particle types measured by ATOFMS in good agreement with other clustering algorithms such as ART-2a and hierarchical clustering (Rebotier and Prather, 2007, Giorio et al. 2012). The clustering results are used to evaluate the mixing state of ambient particles measured in downtown Toronto and to validate the interpretation of factors from PMF analysis of simultaneously obtained LS-SP-AMS ensemble measurement data.

2 Experiment

2.1 Sampling location and instruments

An Aerodyne soot particle aerosol mass spectrometer (Aerodyne Research Inc.) equipped with light scattering module (LS-SP-AMS) was deployed to measure both NR-PM (i.e., ammonium, nitrate, sulfate and organic) and rBC of the ensemble aerosol and for single particles. A co-located scanning mobility particle sizer (SMPS; TSI Inc., model 3936L76) was used to measure ambient particle number concentrations and size distributions. The SMPS was set to scan every 4 min. The sheath-to-aerosol flow ratio was held at 10:1.

The urban sampling site was located at the St. George campus of University of Toronto in downtown Toronto and the sampling period occurred during September 18-22, 2012 (from Tuesday evening to Saturday afternoon). The instruments were located on the 3rd floor of Lash Miller Chemical Laboratories (~10 m above ground level). The building is located near the intersection of St. George Street and Willcocks Street (Figure S1). St. George Street has a modest, but steady traffic load during weekday rush hours. The aerosol sampling inlet was a 3/8 inch stainless steel tubing with the total flow rate of ~4 L/min and was pointing towards Willcocks Street, which has been blocked to traffic. There are a few catering facilities including a university canteen near the Lash Miller building and food carts along St. George Street.

2.2 Soot particle aerosol mass spectrometer

The working principle of the SP-AMS has been reported in detail previously (Onasch et al. 2012). In brief, the SP-AMS is a standard HR-ToF-AMS (DeCarlo et al. 2006) coupled with a diode-pumped Nd:YAG intracavity 1064 nm infrared (IR) laser vaporizer (see Figure 1). In the standard AMS configuration, a resistively heated tungsten vaporizer is operated at ~600^{o}C to vaporize the NR-PM (Canagaratna et al. 2007). The addition of the laser vaporizer expands the utility of the standard AMS to vaporize near-IR light absorbing aerosol particles, especially rBC. The rBC-containing particles are heated by absorbing IR energy to ~4000K to facilitate their vaporization. The resulting gas phase species from either the laser or tungsten vaporizer are ionized with electron impact (EI) ionization (70 eV). The ions are then detected by a high-resolution time-of-flight mass spectrometer operated in V-mode, which provides a lower mass resolving power (~2000) but a higher sensitivity compared to W-mode (mass resolving power ~ 4000) (DeCarlo et al. 2006).

The SP-AMS was operated with two vaporizer configurations during sampling, laser-on and laser-off, to maximize the information obtained and to enable comparisons and correlations between the two different vaporizers.. In particular, previous work has shown vaporizer-dependent differences in collection efficiencies and fragmentation patterns (Onasch et al. 2012; Willis et al., 2014). When the IR laser was off, the LS-SP-AMS was operated as a standard HR-ToF-AMS for measuring NR-PM as described above, whereas the instrument operated with the IR laser-on detected both rBC and NR-PM. An aerodynamically focused particle beam overlaps perpendicularly with the IR laser vaporizer before it hits the tungsten vaporizer, and hence the NR-PM that is internally mixed with rBC is vaporized by the IR laser (Onasch et al. 2012). A single slit chopper with ~2% throughput was used in our LS-SP-AMS. In addition to the ensemble measurements (i.e., mass spectrum (MS) and particle time-of-flight (PToF) modes to measure bulk and size-resolved chemical composition, respectively), a light scattering module was integrated into the SP-AMS for detecting single particle mass spectra (LS mode, see Section 2.4 for details). The single particle data are particularly useful for determining the mixing state of ambient aerosol particles. Information on menu switching (90 seconds each) in the LS-SP-AMS is shown in Table 1.

2.3 Calibration and ensemble data analysis

Ammonium nitrate (NH_4NO_3) particles generated by a constant output atomizer (TSI Inc., Model 3076) were dried using a diffusion dryer, and subsequently size selected at 300 nm using a differential mobility analyzer (DMA, TSI Inc., Model 3081) for determining the ionization efficiency of the LS-SP-AMS when operated in the IR laser-off mode. Similarly, a water suspension of Regal Black (Regal 400R Pigment Black, Cabot Corp., a calibration standard recommended by Onasch et al. 2012) was atomized to generate standard rBC particles. Dried 300 nm Regal Black particles were used to determine the mass-based ionization efficiency of rBC, for calculation of the ionization efficiency relative to nitrate (RIE_{rBC}) (Onasch et al. 2012).

The ensemble data were processed using the AMS data analysis software (Squirrel, version 1.51H for unit mass resolution (UMR) data and Pika, version 1.10H for high resolution peak fitting, http://cires.colorado.edu/jimenez-group/ToFAMSResources/ToFSoftware/index.html) with the corrected air fragment column of the standard fragmentation table (Allan et al. 2004, DeCarlo et al. 2006).

Signals of rBC were quantified by the sum of carbon ion clusters (C_x^+) using high resolution mass spectral data up to m/z 120. The product of density and shape factor of the dried 300 nm Regal Black particles is ~0.8 g/cm^3, which is derived from the ratio of the vacuum aerodynamic diameter (d_{va}) measured by the PToF mode of the LS-SP-AMS to the mobility diameter (d_m) determined by the DMA (DeCarlo et al. 2004) as follows:

$$d_{va} = \rho * S * d_m / \rho_0 \qquad \text{(Eq. 1)}$$

where ρ and S are the density and Jayne shape factor of Regal Black particles, respectively, and ρ_0 is the unit density. The RIE_{rBC} determined in this study was 0.4, and the default RIE values of nitrate (1.1), sulfate (1.2), organics (1.4) and ammonium (4) were used (Jimenez et al. 2003). The average C_1^+ to C_3^+ ratio (0.61) obtained from Regal Black was used to correct the interference in C_1^+ from the non-refractory organics in ambient aerosol. The size distribution of rBC was calculated by adding an rBC column (C_1^+ to C_5^+ fragments) to the fragmentation table in Squirrel as shown Table S1. Note that Willis et al. (2014) reported that the collection efficiency (CE) of bare Regal Black is about 0.6 for our instrument. Onasch et al. (2012) reported that the 3σ detection limit for rBC mass concentration measurements is 0.03 µgm−3 for 1 min collection.

2.4 Light scattering module for single particle detection

The design and working principles of the light scattering module have been previously described in detail (Cross et al. 2009, Freutel et al. 2013, Liu et al. 2013). Briefly, the light scattering module consists of a 50 mW diode pumped 405 nm continuous wave laser (CrystaLaser, LC BCL-050-405) that overlaps perpendicularly with the particle beam ~0.265 m downstream of the chopper and ~0.130 m upstream of the tungsten vaporizer as shown in Figure 1. Note that the laser beam is not focused and diverges in order to ensure a complete overlap between the laser and particle beams (Cross et al. 2007). Scattered light from sampled particles is collected using an ellipsoidal mirror and detected with a photomultiplier tube (PMT). A light scattering signal can be obtained if a sampled particle is larger than the optical detection limit. The 50% cut-off mobility diameter (d_m) (i.e., a diameter that represents 50% counting efficiency of particle number when compared to a CPC) of our light scattering module determined using dry NH_4NO_3 particles is ~250 nm, which is approximately equal to a vacuum aerodynamic diameter (d_{va}) of ~340 nm (the density and shape factor of NH_4NO_3 particles are 1.72 g/cm^3 and 0.8, respectively). Note that some ambient particles with lower particle densities may have a lower cut-off d_{va} than that determined for the dried NH_4NO_3 particles. For example, a hydrocarbon oil droplet (i.e., shape factor = ~1 and density = ~1 g/cm^3) likely has a light scattering cut-off in the range of 225-250 nm d_{va}.

2.5 Single particle categorization

Once a light scattering signal is detected, the computer is triggered to save the whole PToF trace, from which the single particle mass spectrum is subsequently obtained. The PToF data (i.e., particle flight time between the running chopper and the light scattering laser or laser/tungsten vaporizer) can be used to calculate the d_{va} of all recorded single particles so that a size distribution of the entire single particle dataset can be obtained. There are two major timing uncertainties for particle sizing measurement: 1) the initial time of the chopper cycle due to the slit width of the spinning chopper (~2%), and 2) the extra time required for vaporization, ionization and detection. Light scattering and single particle mass spectral measurements were processed using the AMS light scattering data processing software (Sparrow, 1.04E, http://cires.colorado.edu/jimenez-group/ToFAMSResources/ToFSoftware/index.html), which is designed for analyzing mass spectra with unit mass resolution (UMR) only.

Weak scattering trigger events (i.e., a total scattering signal less than 0.2 volts or a signal-to-noise ratio less than 5) were classified as “noise” events, and they were not included in the subsequent particle categorization. For particles that gave a sufficiently strong LS trigger event (i.e. those are not classified to as “noise”) and a total number of ions ≥ 6 in their mass spectra (calculated by integrating the ion signals in the single particle mass spectrum), they were either categorized as “prompt”, “early” or “delayed” particle types based on their PToF information (see supplementary information for information on setting the LS signal and total number of ions thresholds). When the PToF recorded by the light scattering signal (LS_{PToF}) can accurately predict the particle arrival time to the mass spectrometer (MS_{PToF}) the particle is categorized as prompt. The Gaussian fit of the difference between LS_{PToF} and MS_{PToF} (i.e., LS_{PToF} - MS_{PToF}) was used to define the prompt particle boundaries (i.e., particles falling outside the Gaussian fit boundaries (3σ) were either assigned as “early” or “delayed” particle types) (Figure S2). The delayed particle type can be due to the phenomenon of particle bounce upon impact with the thermal vaporizer surface (i.e. delayed vaporization) (Cross et al., 2009) but the physical meaning of early particle type remains unclear.

The calculation of total ion signals of an individual particle was modified in the standard software. Instead of using the default output from the fragmentation table, the total number of ions was calculated as the sum of all ion signals except m/z 14 (N^+), 15 (NH^+), 16 (NH_2^+), 17 (NH_3^+), 18 (H_2O^+), 28 (N_2^+), 32 (O_2^+) and 39 (K^+) either due to the strong interferences from air and instrument background (i.e. surface ionization on the tungsten vaporizer for K^+) or the noisy baseline of ammonium fragment ions. Multiple scattering signals observed in a trigger event and weak total ion signal (< 6 ions) were recognized as “coincidence” and “null” particle types, respectively. A summary of the particle categorization in different LS-SP-AMS modes is presented in Table 1. The size distributions of prompt particles in terms of light scattering signal intensity and total number of ions in an individual particle spectrum are shown in Figure S3. It is apparent that the particle categorization procedure effectively separates the prompt particles from the full collected single particle dataset.

2.6 Cluster analysis of single particle data

Cluster analysis was performed to investigate the mixing state of prompt particles based on the k-means algorithm in IGOR Pro (WaveMetrics Inc., version 6.2.2.2). Including other particle types with a lower confidence on their PToF d_{va} (i.e. early and delayed) to the cluster analysis would not affect the major observations, as they contributed only ~1% of the particle LS trigger events (Table 1). K-means cluster analysis has been extensively applied to analyze single particle data measured from the TSI aerosol time-of-flight mass spectrometer (ATOFMS) (Rebotier and Prather, 2007, Friedman et al. 2009, Giorio et al. 2012, Gross et al. 2010, Healy et al. 2010, Healy et al. 2013, Pagels et al. 2013) and more recently a standard HR-ToF-AMS with a light scattering module (Liu et al. 2013). It is worth noting that k-means clustering can classify ambient particles measured by ATOFMS into particle types that are highly consistent with other clustering algorithms such as ART-2a and hierarchical clustering (Rebotier and Prather, 2007, Giorio et al. 2012). Similar to the calculation of total ion signals in a single particle mass spectrum, m/z 14, 15, 16, 17, 18, 28, 32 and 39 were excluded in the cluster analysis. All single particle mass spectra were normalized by their total ion signal, and solutions with up to 25 clusters were tested. Euclidian distance (the square root of the sum of the squares of the differences between corresponding values) was used to evaluate the total distance between the cluster centers and each single particle. In general, increasing the number of clusters can better represent the dataset mathematically (i.e., reduce the total distance) as shown in Figure S4. However, a very large number of clusters compromises the physical meaning of each cluster.

A Cluster Analysis Panel (CAP) recently developed by our group was used to perform the built-in k-means clustering algorithm in IGOR Pro. The following information for each cluster can be directly generated by CAP: (1) number of particles, (2) normalized ion-weighted average unit mass resolution mass spectrum, (3) normalized histogram of the frequency of occurrence for each m/z ion signal for each single particle, and (4) average, time- and size-resolved chemical composition (nitrate, sulfate, organics and rBC) in terms of ion counts. Note that the CAP can also merge multiple clusters into a single particle class if they have similar mass spectral features and size distributions, whereas other clusters remain unchanged. To avoid generating negative ion signals from the default fragmentation table in Sparrow, a simplified version of the fragmentation table was applied for calculating the chemical composition as shown in Table S2 of the supplementary information.

3 Results and Discussion

The results and discussion section is divided into two main parts. The first part (Section 3.1-3.3) presents the observations from SP-AMS ensemble aerosol mesurements and PMF analysis of the organic components. The second part (Section 3.4-3.9) focuses on identification of particle types and characterizing the mixing state of carbonaceous aerosols based on cluster analysis of LS-SP-AMS single particle measurements. Note that the ensemble measurements detect particles with d_{va} starting from ~50 nm and up to ~1 µm, whereas the single particle measurements only detect particles greater than 200 nm d_{va} (the LS cut-off diameter for different particle types will the discussed in Section 3.4).

3.1 Overview of ensemble measurements

Figure 2a shows the time series of NR-PM, measured by the IR laser-off mode (i.e., the standard HR-ToF-AMS configuration), and rBC, measured in IR laser-on mode, of the whole sampling period in downtown Toronto. In general, organics dominated the particulate mass, whereas rBC contributed 4-9% of the average particle mass, assuming the collection efficiency (CE) for ambient rBC varies between 0.6 and 1 (i.e., CE range for bare and heavily coated Regal Black particles, respectively) (Willis et al. 2014) and the CE for all NR-PM evaporated from the tungsten vaporizer varies between 0.5 and 1 depending on chemical composition (Middlebrook et al. 2012) (see Figure S5 and calculation details based on single particle data in supplementary information). Willis et al. (2014) reported that the particle beam width (i.e., a primary parameter that governs the CE of rBC in SP-AMS) of ambient rBC particles measured at the same location of downtown Toronto is similar to that of heavily coated Regal Black particles generated in the laboratory. The total particle mass loading measured by the LS-SP-AMS is similar to that inferred from a simultaneous measurement using a Scanning Mobility Particle Sizer (SMPS, TSI Inc.,) (slope ~ 1.02, R^2 = 0.76), suggesting that the estimated CEs for NR-PM, vaporized from the heated tungsten vaporizer, and rBC, vaporized from the laser vaporizer, are within reasonable ranges (see Figure S5 in supplementary information).

The average mass spectrum of rBC was dominated by carbon ion clusters from C_1^+ to C_5^+ (~95%), with the strongest rBC signal at C_3^+ (Figure 2b). These spectral characteristics are similar to previous SP-AMS measurements (Massoli et al. 2012, Onasch et al. 2012) and the calibration standard used in the current study (Regal Black, see insert of Figure 2b). Fullerene type rBC spectral features (i.e., C_x^+ fragments with carbon number > 32) cannot be evaluated because their C_x^+ peaks are out of the m/z range (up to ~300) investigated in this study. Onasch et al. (2012) observed carbon cluster ions up to C_{82}^+ in laboratory generated ethylene flame soot particles and detected C_{32}^+ to C_{70}^+ that accounted for about 4% of the total rBC signals at an urban roadside environment. Furthermore, Dallmann et al. (2014) has demonstrated the capability of the SP-AMS to detect trace metals such as zinc in on-road gasoline and diesel vehicles emissions. However, no trace metals were clearly observed in this study.

Figure 2c displays the average ensemble size distributions (PToF d_{va}) of NR-PM and rBC. Secondary inorganic species, nitrate and sulfate, peaked at ~300-400 nm with much less contribution to the mass of smaller size particles. In contrast, the rBC signals peaked at ~100 nm. Since ambient rBC is only emitted from primary sources, this suggests that a significant portion of sampled rBC was freshly emitted or only slightly aged particles. This is consistent with the fact that vehicle emission are a major local source of rBC in the downtown area of Toronto. Organic species covered a wide range of particle sizes, indicating that they may be internally mixed with rBC and inorganic species. The organic fragment at m/z 44 (Org 44, CO_2^+) that can be used as a tracer of oxygenated organic aerosol (OOA) (e.g., organic acids) exhibited a bimodal distribution with the larger particle mode comparable to sulfate and nitrate (Figure 2c). Nevertheless, additional information such as single particle characterization is required to confirm the mixing state of ambient particles. The average O/C and H/C ratios of total organics obtained from elemental analysis of high resolution mass spectral data are 0.28 (ranged from 0.05 to 0.57) and 1.65 (ranged from 1.47 to 1.82), respectively (see the Van Krevelen diagram in Figure S6). The relatively low fraction of oxygenated organic aerosol indicates that the sampling site was strongly influenced by local anthropogenic sources, such as vehicle and cooking related emissions, matching well with the site characteristics (see Section 2.1).

3.2 PMF analysis of ensemble measurements

Positive matrix factorization (PMF) has been widely applied to analyze ambient AMS datasets to identify the potential sources of organic aerosol (Ulbrich et al. 2009, Zhang et al. 2011). PMF analysis separates the total organics measured in this study (Figure 3a-c) into factors that have been commonly observed in AMS measurements: hydrocarbon-like organic aerosol (HOA), cooking emission organic aerosol (COA), and oxygenated organic aerosol (OOA) (Zhang et al.

2011 and references therein). In brief, the HOA spectrum exhibits fragmentation patterns associated with hydrocarbon structures (e.g., m/z 57 ($C_4H_9^+$), 69 ($C_5H_9^+$), etc.), and is comparable to those of gasoline/diesel vehicle exhaust and lubricating oil (Canagaratna et al. 2004, Massoli et al. 2012, Mohr et al. 2009). The COA and HOA spectra are similar to each other; however, the COA factor tends to have a higher ratio of m/z 55 to 57 (Allan et al. 2010, Mohr et al. 2012, Mohr et al. 2009). Lastly, the OOA spectrum is composed of a relatively high fraction of m/z 44 (CO_2^+), indicating that the OOA material has a higher photochemical age (Jimenez et al. 2009, Ng et al. 2010). The O/C and H/C ratios of the laser-off mode PMF factors and their coordinates in the Van Krevelen diagram are shown in Figure 3a-c and S6, respectively.

Figure 4 shows the time series of the three-factor PMF solution obtained with the IR laser-off. Significant contributions of HOA and COA to the total organic mass (average ± standard deviation = 52% ± 20%) indicate that the sampling site was strongly influenced by anthropogenic emissions (Figure S7). In particular, the temporal variations in rBC and the laser-off HOA factor showed a significant correlation (Figure 4a), demonstrating that the HOA was primarily emitted from combustion sources such as engine exhaust. The substantial COA mass loading is consistent with the fact that many catering facilities are close to the sampling site (Figure 4b). The strong diurnal cycle of the COA factor was likely due to the active cooking activities from noon to night every day. The OOA factor represents the ambient level of oxygenated organic aerosol that originated from secondary sources and/or was produced by photochemical aging (e.g., transported/regional emissions from outside the city) (Figure 4c). Similar PMF results were obtained for the IR laser-on measurements (excluding rBC signals in the PMF analysis) and are shown in Figures S8 and S9. Including the rBC signals only slightly modified the PMF results of the laser-on measurements as displayed in Figures 3d-f and S8. Based on the PMF analysis, the rBC mass in HOA, COA and OOA factors accounted for about 51% (±20%), 9% (±11%) and 40% (±18%), respectively, of the total rBC mass loading on average (± standard deviation). The temporal variations of the rBC mass fractions contributed by each factor are shown in Figure 3g. The comparison between PMF and single particle cluster analysis (Figure 4, line vs. filled area) will be discussed in Section 3.9.

3.3 Comparison of laser-on and off ensemble measurements

The IR laser-on mode exhibited a higher sensitivity to all NR-PM components than the IR laser-off mode by ~10-20%, depending on the chemical species (Figure S10). There are two likely explanations for these observations, both of which may account for all or part of the discrepancies. (1) The observed discrepancies may be due to different CE issues for the two vaporizers (i.e., incomplete particle-laser beam overlap for laser vaporizer (Willis et al., 2014) and particle bounce issues for tungsten vaporizers (Matthew et al. 2008)). For example, the instrument operated in the laser-off mode might have a lower CE for rBC-containing particles due to particles bouncing off the tungsten vaporizer, an effect which would depend on the coating thickness, morphology and properties. As a result, some NR-PM components that are internally mixed with rBC may not be detected in the laser-off mode. In particular, it is well known that solid/semi-solid particles have a more pronounced bouncing effect than liquid particles (Docherty et al. 2013, Matthew et al. 2008). (2) Particle vaporization by the IR laser and the tungsten vaporizer do not occur at exactly the same location inside the ion chamber, possibly resulting in different ionization rates and ion transmission efficiencies (i.e., from the ion chamber to the ion focusing optics) between the two operational modes. This difference may also be a reason for the observed enhancements in the RIE of NR-PM evaporated from rBC particles.

Although the main driver of the observed sensitivity enhancement remains unclear, a larger difference between the two modes would imply that a higher mass fraction of a particular aerosol component coexists with rBC, because rBC-containing ambient particles are evaporated by the IR laser before they can reach the tungsten surface. Compared to the standard AMS measurements, in the laser-on mode the HOA, COA and OOA mass loadings are higher by about 40%, 10%, and 23%, respectively (Figure S11a-c). Figure S11d explicitly demonstrates that the percentage difference of each PMF factor between the laser-on and off operational modes is positively correlated with the mass fraction of rBC signal in each factor (mass fraction of rBC in laser-on HOA = 0.15, COA = 0.02, and OOA = 0.06). This is indirect evidence that a larger fraction of HOA material was internally mixed with rBC compared to the COA and OOA components. Further, we note that HOA and COA (oil-like droplets) dominated the organic aerosol mass and, as indicated earlier (see Section 3.1, and Figure S5 and description in supplementary information), these chemical components have CE's from the heated tungsten vaporizer close to unity, which would minimize the effects of the first argument. Therefore, the second argument is likely more appropriate to explain our observations for organic aerosol. For inorganic species, the enhancement of NH_4^+ mass between the two operational modes is smaller than those observed in the case of NO_3^- and SO_4^{2-} (Figure S10). The reason of this observation is unclear but one of the possibilities is that some refractory nitrate and sulfate (e.g., Na_2SO_4) coexisted with rBC. The direct measurements of mixing state from the single particle data will be discussed in the following sections.

3.4 Overview of single particle dataset

The single particle statistics of the LS measurement are summarized in Table 1. The IR laser-on and off modes had 113,120 and 112,441 total light scattering (LS) trigger events, respectively, and 75% of them in both laser-on and laser-off mode were recognized as particle LS trigger events. Approximately 41% (35,001) and 34% (28,322) of the particle LS trigger events were categorized as prompt particles in the laser-on and off modes, respectively. Figure 5 shows the prompt single particle results for laser-on and off modes, and the difference, as a function of the measured particle sizes (dva, nm). A higher fraction of prompt particles observed in the IR laser-on mode could be due to (1) the extra ions generated from rBC, (2) the different CE for laser and tungsten vaporizers especially for inorganic particles in the accumulation mode (see Figure S5 and description in supplementary information), and (3) a higher mass spectral sensitivity (i.e. a higher RIE of NR-PM) in the laser-on mode as described in Section 3.3. Cross et al. (2009) and Liu et al. (2012) reported that null particles accounted for ~50% of the particle LS trigger events, which is somewhat lower than those determined in this study (Table 1). This may arise from the fact that all ammonium fragments (m/z 14, 15, 16) were excluded in our calculation of total ion signals in the particle categorization procedure. It is also worth noting that Cross et al. (2009) deployed a more sensitive compact ToF-AMS (CToF-AMS) in their measurements.

Figure 6 shows some representative examples of single particle mass spectra of rBC-containing particles. Using the ensemble spectrum of rBC as a reference (Figure 2b), it is clear that ambient rBC can exist as nearly externally mixed (Figure 6a) or can be associated with various types of coating materials such as HOA (Figure 6b), OOA and inorganics (Figure 6c). Figure 7 shows the chemically speciated size distributions of all prompt particles. A comparison between the single particle size distributions (Figure 7) and the ensemble PTOF data (Figure 2c) illustrates the effect of the light scattering cut-off, showing that a significant portion of small particles cannot be detected in the LS measurements. A light scattering cut-off d_{va} of ambient nitrate and sulfate match well with that calibrated by the dried NH_4NO_3 particles, whereas ambient organic particles that are mainly composed of HOA and COA materials (see Section 3.5) have a cut-off d_{va} similar to that estimated for spherical hydrocarbon oil droplets (~250 nm, the pink dashed line in Figures 5 and 7). Furthermore, the LS mode can detect rBC-containing particles and the associated coating materials down to ~100 nm d_{va}. This is because ambient BC/soot agglomerates can have low effective particle densities due to their fractal morphologies (China et al. 2013, 2014, Slowik et al. 2004). In other words, the ambient rBC particles that have small d_{va} can be physically large enough to be detected by the light scattering module (see Eq. 1) and can produce sufficient signal for mass spectrometric detection.

The differences in overall and chemically speciated size distribution of ion signals between the laser-on and off modes are shown in Figures 5 and 7c, respectively. Accumulation mode particles peaked at ~400 nm d_{va} (mainly composed of secondary aerosol components such as nitrate, sulfate and oxygenated organic species) and exhibited the largest differences between the two operational modes. Organics with mid-range d_{va} (i.e., peak at ~300 nm) show a relatively small difference compared to accumulation mode organics, suggesting that those organic particles are likely less sensitive to the types of particle vaporization (i.e., no rBC core). Note that those mid-range d_{va} organic particles are dominated by HOA and COA materials with a relative small mass fraction of rBC (see Section 3.5). Similar observations are also obtained from particle number size distributions as shown in Figure S12a. The laser-on-to-laser-off ratios in terms of total ion signals and particle number are biased higher in the large and small particle size ranges. The former is suggestive of potential bounce effects on the tungsten vaporizer and/or better ion transmission efficiency in the laser-on mode as discussed in Section 3.3; the latter, for particles smaller than 200 nm, is likely due to rBC particles dominating the ion signals (Figure S12b).

3.5 Cluster analysis of single particle dataset

The k-means clustering algorithm was used to separately classify all the prompt particle mass spectra into chemically distinct groups for both laser-on and laser-off datasets. The overall cluster analysis results for NR-PM are similar for both the IR laser-on and off datasets, with the primary exception being an additional particle class, rBC, obtained from the laser-on mode single particle data. The major NR-PM particle classes obtained via independent cluster analysis for both datasets included nitrate, sulfate, HOA, COA, and 2 types of OOA (Figure 8). These particle classes represented similar particle number fractions and time series, and differed only slightly in average mass spectra (not shown).

To demonstrate the capability of the LS-SP-AMS to investigate the mixing state of ambient aerosol particles, the twelve-cluster solution from the laser-on mode measurements is presented here. The number of particles and the ion fractions of nitrate, sulfate, organics and rBC in each cluster are shown in Figure S13. Increasing the number of clusters from 12 to 25 only gradually reduces the total Euclidian distance between the cluster centers and each single particle mass spectrum (Figure S4), and does not generate any new particles classes with significant physical meaning (i.e. determined by clusters re-combination as discussed in the next paragraph). Note that an rBC-rich particle class (see Section 3.5.2) can be clearly identified starting from the nine-cluster solution (up to twenty five-cluster solution). However, for the eleven-cluster solution, the rBC-rich particle class cannot be separated from OOA in the accumulation mode (i.e. dva peak at ~ 400 nm). Therefore, the twelve-cluster solution is considered as the optimal clustering solution.

By comparing the mass spectra, time series, and size distributions of the twelve clusters, it is clear that some clusters must be re-combined into a single particle class to provide physically meaningful results. For example, four preliminary clusters obtained from the k-means clustering (cluster #1, 6, 8 and 11 in Figure S13) are rich in nitrate signatures with similar temporal variations and/or size distributions (Figure S14), and hence they were merged to produce a single nitrate-rich class. Merging preliminary clusters into a single final particle class has been widely applied to cluster analysis of ATOFMS data (e.g., Healy et al. 2013). A tracer for rBC (C_3^+ at m/z 36) is used to examine the mixing state of ambient rBC. The potential isobaric interference from HCl^+ was evaluated based on the cluster analysis of the IR laser-off dataset (Table 2, see discussion below).

3.5.1 Inorganic Classes

Figure 8 summarizes the unit mass resolution (UMR) spectra, mass spectral histograms and size distributions of the seven final particle classes. Figure 8a shows a nitrate-rich class that consists of significant ion signals at m/z 30 (NO^+) and m/z 46 (NO_2^+) with comparable intensities, and a sulfate-rich class with a mass spectrum dominated by m/z 48 (SO^+), 64 (SO_2^+), 80 (SO_3^+), 81 (HSO_3^+) and 98 ($H_2SO_4^+$). These inorganic classes have narrow size distributions and peak at ~400 nm (Figure 8p and 8q), which is consistent with the PToF ensemble data. A significant fraction of the particles in these two classes are internally mixed with a substantial amount of organic material (see Section 3.6 for the discussion of mixing state of secondary species in an accumulation mode particle). The mass spectra of these organics are similar to the OOA class 1 identified in this work (i.e., strong signals at m/z 29 and 43, Figure 8f). In particular, approximately 60-70 % of the nitrate- and sulfate-rich particles exhibit organic signal at m/z 43 (Figure 8h and 8i). Furthermore, the tracer of rBC (C_3^+ at m/z 36) indicates that rBC has only a minor contribution to the nitrate- and sulfate-rich particles (i.e., a similar percentage of particles contributed to m/z 36 between laser-on and off modes (< 2%) in these clusters) as shown in Table 2.

3.5.2 HOA and rBC Classes

A cluster with mass spectral fragmentation patterns for hydrocarbons (i.e. $C_xH_y^+$ ions) is assigned as a HOA-rich class (Figure 8c). Most of the HOA-rich particles do not contain any inorganic species (Figure 8c and 8j). About 6% of the HOA-rich particles were composed of a detectable signal at m/z 36 that originates from rBC (Table 2) and the mass contribution of rBC to this cluster was about 3% on average (RIE_{org} = 1.4 and RIE_{rBC} = 0.4). Instead, the cluster analysis yields a separate rBC class without substantial organic coating (Figure 8d). Although the mass fraction contribution of organics to this particle type is only 0.28, ~60-80% of the particles consist of detectable organic signals at m/z 41, 43, 55, and 57 (Figure 8k). The rBC-rich class has a C_1^+/C_3^+ ratio of about 0.53, which is slightly smaller than the ratio obtained from the calibration standard (Regal Black). The mass spectral character of the organic coating is similar to the spectrum of PMF-HOA in general, but with a slightly higher fraction of m/z 44 and lower fraction of m/z 55 and 57 compared to the HOA-rich class (insert of Figure 8d). We emphasize that while PMF analysis showed that rBC and HOA materials likely have the same emission sources, this approach does not provide direct information about the ambient particle mixing state. In contrast, the cluster analysis clearly suggests that two major types of particles, which have different size distributions (Figure 8r and 8s) and extents of internal mixing of HOA and rBC (see Section 3.7), contributed to the PMF-HOA factor.

3.5.3 COA and OOA Classes

The mass spectrum of a COA class is shown in Figure 8e. The COA cluster covers a range of particles with d_{va} peaking at ~300 nm (Figure 8t). Similar to the PMF-COA factor, the COA class is dominated by fragments at m/z 41 and m/z 55 with a relatively high m/z 55 to 57 ratio compared to the HOA. Two OOA classes were also identified (Figure 8f and 8g). These particle types likely represent aged organic aerosol components because a large fraction of the particles (> 50 %) are associated with secondary nitrate and sulfate (see Section 3.6). While OOA class 1 represents the less oxygenated organics (i.e., strong signal from less oxygenated fragments such as CHO^+ at m/z 29 and $C_2H_3O^+$ at m/z 43), OOA class 2 has the distinct spectral feature of highly oxygenated organics produced via photochemical aging (i.e., intense signal at m/z 44 (CO_2^+) from organic acids). Both OOA classes have size distributions similar to the inorganic classes (see Section 3.6 for the discussion of mixing state of secondary species in an accumulation mode particle). The major exception is that the OOA class 1 has another peak with a smaller mean particle diameter, suggesting that this particle type may consist of ambient particles with a different degree of aging (e.g., fewer condensed materials such as inorganic species on the smaller particles). The majority of the particles in the COA and OOA classes (96-97%) were not associated with rBC signals (Table 2).

3.6 Mixing of secondary species in accumulation mode particles (d_{va} ~ 400 nm)

Although seven particle classes with their distinct mass spectral features are identified based on cluster analysis, atmospheric aerosol particles are likely internal mixtures with varying relative compositions of the different chemical components. As shown in Section 3.5, a few particle classes dominated by secondary species, including nitrate, sulfate, and OOA, are predominately measured by size to be in the accumulation mode (Figure 8). To understand the mixing state of these secondary components, the relative mass contributions of nitrate, sulfate and organic (i.e., OOA) in each particle type are examined using ternary diagrams as shown in Figure 9. The input parameters of ternary diagrams are converted from ion counts to mass-based data using default RIE of nitrate, sulfate and organic (See Section 2.3). Overall, all these particle types are internal mixtures of nitrate, sulfate and organic to different degrees. Most of the classified as nitrate-rich are composed of nitrate and organic, though some particles have significant sulfate content (up to ~50 wt% of these secondary species) (Figure 9a). Figure 9b shows that the sulfate-rich class is dominated by internal mixtures of sulfate and organic with relatively low nitrate mass (up to ~30 wt%). OOA1 and OOA2 classes are dominated by organic-rich particles with a variable degree of internal mixing with sulfate and nitrate (up to ~40 and ~30 wt%, respectively) (Figure 9c). In contrast, a very low degree of internal mixing of inorganic components with COA, HOA and rBC classes are observed (see ternary diagrams shown in Figure S15 in the supplementary information), which is consistent with the COA, HOA and rBC particle types being predominantly externally mixed primary particles with little gas-to-particle condensation (or coagulation) of secondary particulate material prior to sampling (see Figure 8).

3.7 Mixing of rBC-containing particles

Ternary diagrams that show the relative mass contributions of inorganic (nitrate and sulfate), organic and rBC in each particle class are used to evaluate the mixing states of rBC-containing particles in the sampled urban environment (see Figure S16 in supplementary information). According to Figure S16 and Table 2, rBC is only a minor contributor to all particle types except the rBC class. The normalized number fraction of single particles, for each particle class, is shown in Figure 10a as a function of the rBC mass fraction per single particle, demonstrating that only a small portion of particles from each class (except for the rBC class) is internally mixed with rBC (up to 60 wt%). Note that the total mass of each particle presented in Figure 10a-c is calculated as the sum of organic, rBC, ammonium nitrate, and ammonium sulfate, assuming that all particles are completely neutralized (i.e., all nitrate and sulfate are in the form of ammonium salts, see Figure S5c). Although the nitrate-rich class has an apparent relatively high rBC content compared to other classes, it is possibly due to the interference from HCl^+ signal as discussed previously (Section 3.5 and Table 2).

Figure 10b and 10c further shows the number distributions of particles categorized to the rBC and HOA classes, respectively, as a function of rBC mass fraction and particle d_{va}. Apparently, most of the HOA-rich particles contain very little (i.e., below detection limits) rBC mass as shown in the bar graph in Figure 10c. A tail of the number distribution indicates that some small particles (~200 nm) are internally mixed with rBC up to ~50% by mass. On the other hand, Figure 10b suggests that rBC-rich particles are more gradually mixed with HOA materials with the average rBC mass fraction of ~0.7. Some nearly pure rBC particles are also observed in this study (i.e. mass fraction of rBC ~1). The number distributions of particles classified to other classes as a function of rBC mass fraction and particle d_{va} are shown in Figure S17. The rBC content in the accumulation mode particles is mainly associated with the secondary components, indicating that those rBC-containing particles are chemically aged.

3.8 Low to mid-range d_{va} (~200-400 nm), organic-rich particles

The results provide a valuable, new perspective into the chemical composition and potential sources for low to mid-range d_{va} (~200-400 nm), organic-rich particles (i.e., dominated by particles in the HOA and COA clusters) using both ensemble and single particle techniques. Specifically, we made two sets of observations: (a) LS-SP-AMS ensemble data suggest that HOA and rBC were highly correlated in several ways: (1) time traces in Figure 4a, (2) PToF size distributions in Figure 2c, and (3) laser-on-to-laser-off ratios for PMF factors in Figures S10 and S11; and (b) LS-SP-AMS single particle results suggest that HOA- and COA-rich particles were nearly externally mixed with rBC. The strong correlation between HOA and rBC has, for the most part, been noted previously (Zhang et al. 2011 and references therein). The new observations obtained with the LS-SP-AMS single particle data and k-means cluster analysis suggest that the low to mid-range d_{va}, organic-rich particles in a typical urban environment largely arise from low density organic materials, such as nearly pure HOA and COA particles (> 95 wt% of organics) emitted from primary sources (e.g., vehicle exhaust and cooking emissions).

Even though the HOA-rich particles exhibit near external mixing with rBC, we note that HOA materials are nevertheless still more closely associated with rBC than are other particle constituents. As noted above, the laser-on-to-laser-off ratio increases by organic PMF factor in the following manner: HOA > OOA > COA (Figure S11). This trend correlates well with the observed ensemble rBC mass fractions for each PMF factor. Hence, the difference between the PMF-HOA mass loadings from the laser-on and off modes suggests that HOA materials were more associated with rBC-containing particles than were OOA and COA. Furthermore, the HOA coating on rBC-rich particles alone is likely insufficient to explain the PMF-HOA difference between laser-on and off modes, at least for the current single particle size range. This suggests that the some HOA-rich particles were likely associated with small rBC cores.

Quantitatively, the single particle data analysis demonstrates that: (1) a significant portion of HOA- and COA-rich particles (> 90%) with particle d_{va} larger than ~200 nm did not contain a detectable amount of rBC, e.g., organic-rich particles containing a small rBC core or no rBC (with a mass contribution of rBC to the HOA- and COA-rich classes about 3% on average), and (2) the rBC-rich particles were mixed with ~28 wt% HOA-like material on average, e.g., a thinly HOA coated rBC particle, assuming uniform coating thickness. For example, applying a simple core-shell spherical structure (i.e. rBC core plus uniform HOA coating), a 200 nm d_{va} rBC-rich particle has a coating thickness of ~10 nm with HOA and rBC densities equal to 0.9 and 0.8 g/cm^3, respectively. rBC was mixed to a minor extent with other inorganic and organic materials. The total organic-to-rBC ratios are relatively constant across the size range of the rBC-rich cluster. However, whether this fact allows us to extend our mixing state conclusions to particles that are smaller than the nominal detection limit of the light scattering module is unknown.

The number fraction of rBC-containing particles to total prompt particles determined in the current study is about 7-11% using m/z 36 as an rBC tracer and considering the potential interference from HCl^+ (Table 2). Willis et al. (2014) showed that the SP-AMS could measure rBC mass fractions down to at least 5% by mass for laboratory-generated particle ensembles.

The current data suggest that per particle rBC mass fractions for many of the HOA- and COA-rich single particles are less than 5% (Table 2). We cannot rule out that the LS-SP-AMS is missing ion signals from small rBC cores in these particle types. The fact that the RIE_{rBC} (usually from 0.2 to 0.4) is smaller than the RIE of other major NR-PM species indicates that that we are getting fewer ion signals per mass from rBC compared to other NR-PM components, making it harder to determine if rBC is in any given particle. Using 6 ions as a detection limit of a single particle (i.e. a criteria for "prompt" particle type) and a mass-based ionization efficiency of Regal Black determined by calibration, it can be estimated that the detection limit of a pure rBC single particle is ~25 fg of rBC per particle. Therefore, the single particle mixing state measurements here may under represent rBC-containing particle number (and mass) not only for low to mid-range d_{va}, organic-rich particles but also for all identified clusters.

3.9 Comparison of clustering observations with PMF factors

In addition to the mass spectral comparison provided in the previous section, Figure 4 displays a comparison between the time series of organic classes (HOA, COA, and OOA classes, in ion signal) and PMF factors (in mass loadings). The total signals of the OOA classes shown in Figure 4c were determined by the sum of organic signals from the nitrate, sulphate, OOA 1 and OOA 2 classes as they all contain oxygenated organic aerosol materials. The COA class completely captures the diurnal cycle of the PMF-COA (Figure 4b), and the PMF-OOA agrees well with the OOA classes (Figure 4c). The PMF-HOA factor exhibited three major peaks during the sampling period indicated by red dashed rectangles in Figure 4a. However, the HOA class only captures the first two periods and not the last one. It is possible that most of the HOA material in this final period was associated with extremely small particles, which could not be detected by the light scattering module. The HOA class organic signals displayed in Figure 4a are not significantly altered by the addition of organic signals from the rBC class. Overall, the temporal variations of these organic particle classes and PMF factors correlate very well indicating that this single particle approach is able to largely capture the variability in the major aerosol components observed by LS-SP-AMS ensemble measurements.

4 Summary and concluding remarks

This work represents the first report of single particle characterization of rBC particles with the LS-SP-AMS. PMF analysis of ensemble data is a standard approach used to investigate the sources of ambient organic aerosol. Noting that the single particle data are direct measurements of aerosol composition whereas PMF analysis is a statistical tool, one of the major results from this paper is the temporal and compositional agreement between k-means single particle clusters and the PMF factors, which validate the PMF result and their relation to particulate matter sources. That being said, it is important to note that because the LS-SP-AMS may not be able to detect certain primary aerosol components, such as mineral dust, and non-IR absorbing refractory PM, and therefore the mixing state measurements obtained may not reflect the mixing state of the entire aerosol population.

Additional information regarding the mixing state of ambient particles and their size distributions (down to the detection limit of the light scattering module) is important for improving our understanding of the environmental impacts of atmospheric aerosol particles. While Liu et al. (2013) first applied the k-mean clustering algorithm to LS-ToF-AMS data, this work successfully extends the application of the k-means clustering approach to analyze LS-SP-AMS data to evaluate the mixing state of ambient rBC particles and other, non-refractory aerosol components. The approach presented here can be applied to assess the magnitude of the contributions of different sources when performing source-receptor analysis.

PMF analysis of ensemble measurements can provide information to evaluate the potential sources and aging of organic aerosol. While it is recognized that HOA factors, identified by PMF analysis of standard HR-ToF-AMS data, and rBC originate from combustion sources, the mixing states of these primary aerosol species cannot be easily characterized in this manner without the support of single particle measurement. Within the constraints of the instrumentation that may under represent the number of rBC-containing particles (see Sections 3.3 and 3.8), the single particle data analysis demonstrates quantitatively that there were two types of particles associated with HOA materials: (1) HOA-rich particles associated with ~3 wt% of rBC (e.g.,, a small rBC core with a high HOA content), and (2) rBC-rich particles mixed with ~28 wt% HOA-like material on average (e.g., a rBC particle with a thin, uniform HOA content). Other inorganic and organic materials were mixed to a lesser extent with rBC. The single particle data also provide insight to the sources of low to mid-range d_{va} organics (~200-400 nm) in a typical urban environment. According to our cluster analysis, those organics are mainly composed of HOA- and COA-rich particles (with rBC content about 3% on average) emitted from primary sources such as vehicle exhaust and kitchen emissions instead of processed particles associated with condensed secondary materials.

During our study, most of the rBC was likely freshly emitted from nearby vehicle exhaust and therefore we did not observe significant mixing, even though missing ion signal from small rBC cores in the aged particle types is possible. Further deployment of the LS-SP-AMS in remote environments will provide insight into the mixing state of aged ambient rBC. Freutel et al. (2013) recently developed a new particle categorization algorithm based on reference spectra comparison, which is potentially useful to identify unknown rBC particle types from LS-SP-AMS measurements.

Acknowledgements:

This work was financially supported by Natural Sciences and Engineering Research Council (NSERC) of Canada, the Canada Foundation for Innovation and the Marie Curie Action FP7-PEOPLE-IOF-2011 (Project: CHEMBC, No. 299755).

References:

Allan, J. D., Williams, P. I., Morgan, W. T., Martin, C. L., Flynn, M. J., Lee, J., Nemitz, E., Phillips, G. J., Gallagher, M. W. and Coe, H.: Contributions from transport, solid fuel burning and cooking to primary organic aerosols in two UK cities, Atmos. Chem. Phys., 10, 647-668, 2010.

Allan, J., Delia, A., Coe, H., Bower, K., Alfarra, M., Jimenez, J., Middlebrook, A., Drewnick, F., Onasch, T., Canagaratna, M., Jayne, J. and Worsnop, D.: A generalised method for the extraction of chemically resolved mass spectra from Aerodyne aerosol mass spectrometer data, J. Aerosol Sci., 35, 909-922, 2004.

Baumgardner, D., Kok, G. and Raga, G.: Warming of the Arctic lower stratosphere by light absorbing particles, Geophys. Res. Lett., 31, L06117, 2004.

Bond, T. C., Doherty, S. J., Fahey, D. W., Forster, P. M., Berntsen, T., DeAngelo, B. J., Flanner, M. G., Ghan, S., Kaercher, B., Koch, D., Kinne, S., Kondo, Y., Quinn, P. K., Sarofim, M. C., Schultz, M. G., Schulz, M., Venkataraman, C., Zhang, H., Zhang, S., Bellouin, N., Guttikunda, S. K., Hopke, P. K., Jacobson, M. Z., Kaiser, J. W., Klimont, Z., Lohmann, U., Schwarz, J. P., Shindell, D., Storelvmo, T., Warren, S. G. and Zender, C. S.: Bounding the role of black carbon in the climate system: A scientific assessment, J.Geophys. Res.-Atmos., 118, 5380-5552, 2013.

Canagaratna, M. R., Jayne, J. T., Ghertner, D. A., Herndon, S., Shi, Q., Jimenez, J. L., Silva, P. J., Williams, P., Lanni, T., Drewnick, F., Demerjian, K. L., Kolb, C. E. and Worsnop, D. R.: Chase studies of particulate emissions from in-use New York City vehicles, Aerosol Sci. Technol., 38, 555-573, 2004.

Canagaratna, M. R., Jayne, J. T., Jimenez, J. L., Allan, J. D., Alfarra, M. R., Zhang, Q., Onasch, T. B., Drewnick, F., Coe, H., Middlebrook, A., Delia, A., Williams, L. R., Trimborn, A. M., Northway, M. J., DeCarlo, P. F., Kolb, C. E., Davidovits, P. and Worsnop, D. R.: Chemical and microphysical characterization of ambient aerosols with the aerodyne aerosol mass spectrometer, Mass Spectrom. Rev., 26, 185-222, 2007.

Cahill, J. F., Suski, K., Seinfeld, J. H., Zaveri, R. A. and Prather, K. A.: The mixing state of carbonaceous aerosol particles in northern and southern California measured during CARES and CalNex 2010, Atmos. Chem. Phys., 12(22), 10989–11002, doi:10.5194/acp-12-10989-2012, 2012.

Cappa, C. D., Onasch, T. B., Massoli, P., Worsnop, D. R., Bates, T. S., Cross, E. S., Davidovits, P., Hakala, J., Hayden, K. L., Jobson, B. T., Kolesar, K. R., Lack, D. A., Lerner, B. M., Li, S., Mellon, D., Nuaaman, I., Olfert, J. S., Petaja, T., Quinn, P. K., Song, C., Subramanian, R., Williams, E. J. and Zaveri, R. A.: Radiative Absorption Enhancements Due to the Mixing State of Atmospheric Black Carbon, Science, 337, 1078-1081, 2012.

China, S., Mazzoleni, C., Gorkowski, K., Aiken, A. C. and Dubey, M. K.: Morphology and mixing state of individual freshly emitted wildfire carbonaceous particles, Nat. Commun., 4, 2122, 2013.

China, S., Salvadori, N. and Mazzoleni, C.: Effect of traffic and driving characteristics on morphology of atmospheric soot particles at freeway on-ramps, Environ. Sci. Technol., ASAP, 2014.

Corbin, J. C., Sierau, B., Gysel, M., Laborde, M., Keller, A., Kim, J., Petzold, A., Onasch, T.B., Lohmann, U. and Mensah, A. A.: Mass spectrometry of refractory black carbon particles from six sources: carbon cluster and oxygenated ions, Atmos. Chem. Phys., 14, 2591-2603, 2014.

Cross, E. S., Onasch, T. B., Canagaratna, M., Jayne, J. T., Kimmel, J., Yu, X. -., Alexander, M. L., Worsnop, D. R. and Davidovits, P.: Single particle characterization using a light scattering module coupled to a time-of-flight aerosol mass spectrometer, Atmos. Chem. Phys., 9, 7769-7793, 2009.

Cross, E. S., Onasch, T. B., Ahern, A., Wrobel, W., Slowik, J. G., Olfert, J., Lack, D. A., Massoli, P., Cappa, C. D., Schwarz, J. P., Spackman, J. R., Fahey, D. W., Sedlacek, A., Trimborn, A., Jayne, J. T., Freedman, A., Williams, L. R., Ng, N. L., Mazzoleni, C., Dubey, M., Brem, B., Kok, G., Subramanian, R., Freitag, S., Clarke, A., Thornhill, D., Marr, L. C., Kolb, C. E., Worsnop, D. R. and Davidovits, P.: Soot Particle StudiesInstrument Inter-ComparisonProject Overview, Aerosol Sci. Technol., 44, 592-611, 2010.

Cross, E. S., Slowik, J. G., Davidovits, P., Allan, J. D., Worsnop, D. R., Jayne, J. T., Lewis, D. K., Canagaratna, M. and Onasch, T. B.: Laboratory and ambient particle density determinations using light scattering in conjunction with aerosol mass spectrometry, Aerosol Sci. Technol., 41, 343-359, 2007.

Dallmann, T. R., Onasch, T. B., Kirchstetter, T. W., Worton, D. R., Fortner, E. C., Herndon, S. C., Wood, E. C., Franklin, J. P., Worsnop, D. R., Goldstein, A. H. and Harley, R. A.: Characterization of particulate matter emissions from on-road gasoline and diesel vehicles using a soot particle aerosol mass spectrometer, Atmos. Chem. Phys., 14(14), 7585–7599, doi:10.5194/acp-14-7585-2014, 2014.

DeCarlo, P. F., Kimmel, J. R., Trimborn, A., Northway, M. J., Jayne, J. T., Aiken, A. C., Gonin, M., Fuhrer, K., Horvath, T., Docherty, K. S., Worsnop, D. R., and Jimene, J. L.: Field-deployable, high-resolution, time-of-flight aerosol mass spectrometer, Anal. Chem., 78, 8281–8289, 2006.

DeCarlo, P. F., Slowik, J. G., Worsnop, D. R., Davidovits, P., and Jimenez, J. L.: Particle morphology and density characterization by combined mobility and aerodynamic diameter measurements. Part 1: Theory, Aerosol Sci. Technol., 38, 1185–1205, 2004.

Drewnick, F., Hings, S. S., DeCarlo, P. F., Jayne, J. T., Gonin, M., Fuhrer, K., Weimer, S., Jimenez, J. L., Demerjian, K. L., Borrmann, S. and Worsnop, D. R.: A new time-of-flight aerosol mass spectrometer (TOF-AMS) - Instrument description and first field deployment, Aerosol Sci. Technol., 39, 637–658, 2005.

Docherty, K. S., Jaoui, M., Corse, E., Jimenez, J. L., Offenberg, J. H., Lewandowski, M. and Kleindienst, T. E.: Collection Efficiency of the Aerosol Mass Spectrometer for Chamber-Generated Secondary Organic Aerosols, Aerosol Sci. Technol., 47, 294-309, 2013.

Freutel, F., Drewnick, F., Schneider, J., Klimach, T. and Borrmann, S.: Quantitative single-particle analysis with the Aerodyne aerosol mass spectrometer: development of a new classification algorithm and its application to field data, Atmos. Meas. Tech., 6, 3131-3145, 2013.

Friedman, B., Herich, H., Kammermann, L., Gross, D. S., Arneth, A., Holst, T. and Cziczo, D. J.: Subarctic atmospheric aerosol composition: 1. Ambient aerosol characterization, J.Geophys. Res.-Atmos., 114, D13203, 2009.

Giorio, C., Tapparo, A., Dall'Osto, M., Harrison, R. M., Beddows, D. C. S., Di Marco, C. and Nemitz, E.: Comparison of three techniques for analysis of data from an Aerosol Time-of-Flight Mass Spectrometer, Atmos. Environ., 61, 316-326, 2012.

Gross, D. S., Atlas, R., Rzeszotarski, J., Turetsky, E., Christensen, J., Benzaid, S., Olson, J., Smith, T., Steinberg, L., Sulman, J., Ritz, A., Anderson, B., Nelson, C., Musicant, D. R., Chen, L., Snyder, D. C. and Schauer, J. J.: Environmental chemistry through intelligent atmospheric data analysis, Environ. Modell. Softw., 25, 760-769, 2010.

Healy, R. M., Hellebust, S., Kourtchev, I., Allanic, A., O'Connor, I. P., Bell, J. M., Healy, D. A., Sodeau, J. R. and Wenger, J. C.: Source apportionment of PM2.5 in Cork Harbour, Ireland using a combination of single particle mass spectrometry and quantitative semi-continuous measurements, Atmos. Chem. Phys., 10, 9593-9613, 2010.

Healy, R. M., Sciare, J., Poulain, L., Crippa, M., Wiedensohler, A., Prevot, A. S. H., Baltensperger, U., Sarda-Esteve, R., McGuire, M. L., Jeong, C. -., McGillicuddy, E., O'Connor, I. P., Sodeau, J. R., Evans, G. J. and Wenger, J. C.: Quantitative determination of carbonaceous particle mixing state in Paris using single-particle mass spectrometer and aerosol mass spectrometer measurements, Atmos. Chem. Phys., 13, 9479-9496, 2013.

Jacobson, M.: Strong radiative heating due to the mixing state of black carbon in atmospheric aerosols, Nature, 409, 695-697, 2001.

Jayne, J.T., Leard, D.C., Zhang, X., Davidovits, P., Smith, K.A., Kolb, C.E. and Worsnop, D.R.: Development of an Aerosol Mass Spectrometer for Size and Composition. Analysis of Submicron Particles, Aerosol Sci. and Technol, 33, 49-70, 2000.

Jimenez, J. L., Canagaratna, M. R., Donahue, N. M., Prevot, A. S. H., Zhang, Q., Kroll, J. H., DeCarlo, P. F., Allan, J. D., Coe, H., Ng, N. L., Aiken, A. C., Docherty, K. S., Ulbrich, I. M., Grieshop, A. P., Robinson, A. L., Duplissy, J., Smith, J. D., Wilson, K. R., Lanz, V. A., Hueglin, C., Sun, Y. L., Tian, J., Laaksonen, A., Raatikainen, T., Rautiainen, J., Vaattovaara, P., Ehn, M., Kulmala, M., Tomlinson, J. M., Collins, D. R., Cubison, M. J., Dunlea, E. J., Huffman, J. A., Onasch, T. B., Alfarra, M. R., Williams, P. I., Bower, K., Kondo, Y., Schneider, J., Drewnick, F., Borrmann, S., Weimer, S., Demerjian, K., Salcedo, D., Cottrell, L., Griffin, R., Takami, A., Miyoshi, T., Hatakeyama, S., Shimono, A., Sun, J. Y., Zhang, Y. M., Dzepina, K., Kimmel, J. R., Sueper, D., Jayne, J. T., Herndon, S. C., Trimborn, A. M., Williams, L. R., Wood, E. C., Middlebrook, A. M., Kolb, C. E., Baltensperger, U. and Worsnop, D. R.: Evolution of Organic Aerosols in the Atmosphere, Science, 326, 1525-1529, 2009.

Jimenez, J. L., Jayne, J. T., Shi, Q., Kolb, C. E., Worsnop, D. R., Yourshaw, I., Seinfeld, J. H., Flagan, R. C., Zhang, X., Smith, K. A., Morris, J. W. and Davidovits, P.: Ambient aerosol sampling using the Aerodyne Aerosol Mass Spectrometer, J.Geophys. Res.-Atmos, 108, 8425. doi:10.1029/2001JD001213, 2003.

Lack, D. A., Langridge, J. M., Bahreini, R., Cappa, C. D., Middlebrook, A. M. and Schwarz, J. P.: Brown carbon and internal mixing in biomass burning particles, Proc. Natl. Acad. Sci. U. S. A., 109, 14802-14807, 2012.

Lanz, V. A., Alfarra, M. R., Baltensperger, U., Buchmann, B., Hueglin, C., and Prevot, A. S. H.: Source apportionment of submicron organic aerosols at an urban site by factor analytical modelling of aerosol mass spectra, Atmos. Chem. Phys., 7, 1503–1522, 2007.

Liu, S., Russell, L. M., Sueper, D. T. and Onasch, T. B.: Organic particle types by single-particle measurements using a time-of-flight aerosol mass spectrometer coupled with a light scattering module, Atmos. Meas. Tech., 6, 187-197, 2013.

Massoli, P., Fortner, E. C., Canagaratna, M. R., Williams, L. R., Zhang, Q., Sun, Y., Schwab, J. J., Trimborn, A., Onasch, T. B., Demerjian, K. L., Kolb, C. E., Worsnop, D. R. and Jayne, J. T.: Pollution Gradients and Chemical Characterization of Particulate Matter from Vehicular Traffic near Major Roadways: Results from the 2009 Queens College Air Quality Study in NYC, Aerosol Sci. Technol., 46, 1201-1218, 2012.

Matthew, B. M., Middlebrook, A. M. and Onasch, T. B.: Collection efficiencies in an Aerodyne Aerosol Mass Spectrometer as a function of particle phase for laboratory generated aerosols, Aerosol Sci. Technol., 42, 884-898, 2008.

McMeeking, G. R., Good, N., Petters, M. D., McFiggans, G. and Coe, H.: Influences on the fraction of hydrophobic and hydrophilic black carbon in the atmosphere, Atmos. Chem. Phys., 11, 5099-5112, 2011.

Metcalf, A. R., Loza, C. L., Coggon, M. M., Craven, J. S., Jonsson, H. H., Flagan, R. C. and Seinfeld, J. H.: Secondary Organic Aerosol Coating Formation and Evaporation: Chamber Studies Using Black Carbon Seed Aerosol and the Single-Particle Soot Photometer, Aerosol Sci. Technol., 47, 326-347, 2013.

Moffet, R. C. and Prather, K. A.: In-situ measurements of the mixing state and optical properties of soot with implications for radiative forcing estimates, Proc. Natl. Acad. Sci., 106(29), 11872–11877, 2009.

Mohr, C., DeCarlo, P. F., Heringa, M. F., Chirico, R., Slowik, J. G., Richter, R., Reche, C., Alastuey, A., Querol, X., Seco, R., Penuelas, J., Jimenez, J. L., Crippa, M., Zimmermann, R., Baltensperger, U. and Prevot, A. S. H.: Identification and quantification of organic aerosol from cooking and other sources in Barcelona using aerosol mass spectrometer data, Atmos. Chem. Phys., 12, 1649-1665, 2012.

Mohr, C., Huffman, J. A., Cubison, M. J., Aiken, A. C., Docherty, K. S., Kimmel, J. R., Ulbrich, I. M., Hannigan, M. and Jimenez, J. L.: Characterization of Primary Organic Aerosol Emissions from Meat Cooking, Trash Burning, and Motor Vehicles with High-Resolution Aerosol Mass Spectrometry and Comparison with Ambient and Chamber Observations, Environ. Sci. Technol., 43, 2443-2449, 2009.

Moteki, N. and Kondo, Y.: Effects of mixing state on black carbon measurements by laser-induced incandescence, Aerosol Sci. Technol., 41, 398-417, 2007.

Ng, N. L., Canagaratna, M. R., Zhang, Q., Jimenez, J. L., Tian, J., Ulbrich, I. M., Kroll, J. H., Docherty, K. S., Chhabra, P. S., Bahreini, R., Murphy, S. M., Seinfeld, J. H., Hildebrandt, L., Donahue, N. M., DeCarlo, P. F., Lanz, V. A., Prevot, A. S. H., Dinar, E., Rudich, Y. and Worsnop, D. R.: Organic aerosol components observed in Northern Hemispheric datasets from Aerosol Mass Spectrometry, Atmos. Chem. Phys., 10, 4625-4641, 2010.

Onasch, T. B., Trimborn, A., Fortner, E. C., Jayne, J. T., Kok, G. L., Williams, L. R., Davidovits, P. and Worsnop, D. R.: Soot Particle Aerosol Mass Spectrometer: Development, Validation, and Initial Application, Aerosol Sci. Technol., 46, 804-817, 2012.

Pagels, J., Dutcher, D. D., Stolzenburg, M. R., McMurry, P. H., Gaelli, M. E. and Gross, D. S.: Fine-particle emissions from solid biofuel combustion studied with single-particle mass spectrometry: Identification of markers for organics, soot, and ash components J.Geophys. Res.-Atmos., 118, 859-870, 2013.

Pratt, K. A. and Prather, K. A.: Mass spectrometry of atmospheric aerosols: Recent developments and applications. Part II: On-line mass spectrometry techniques, Mass Spectrom. Rev., 31, 17-48, 2012.

Rebotier, T. P. and Prather, K. A.: Aerosol time-of-flight mass spectrometry data analysis: a benchmark of clustering algorithms, Anal. Chim. Acta, 585(1), 38–54, doi:10.1016/j.aca. 2006.12.009, 2007.

Robinson, E. S., Saleh, R. and Donahue, N. M.: Organic aerosol mixing observed by single-particle mass spectrometry., J. Phys. Chem. A, 117(51), 13935–45, doi:10.1021/jp405789t, 2013.

Schwarz, J. P., Gao, R. S., Fahey, D. W., Thomson, D. S., Watts, L. A., Wilson, J. C., Reeves, J. M., Darbeheshti, M., Baumgardner, D. G., Kok, G. L., Chung, S. H., Schulz, M., Hendricks, J., Lauer, A., Kaercher, B., Slowik, J. G., Rosenlof, K. H., Thompson, T. L., Langford, A. O., Loewenstein, M. and Aikin, K. C.: Single-particle measurements of midlatitude black carbon and light-scattering aerosols from the boundary layer to the lower stratosphere, J.Geophys. Res.-Atmos., 111, D16207, 2006.

Shields, L. G., Qin, X. Y., Toner, S. M. and Prather, K. A.: Detection of ambient ultrafine aerosols by single particle techniques during the SOAR 2005 campaign, Aerosol Sci. Technol., 42(8), 674–684, doi:10.1080/02786820802227378, 2008.

Shields, L. G., Suess, D. T. and Prather, K. A.: Determination of single particle mass spectral signatures from heavy-duty diesel vehicle emissions for PM2.5 source apportionment, Atmos. Environ., 41(18), 3841–3852, 2007.

Shiraiwa, M., Kondo, Y., Iwamoto, T. and Kita, K.: Amplification of Light Absorption of Black Carbon by Organic Coating, Aerosol Sci. Technol., 44, 46-54, 2010.

Shiraiwa, M., Kondo, Y., Moteki, N., Takegawa, N., Miyazaki, Y. and Blake, D. R.: Evolution of mixing state of black carbon in polluted air from Tokyo, Geophys. Res. Lett., 34, L16803, 2007.

Slowik, J., Stainken, K., Davidovits, P., Williams, L., Jayne, J., Kolb, C., Worsnop, D., Rudich, Y., DeCarlo, P. and Jimenez, J.: Particle morphology and density characterization by combined mobility and aerodynamic diameter measurements. Part 2: Application to combustion-generated soot aerosols as a function of fuel equivalence ratio, Aerosol Sci. Technol., 38, 1206-1222, 2004.

Sodeman, D. A., Toner, S. M. and Prather, K. A.: Determination of single particle mass spectral signatures from light-duty vehicle emissions, Environ. Sci. Technol., 39(12), 4569–4580, 2005.

Stephens, M., Turner, N. and Sandberg, J.: Particle identification by laser-induced incandescence in a solid-state laser cavity, Appl. Opt., 42, 3726-3736, 2003.

Toner, S. M., Shields, L. G., Sodeman, D. A. and Prather, K. A.: Using mass spectral source signatures to apportion exhaust particles from gasoline and diesel powered vehicles in a freeway study using UF-ATOFMS, Atmos. Environ., 42(3), 568–581, 2008.

Toner, S. M., Sodeman, D. A. and Prather, K. A.: Single particle characterization of ultrafine and accumulation mode particles from heavy duty diesel vehicles using aerosol time-of-flight mass spectrometry, Environ. Sci. Technol., 40(12), 3912–3921, 2006.

Tritscher, T., Juranyi, Z., Martin, M., Chirico, R., Gysel, M., Heringa, M. F., DeCarlo, P. F., Sierau, B., Prevot, A. S. H., Weingartner, E. and Baltensperger, U.: Changes of hygroscopicity and morphology during ageing of diesel soot, Environ. Res. Lett., 6, 034026, 2011.

Ulbrich, I. M., Canagaratna, M. R., Zhang, Q., Worsnop, D. R. and Jimenez, J. L.: Interpretation of organic components from Positive Matrix Factorization of aerosol mass spectrometric data, Atmos. Chem. Phys., 9, 2891-2918, 2009.

Wang, J., Cubison, M. J., Aiken, A. C., Jimenez, J. L. and Collins, D. R.: The importance of aerosol mixing state and size-resolved composition on CCN concentration and the variation of the importance with atmospheric aging of aerosols, Atmos. Chem. Phys., 10, 7267-7283, 2010.

Willis, M. D., Lee, A. K. Y., Onasch, T. B., Fortner, E. C., Williams, L. R., Lambe, A. T., Worsnop, D. R., and Abbatt, J. P. D., Collection efficiency of the soot-particle aerosol mass spectrometer (SP-AMS) for internally mixed particulate black carbon, Atmos. Meas. Tech. Discussion, 7, 5223-5249, 2014.

Zhang, Q., Jimenez, J. L., Canagaratna, M. R., Allan, J. D., Coe, H., Ulbrich, I., Alfarra, M. R., Takami, A., Middlebrook, A. M., Sun, Y. L., Dzepina, K., Dunlea, E., Docherty, K., DeCarlo, P. F., Salcedo, D., Onasch, T., Jayne, J. T., Miyoshi, T., Shimono, A., Hatakeyama, S., Takegawa, N., Kondo, Y., Schneider, J., Drewnick, F., Borrmann, S., Weimer, S., Demerjian, K., Williams, P., Bower, K., Bahreini, R., Cottrell, L., Griffin, R. J., Rautiainen, J., Sun, J. Y., Zhang, Y. M. and Worsnop, D. R.: Ubiquity and dominance of oxygenated species in organic aerosols in anthropogenically-influenced Northern Hemisphere midlatitudes, Geophys. Res. Lett., 34, L13801, 2007.

Zhang, Q., Jimenez, J. L., Canagaratna, M. R., Ulbrich, I. M., Ng, N. L., Worsnop, D. R. and Sun, Y.: Understanding atmospheric organic aerosols via factor analysis of aerosol mass spectrometry: a review, Analyt. Bioanalyt. Chem., 401, 3045-3067, 2011.

Zhang, R., Khalizov, A. F., Pagels, J., Zhang, D., Xue, H. and McMurry, P. H.: Variability in morphology, hygroscopicity, and optical properties of soot aerosols during atmospheric processing, Proc. Natl. Acad. Sci. U. S. A., 105, 10291-10296, 2008.

Tables:

Table 1: Summary of menu switching in the LS-SP-AMS and single particle categorization

Menu	**1**	**2**	**3**	**4**
IR laser mode	ON	ON	OFF	OFF
Data acquisition mode	MS, PToF	LS	MS, PToF	LS
Time intervals (s)	90	90	90	90
Total LS trigger events	--	113,120	--	112,441
"Noise" events	--	28,513	--	28,226
Particle LS trigger events	--	84,607	--	84,218
Coincidence	--	2,190 (2.6%)	--	2,242 (2.7%)
Prompt	--	35,001 (41.4%)	--	28,322 (33.6%)
Early	--	206 (0.2%)	--	83 (0.1%)
Delayed	--	702 (0.8%)	--	340 (0.4%)
Null	--	46,508 (55.0%)	--	53,231 (63.2%)

Table 2: Summary of the rBC contribution to each cluster

Cluster type	**% of particles with measurable m/z 36* signal (# of particles)**			**Mass fraction of rBC (IR laser-on)[#]**
	Laser-on	Laser-off	Difference (laser-on minus off)	
NO_3	11.4% (1063)	10.2% (652)	1.2%	0.035
SO_4	4.4% (130)	2.8% (67)	1.6%	0.019
HOA	8.4% (347)	2.0% (65)	6.4%	0.024
rBC	97.1% (867)	NA	NA	0.722
COA	6.5% (548)	2.9% (205)	3.6%	0.020
OOA 1	8.2% (587)	4.1% (291)	4.1%	0.027
OOA 2	7.4% (153)	3.9% (80)	3.5%	0.028

*Any signal larger than zero, IR laser-on mode: m/z 36 = C_3^+ and HCl^+, IR laser-off mode: m/z 36 = HCl^+ only

The fragmentation table shown in TableS2 was used for quantification of rBC

NA = Not applicable

Figures:

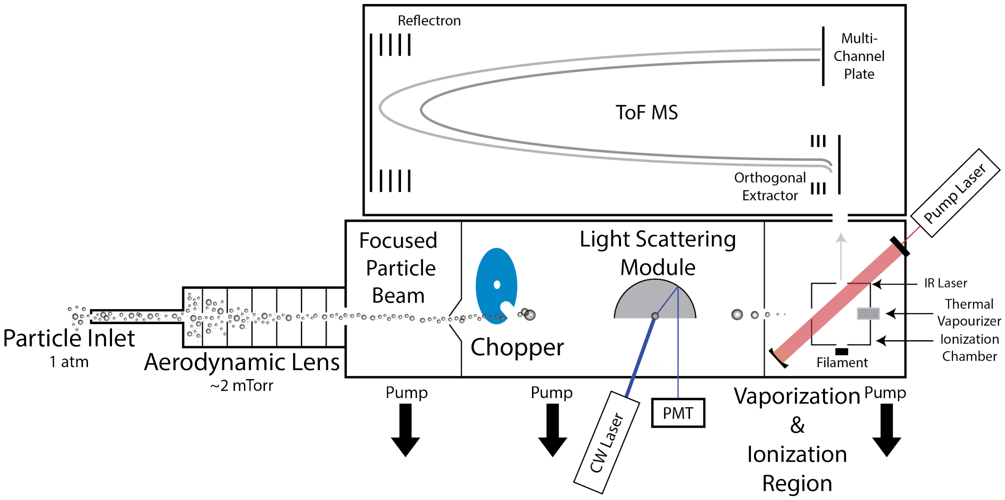

Figure 1: A simplified schematic of the SP-AMS equipped with a light scattering module (LS-SP-AMS) for ensemble measurements and single particle detection.

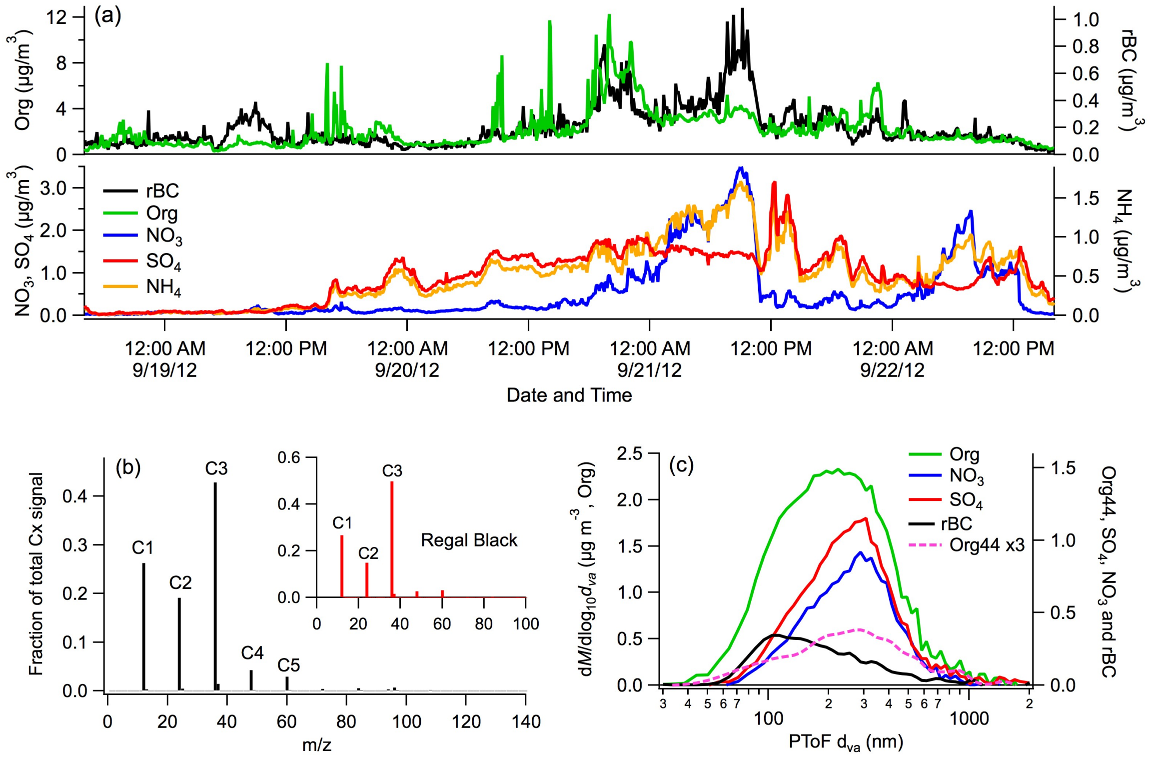

Figure 2: Summary of ensemble measurements (a) Time series (local time) of laser-off (Org, NO_3, SO_4, NH_4) and laser-on (rBC) aerosol compositions. (b) The average mass spectrum of laser-on ambient rBC and Regal Black (insert). (c) Average size distributions of laser-off (Org, NO_3, SO_4, Org44) and laser-on (rBC) aerosol compositions. Org 44 represents the organic signal at m/z 44 (e.g., CO_2^+).

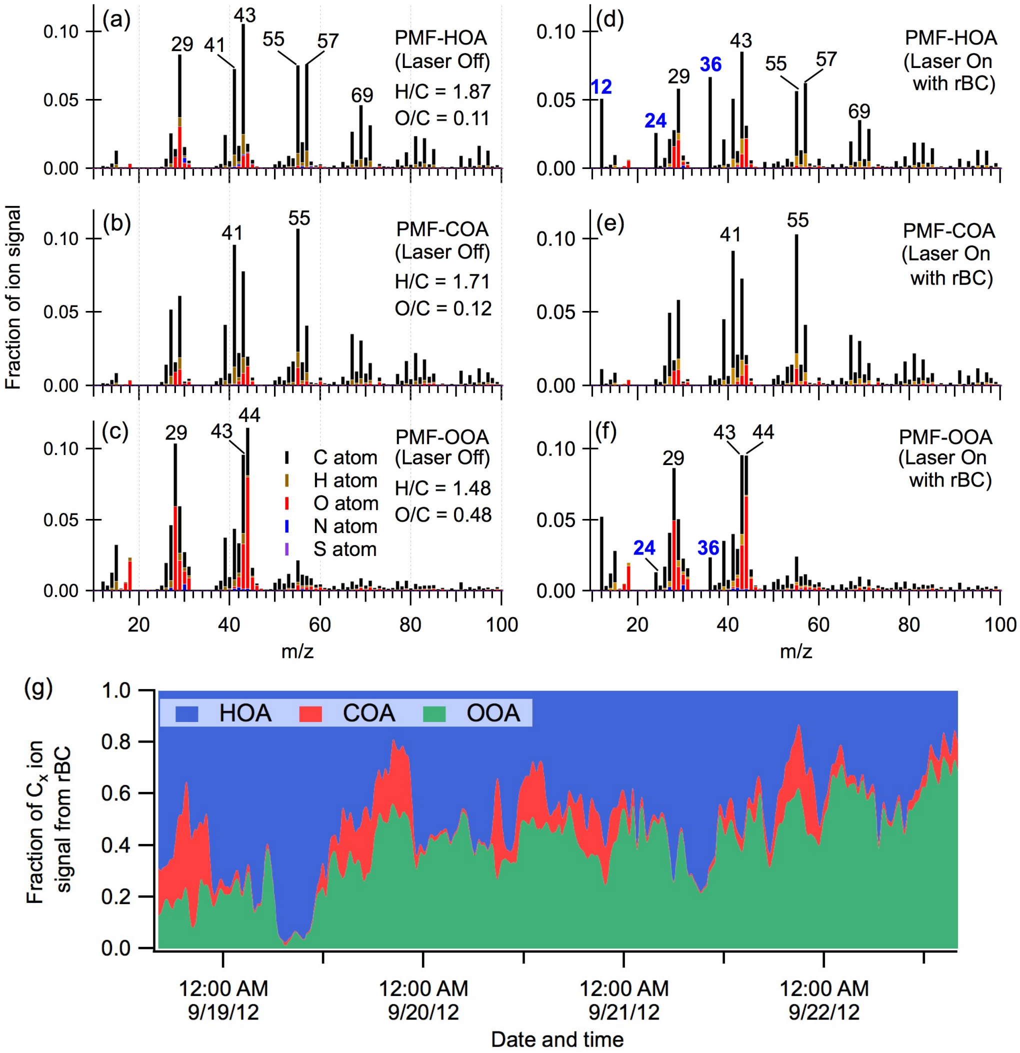

Figure 3: Normalized mass spectra of PMF factors from laser-off (a-c) and laser-on with rBC signals (d-f) mode measurements: (a and d) HOA factor, (b and e) COA factor, (c and f) OOA
5 factor. (g) Mass fraction contribution of total C_x signal from each laser-on mode PMF factor (d-f).

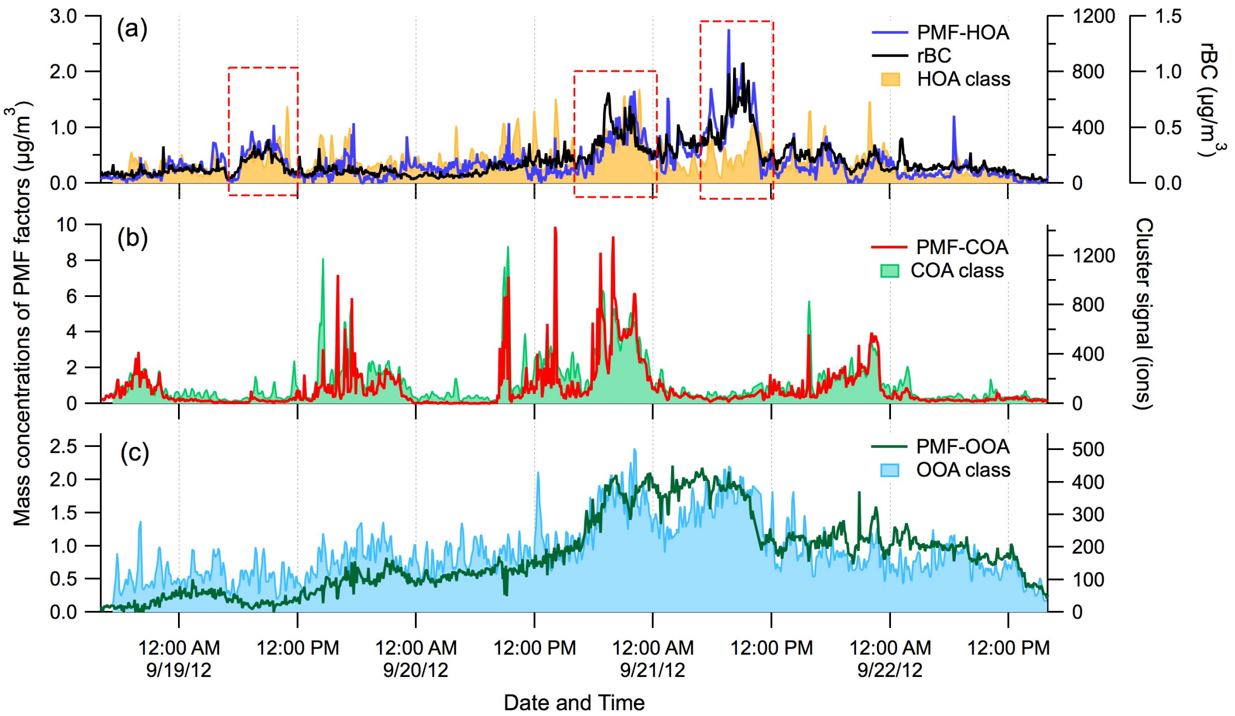

Figure 4: Time series (local time) profiles of rBC, PMF factors of organic components (from laser-off mode MS measurements) and different organic clusters (from laser-on mode LS measurements). The red rectangles indicate three major rBC and HOA peaks throughout the sampling period.

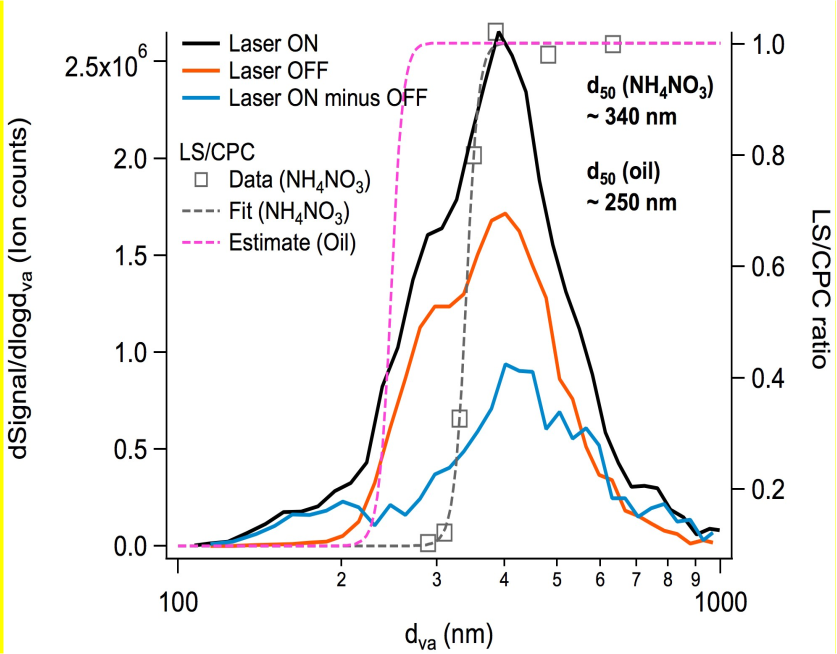

Figure 5: Size distributions of total ion counts from the ambient single particle measurements (Black: laser-on mode, Orange: laser-off mode, Blue: difference between laser-on and laser-off modes). The grey square (data) and grey dashed line (fitting) represents the counting efficiency (the ratio of light scattering counts and condensation particle counter signals (LS/CPC), left axis) of the light scattering module for ammonium nitrate particles. The pink dashed line indicates an estimated light scattering cut-off d_{va} for spherical hydrocarbon oil droplets (i.e., shape factor = 1 and density = 1 g/cm^3).

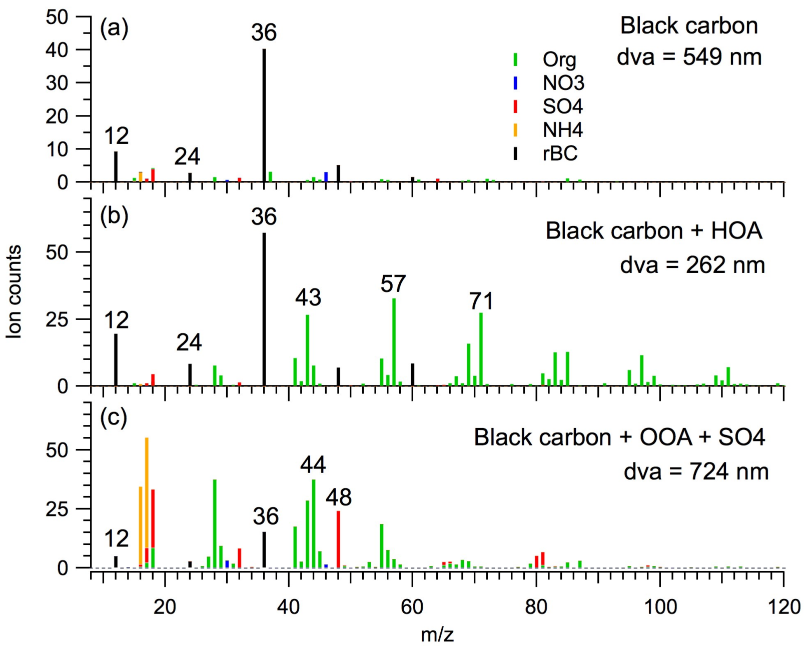

Figure 6: Examples of single particle mass spectra of rBC-containing particles in ambient air: (a) Black carbon, (b) black carbon internally mixed with HOA, and (c) black carbon internally mixed with OOA and sulfate. Particles (a) and (b) are sorted into the rBC cluster, and particle (c) is classified into the OOA cluster 2 identified in this study (See Section 3.5).

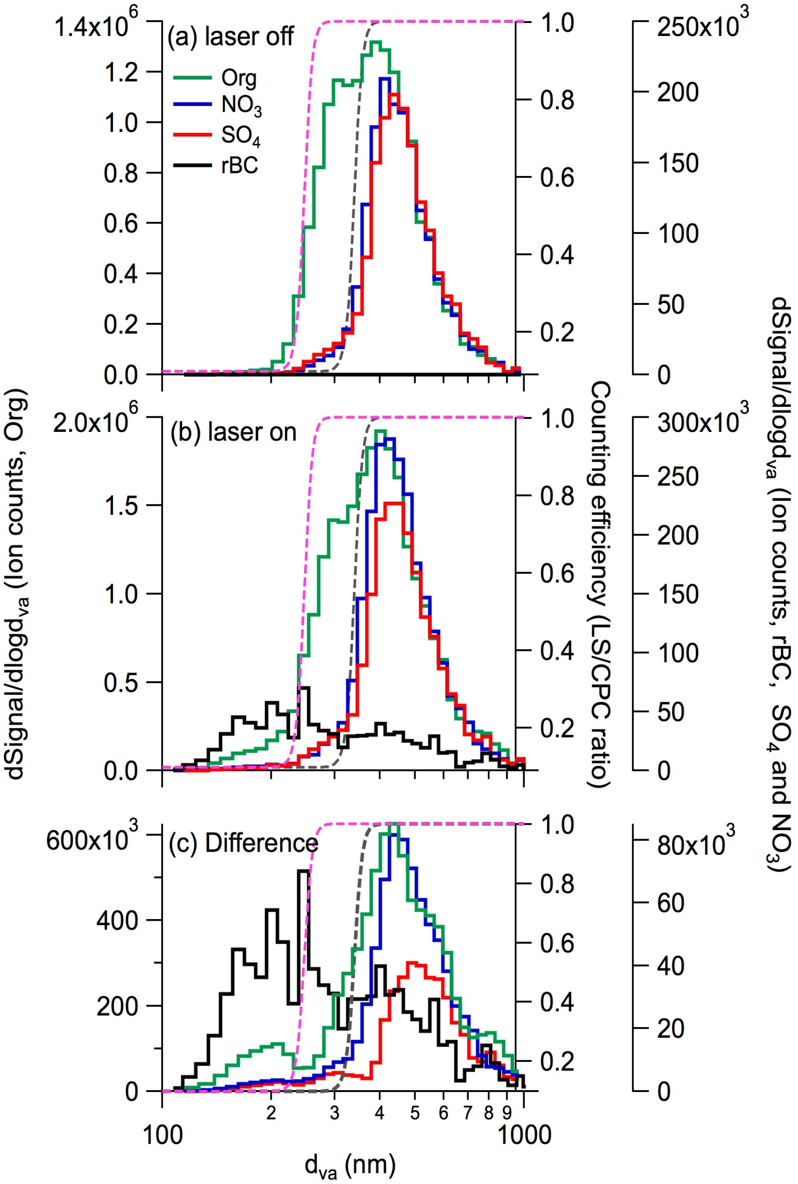

Figure 7: Integrated size distributions of nitrate, sulfate, organics and rBC from the single particle ion signal measurements with IR laser-off (a) and on (b). (c) Differences between laser-on and off modes (i.e., laser-on minus laser-off data). The grey dashed line represents the counting efficiency (LS/CPC) of the light scattering module for ammonium nitrate particles. The pink dashed line indicates an estimated light scattering cut-off d_{va} for spherical hydrocarbon oil droplets.

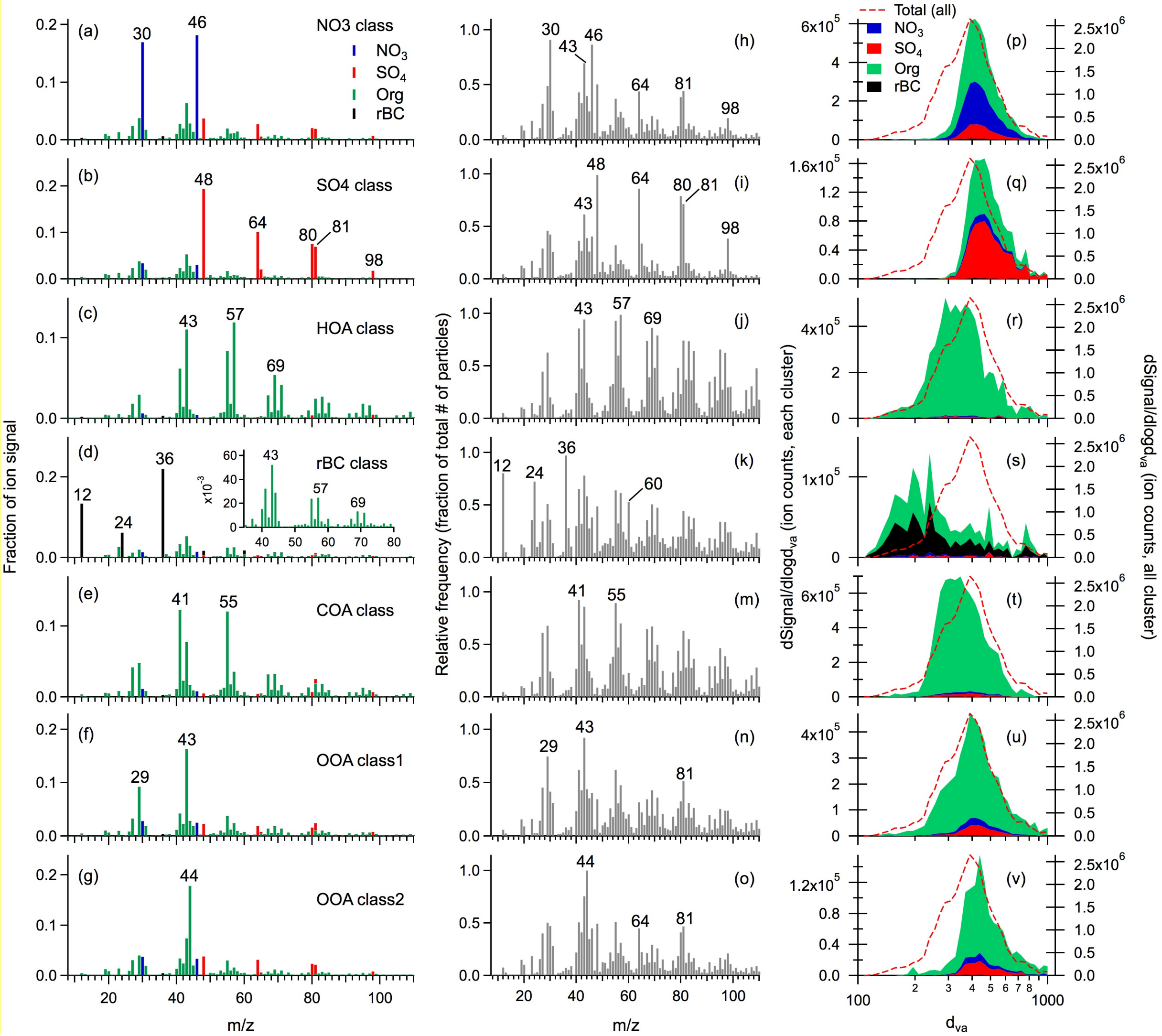

Figure 8: Normalized mass spectra (left column), normalized histograms displaying the relative frequency of each m/z (middle column), and size distributions (right column) of different particle classes identified from k-means clustering of LS-SP-AMS single particle dataset (laser-on): (a, h and p) NO_3 class, (b, i and q) SO_4 class, (c, j and r) HOA class, (d, k and s) rBC class, (e, m and t) COA class, (f, n and u) OOA class 1 – less oxygenated, (g, o and v) OOA class 2 – more oxygenated. The insert in 8d shows the organic mass spectrum associated with rBC-rich particle class.

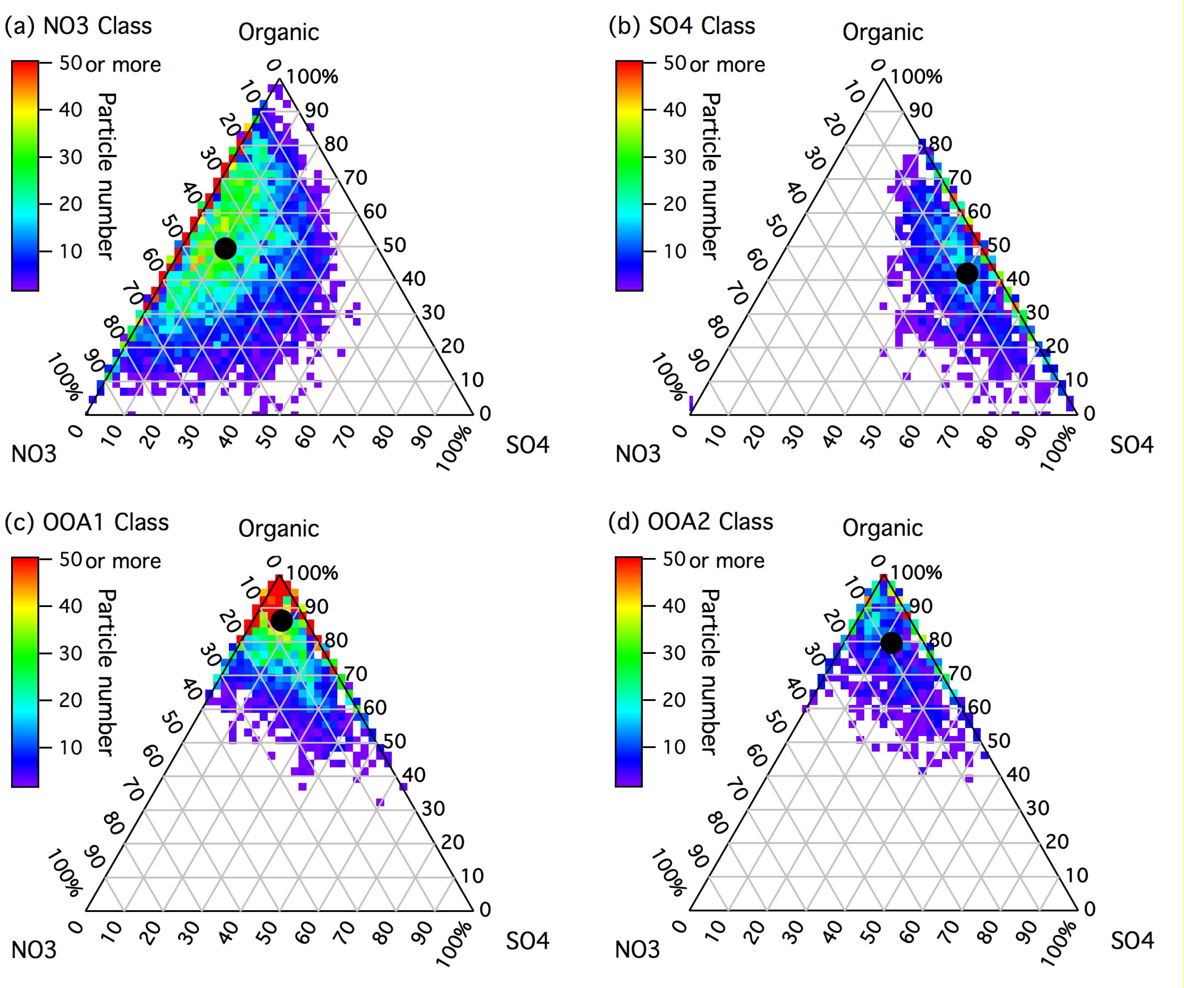

Figure 9: Ternary plot of nitrate, sulfate and organics mass fraction for those particles types identified by cluster analysis: (a) NO_3, (b) SO_4, (c) OOA1, and (d) OOA2. All these particle classes are the major contributors in the accumulation mode particles. The black solid circles indicate the coordinates of average compositions of each particle classes.

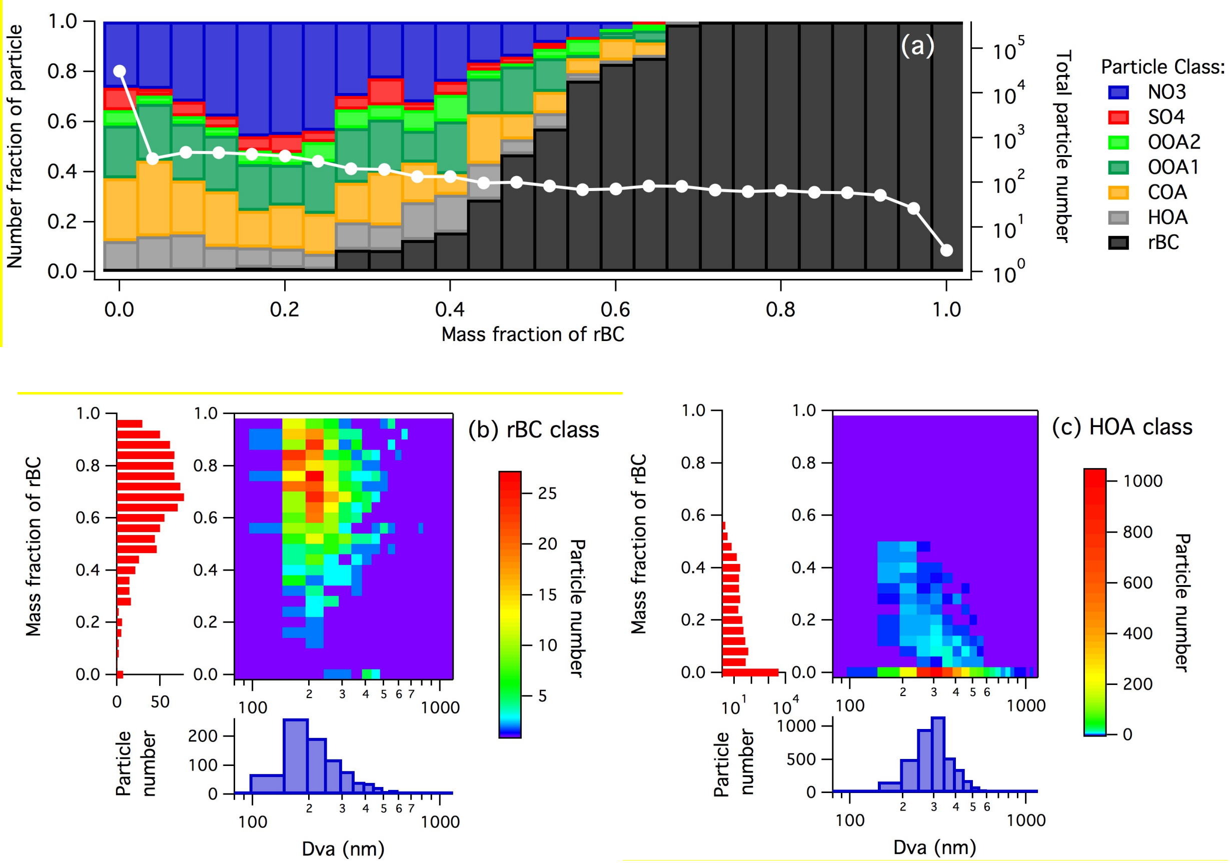

Figure 10: (a) Histogram (normalized to the total number of particles in each bin) of the mass fraction of rBC for all particle classes (left axis). The while circle markers represents the total number of particles (right axis) in each bin. Distributions of particle size and black carbon mass fraction for (b) rBC-rich class, and (c) HOA-rich class.